

AD-A164 182

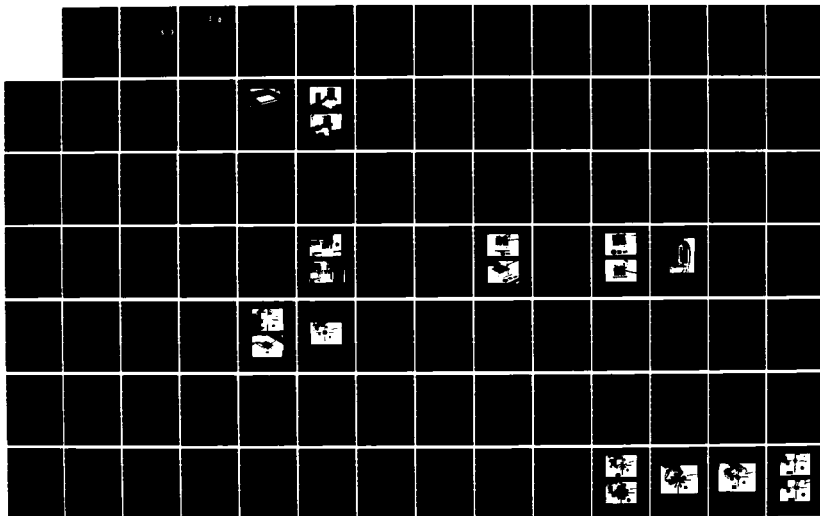
A STUDY OF THE FLUID-DYNAMIC PRESSURE FIELDS ON
COMPRESSOR REED VALVES(U) AIR FORCE INST OF TECH
WRIGHT-PATTERSON AFB OH SCHOOL OF ENGINEERING R D HUNT
DEC 85 AFIT/GAE/AA/85D-09

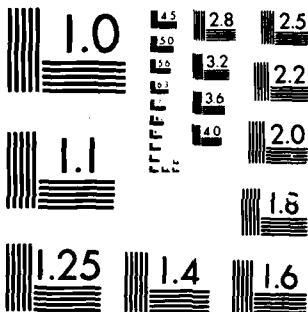
1/2

UNCLASSIFIED

F/G 28/4

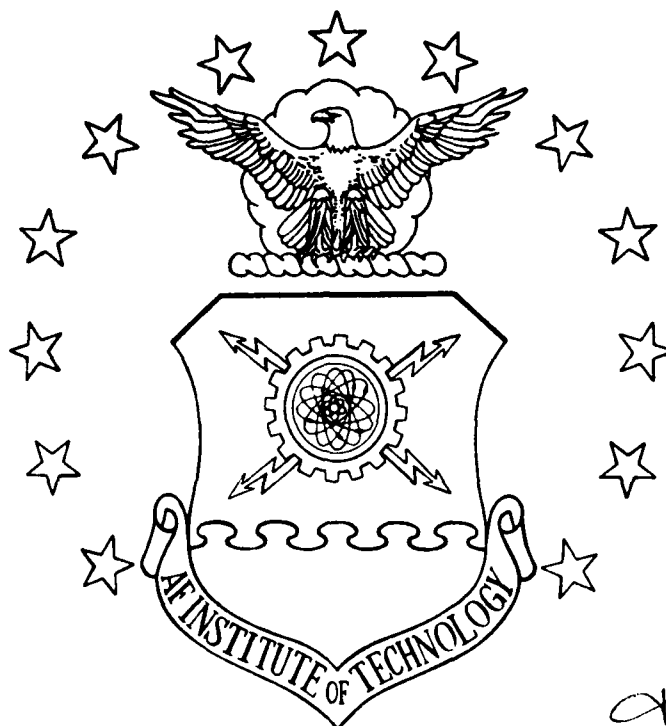
NL





MICROCOPY RESOLUTION TEST CHART
NATIONAL BUREAU OF STANDARDS-1963-A

AD-A164 102



①
DTIC
EL
FEB 14 1986
S
D

A STUDY OF THE FLUID-DYNAMIC PRESSURE
FIELDS ON COMPRESSOR REED VALVES

THESIS

Robert D. Hunt
Captain, USAF

AFIT/GAE/AA/85D-09

DISTRIBUTION STATEMENT A

Approved for public release;
Distribution Unlimited

DEPARTMENT OF THE AIR FORCE
AIR UNIVERSITY

AIR FORCE INSTITUTE OF TECHNOLOGY

Wright-Patterson Air Force Base, Ohio

23 2 14 011

REF ID: A164102

AFIT/GAE/AA/85D-09

DTIC
ELECTE
FEB 14 1986
S D

A STUDY OF THE FLUID-DYNAMIC PRESSURE
FIELDS ON COMPRESSOR REED VALVES

THESIS

Robert D. Hunt
Captain, USAF

AFIT/GAE/AA/85D-09

Approved for public release; distribution unlimited

AFIT/GAE/AA/85D-09

A STUDY OF THE FLUID-DYNAMIC PRESSURE FIELDS
ON COMPRESSOR REED VALVES

THESIS

Presented to the Faculty of the School of Engineering
of the Air Force Institute of Technology
Air University
In Partial Fulfillment of the
Requirements for the Degree of
Master of Science in Aeronautical Engineering



Robert D. Hunt, B.S.
Captain, USAF

December 1985

Accession For	
NTIS CRA&I	<input checked="checked" type="checkbox"/>
DTIC TAB	<input type="checkbox"/>
Unannounced	<input type="checkbox"/>
Justification	
By	
Distribution /	
Availability Codes	
Dist	Avail and/or Special
A-1	

Approved for public release; distribution unlimited

Preface

The purpose of this thesis was to analytically predict and experimentally measure the flow-induced pressure field in a reed-valve arrangement. Reed valves are typically used in sealed compressor units. The thrust of this work was to find an analytic solution, compatible with a small computer system, for a "first-look" at the pressure field on the up-flow side of the reed valve. Analytically, the flow was modeled as one-dimensional, piece-wise isentropic with the possibility of an imbedded normal shock. The experimental portion of the thesis work involved operating an idealized reed-valve model at various steady-state pressures. The pressure field beneath the valve plate was measured using a computerized data acquisition system which relied on a scanivalve as the primary pressure gauge.

An interesting side note identified during this research was that if you make a simple model of the configuration, using a spool of thread, a pin, and a piece of paper, you can create a supersonic flow and a normal shock by blowing through the spool.

Several people gave very valuable assistance throughout this project. My advisor, Lt Col Eric Jumper, provided insight into the analytic solution, provided direction, and shared in the enthusiasm of the experimental work. Nick Yardich and Leroy Cannon were ever ready with their professional advise and assistance. A special thanks is due

to Jay Anderson who diligently assisted me in setting up the computerized data acquisition system. The members of my class, GAE-85D, were very supportive and I'm proud to call each one of them a friend. Finally, my love and thanks are devoutly extended to my wife, Alice. Her encouragement, professional critique and support were invaluable even when the Atlantic Ocean spanned the distance between us.

Bob Hunt

Table of Contents

	Page
Preface	ii
List of Figures	vi
List of Symbols	ix
Abstract	xi
I. Introduction	1
Background	1
Purpose and Scope	3
II. Theory	7
Radial Flow Problem	7
Incompressible Discussion	9
Compressible Solution	14
Numerical Solution	16
Other Theoretical Considerations	28
III. Apparatus and Instrumentation	32
General	32
Test Rig	35
Scanivalve Operation	37
IV. Calibration and Test Procedure	42
Calibration	42
Test Procedure	44
Flow Visualization	45
V. Data Reduction	49
VI. Results and Discussion	54
General	54
Configuration 1	54
Configuration 2	71
Configuration 3	74
Effective Area	75
Flow Visualization	78
Discussion	84

VII. Conclusions and Recommendations	85
Conclusions	85
Recommendations	86
Bibliography	88
Appendix A: SOLVE	90
Appendix B: Intrumentation List	97
Appendix C: TEST	98
Appendix D: REDDATA	100
Appendix E: EFFAREA	103
Vita	105

List of Figures

Figure	Page
1A. Reed-Valve Compressor Plate	4
1B. Reed Valve, Typical Dimensions	4
2A. Spool and Paper Valve Model	5
2B. Spool With Paper Valve Plate in Position	5
3. Cross-section of Problem	8
4. Sectional View of Flow Geometry	10
5. Flow Chart of Program SOLVE	21
6. Flow Chart of Subsonic Solution	23
7. Flow Chart of Supersonic Solution	25
8. Pressure Ratio vs. Location From Analytical Solution	27
9. Radius Ratio vs. Pressure Ratio From Analytical Solution	30
10A. Experimental Work Area, Front View	33
10B. Experimental Work Area, Oblique View	33
11. Schematic of Work Apparatus	34
12A. Test Rig, Overhead View Showing Centering System, Pins, and Valve Plate	36
12B. Test Rig, Oblique View	36
13A. Test Rig With Out Cover Plate, Showing Radial Arm Pattern of Pressure Taps	38
13B. Test Rig, Bottom View	38
14. Scanivalve	39
15. Pressure Transducer Calibration Curve	43

16A. Test Rig Showing Oil Drops for Flow Visualization	46
16B. Test Rig in Inverted Configuration. Note the Reversed Legs	46
16C. Test Rig Showing Knife Edge Technique for Centering the Valve Plate	47
17. Radial Arm Symmetry for Various Valve Plates . .	51
18. Representative Data; Pressure Ratio vs. Radial Location; Five Runs	55
19. Pressure Ratio vs. Location Plots, Theory and Data, for Reservoir Pressure of 14.85 psia . . .	57
20. Pressure Ratio vs. Location Plots, Theory and Data, for Reservoir Pressure of 15.88 psia . . .	58
21. Pressure Ratio vs. Location Plots, Theory and Data, for Reservoir Pressure of 20.46 psia . . .	59
22. Pressure Ratio vs. Location Plots, Theory and Data, for Reservoir Pressure of 24.04 psia . . .	60
23. Pressure Ratio vs. Location Plots, Theory and Data, for Reservoir Pressure of 28.96 psia . . .	61
24. Pressure Ratio vs. Location Plots, Theory and Data, for Reservoir Pressure of 36.39 psia . . .	62
25. Pressure Ratio vs. Location Plots, Theory and Data, for Reservoir Pressure of 48.36 psia . . .	63
26. Pressure Ratio vs. Location Plots, Theory and Data, for Reservoir Pressure of 72.90 psia . . .	64
27. Pressure Ratio vs. Location Plots, Theory and Data, for Reservoir Pressure of 96.03 psia . . .	65
28. Pressure Ratio vs. Location Plots, Theory and Data, for Reservoir Pressure of 104.96 psia . .	66
29. Overlay of Five Theoretical and Five Data Plots of Pressure Ratio vs. Location	67
30A. Pressure Ratio vs. Location Data and Equivalent Nozzle Including Theoretical Supersonic Branch .	69

30B. Similar Plot for Laval Nozzle, Taken From Liepmann and Roshko (10:129)	70
31. Pressure Ratio vs. Location Data for Configuration 2: Three Data Plots; Two for Symmetric Arms, One for Circular Evaluation. Theoretical Plot for Circular Plate Included for Comparison	73
32. Pressure Ratio vs. Location Data for Configuration 3: Four Data Plots; Three for Symmetric Arms, One for Circular Evaluation. Theoretical Plot for Circular Plate Included for Comparison	76
33. Pressure Ratio vs. Location Plots of Data and Three Analytic Techniques: (1) SOLVE, (2) EFFAREA Method 1, (3) EFFAREA Method 2. Reservoir Pressure is 36.39 psia	77
34A. Flow Visualization Configuration 1; Reservoir Pressure is 44 psia	80
34B. Flow Visualization Configuration 1; Reservoir Pressure is 73 psia	80
35. Flow Visualization Configuration 1; Reservoir Pressure is 99 psia. Note Smeared Shock	81
36. Flow Visualization Configuration 2; Reservoir Pressure is 39 psia	82
37A. Flow Visualization Configuration 3; Reservoir Pressure is 39 psia	83
37B. Flow Visualization Configuration 3; Reservoir Pressure is 54 psia	83

List of Symbols

Symbol	Description
A	Area of Stream Tube, ft ²
A*	Throat Area, Star Condition, ft ²
A _c	Area of Inlet Collar, in ²
A _e	Area of Exit Collar, in ²
c	Sonic Velocity, ft/sec
c ₀	Total Sonic Velocity, ft/sec
δ	Nozzle Divergence Half Angle, degrees
E	Section of Exit Collar Area, in ²
FNBOB(M)	Function of Mach Number (cf. Eq(6))
γ	Gamma, Ratio of Specific Heats
h	Height of Valve Plate From Base Plate, in
I	Section of Inlet Area, in ²
m	Mass Flow Rate, slugs/sec
M	Mach Number
M _e , ME	Exit Mach Number
MES	Exit Mach Number, Star Condition
M _i , M(I)	Mach Number at Location I
M ₁	Mach Number, Upstream Side of Normal Shock
M ₂	Mach Number, Downstream Side of Normal Shock
P	Static Pressure, lb/in ²
P _a , PA	Ambient Pressure, lb/in ²
P _e , PE	Exit Pressure, lb/in ²
P ₀	Total Pressure, lb/in ²
P _{res}	Reservoir Pressure, lb/in ²

P_{0v} , PTY	Total Pressure, Downstream Side of Normal Shock, lb/in ²
psia	lb/in ² Absolute
psig	lb/in ² Gauge
PR	Pressure Ratio
PRS	Pressure Ratio, Star Condition
π	P_1 , Approximately 3.14159
Q	Volumetric Flow, ft ³ /sec
R_e	Radius at Exit, in
R_i	Radius at Incremental Location I, in
R_{inlet}	Radius at Inlet, in
s	Entropy
ρ	Static Density, slug/ft ³
ρ_0	Total Density, slug/ft ³
ρ_1	Density at Location 1, slug/ft ³
ρ_2	Density at Location 2, slug/ft ³
T	Static Temperature, degrees Rankine
T_0	Total Temperature, degrees Rankine
u_m	Maximum Velocity in Channel, ft/sec
u_1	Velocity at Location 1, ft/sec
u_2	Velocity at Location 2, ft/sec
V	Velocity, ft/sec

Abstract

The flow-induced pressure field in a reed-valve arrangement was analytically predicted and experimentally measured for steady-state conditions. The flow was found to be supersonic in nature with an imbedded shock for all but the lowest total pressure runs.

The analytic method used one-dimensional isentropic and normal shock relations. The technique provides a good "first-look" at the nature of the flow and is compatible for use on a small computer system.

The experimental data was obtained by using an idealized reed-valve model. The data acquisition system was computerized and used a scanivalve system to measure the pressures in the valve model. Circular, square, and rectangular valve plate geometries were investigated. The inlet was circular for all cases. Flow-visualization oil was also used in a qualitative approach to determine the location and shape of the shock in the flow. The pressure measurements and the flow visualization showed the shock to be circular for all geometries and pressures tested. At high total pressure runs the valve plate began vibrating and the shock location became smeared, suggesting that the shock was also oscillating.

A STUDY OF THE FLUID-DYNAMIC PRESSURE FIELDS
ON COMPRESSOR REED VALVES

I. INTRODUCTION

Background

In piston-type compressors, a spring-metal valve plate is often used for intake and exhaust valves. The valve, hereafter called a reed valve, has wide practical application due to the simplicity of operation and manufacture, and the minimal number of moving parts. These qualities normally mean long life and as such these valves are in common usage in sealed compressor units such as refrigeration systems. These systems are often required to operate for years without direct maintenance.

The design of these valves has historically been by trial and error. Seemingly small design changes can lead to large changes in the operating characteristics of the valve. Rapid and violent opening and closings of the valve during a single stroke of the compressor piston after slight design changes to previously smoothly operating valves have been reported (1). Modeling of the valve by other researchers is often from a structural point of view. In other work, the pressure on the face of the valve has been modeled by directly applying the total pressure of the flow to the area

of the exposed face. The present thesis work investigated a simple fluid-dynamic model of the pressure field for valve-like configurations. The pressure field on the up-flow side of the reed valve was of primary concern in this study.

The thrust of this work was to develop and apply an analytical solution to valve-like geometries and to compare it with experimentally acquired data. Certainly, the problem could be discretized and solved using an elaborate computational fluid dynamics approach, but the intention here was to take a "first look" with the simplest approach. As such, the analytical solution was intended to be compatible with small computer systems.

Initial work on this problem was accomplished by Jumper (2). His work examined the valve problem from a subsonic compressible flow point of view. One-dimensional isentropic flow relations were used throughout. While, as will be shown, the flow does not generally remain subsonic, insight can be derived from his findings. One such insight is the fact that only a small differential between the inlet pressure and the exit pressure is required to choke the flow in the valve. The present work expanded the analytical treatment of Jumper to include supersonic flow and the possibility of a shock wave in the flow.

Following Jumper, it is of interest to recognize the striking geometric similarity between the reed-valve problem and a problem involving a spool of thread and a piece of

paper. The problem involving the spool of thread is that of a child's trick where a pin is centered in a piece of paper, then the paper and pin are placed on the spool of thread. The trick is to blow the paper off of the spool. The interesting feature of the trick is that the paper cannot be blown off. A reed-valve compressor plate and a reed-valve schematic are shown in Figures 1A and 1B, respectively. The spool trick is illustrated in Figures 2A and 2B.

The geometric similarity between the spool trick and the reed valve becomes more obvious when the piece of paper is trimmed to more nearly match that of the reed-valve configuration. The spool trick works even with a piece of paper which barely overlaps the hole of the spool. This simple experimental and visual aid also provided a starting point for the design of the experimental apparatus.

Other flow problems with similar geometry can be found. These problems are typically posed as incompressible (3; 4) or compressible but subsonic as in the case of the radial diffuser (5). To our knowledge, no previous work has been done on the general problem which was the focus of this study.

Purpose and Scope

The purpose and scope of this work was to expand on the work started by Jumper and to compare the analytical

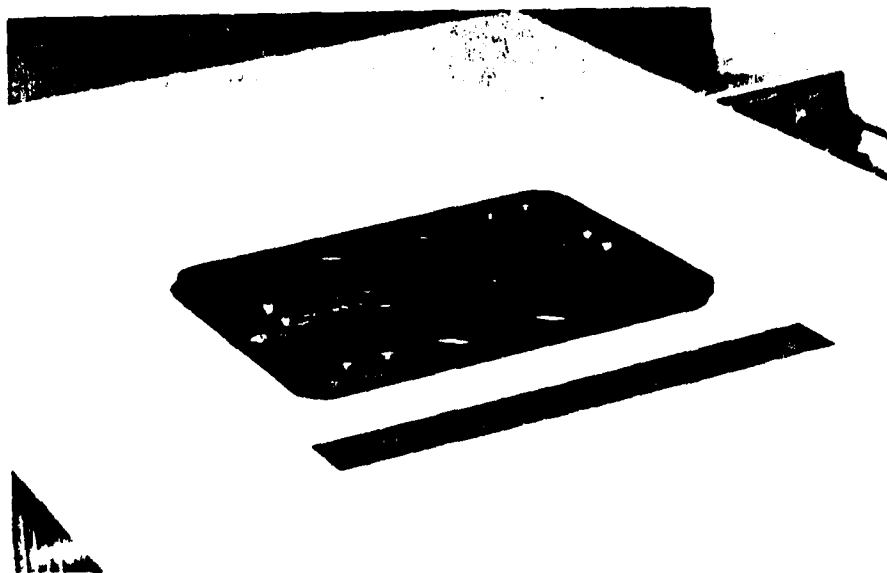


Figure 1A. Reed-Valve Compressor Plate

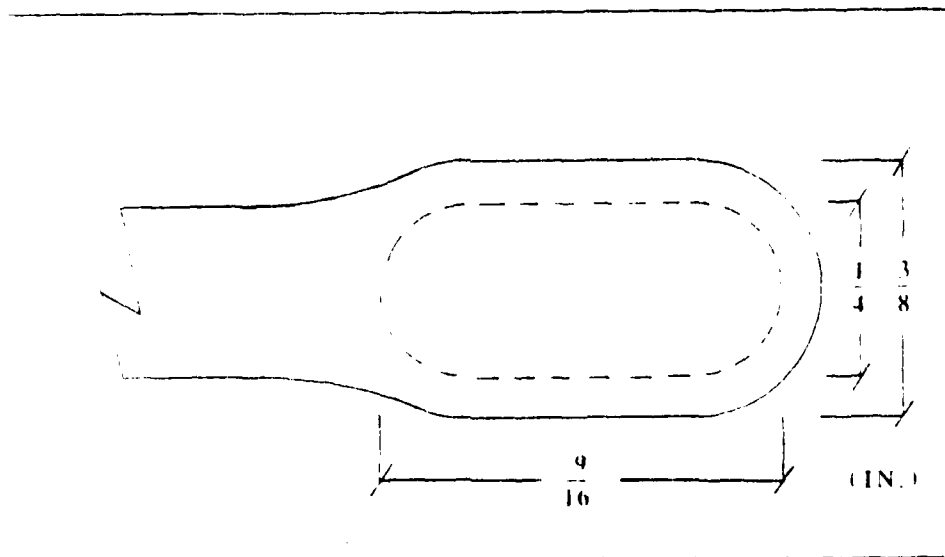


Figure 1B. Reed Valve, Typical Dimensions

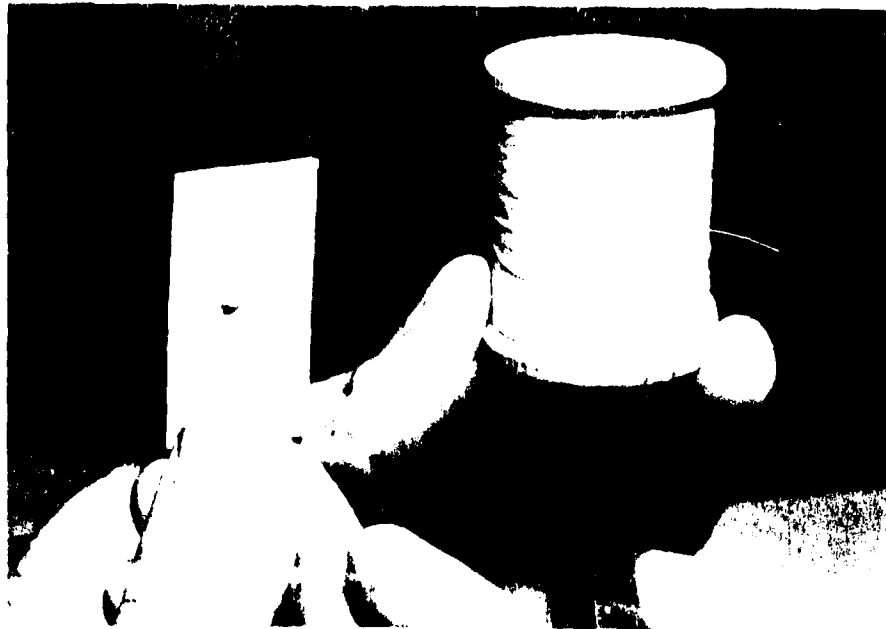


Figure 2A. Spool and Paper Valve Model

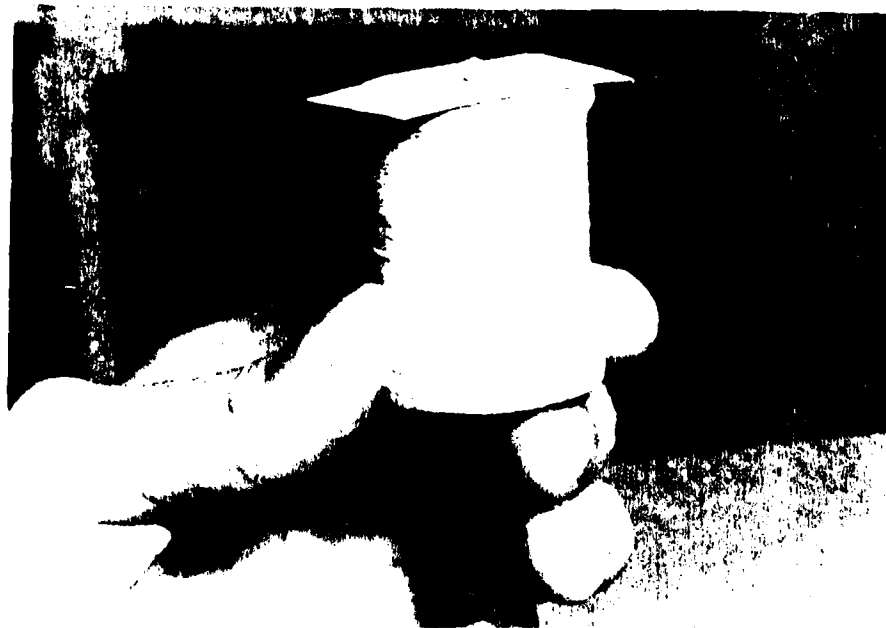


Figure 2B. Spool With Paper Valve Plate in Position

solution with results acquired experimentally. The expanded analytical solution includes subsonic and supersonic theory with the possibility of normal shocks imbedded in the flow. The analytical solution of the problem is specifically tailored to be performed on a small computer system. To experimentally validate the analytical solution, a test rig needed to be designed and operated over a range of conditions for various geometries of reed-valve plates. Pressure measurements were taken for the various geometries and compared with the analytical solution.

II. Theory

Radial Flow Problem

By studying the geometry of the spool trick, solution techniques can be developed. From an abstract point of view, there is little or no difference between the physics of the spool trick and the reed-valve problem at hand. The two problems will be treated here as the same. Figure 3 details the problem in a cross-sectional view. The geometry of the problem prescribes a flow issuing from a circular inlet. The flow then proceeds radially between the base plate of the apparatus and a free-floating circular valve plate. Although in general the results may be applied to any compressible fluid, it will be assumed that air is the fluid which is passing through the valve.

The air enters this idealized reed valve from a relatively high pressure region. This high pressure region can originate from the action of a piston, as in the compressor, a high pressure source, or even from the pressure exerted by the operator of the spool trick trying to blow the piece of paper off of the spool. When the air encounters the valve plate, it is turned and flows radially to the exit of the valve plate. In many situations the exit pressure will be the ambient atmospheric pressure (though this need not be the case). Although the problem at hand will be treated from a compressible point of view, a look at

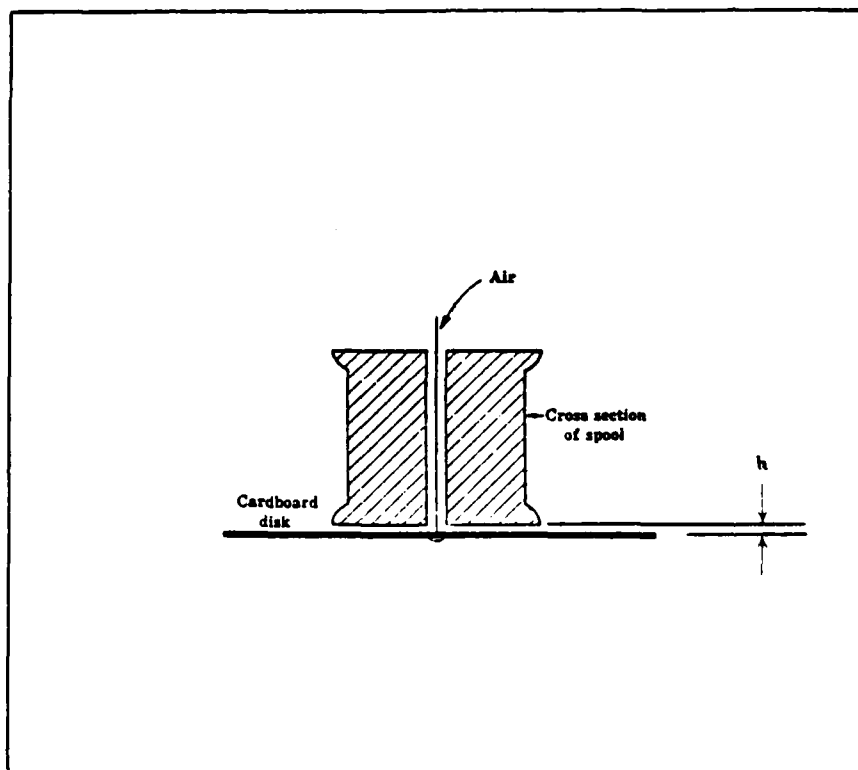


Figure 3. Cross-section of Problem

the incompressible analogue is helpful for a background understanding of the flow.

Incompressible Discussion

Figure 4 shows a section of the flow which is helpful in visualizing the problem as a whole. There are several cross-sectional areas of the flow which are of interest. The first is the area of the inlet. A section of this area is identified as I in Figure 4. The next sectional area shown is that of the annular collar around the inlet; identified as T. Finally the exit annulus is of interest; a section of which is shown as E. The areas T and E are dependent on the height (h) of the valve plate above the base plate of the apparatus. A radial flow of this type, for an incompressible fluid, is similar to a two-dimensional potential source flow (4:134). Now, with a rough idea of the geometry through which the air flows, equations for incompressible flow through a variable-area stream tube may be applied.

In the incompressible case, pressure and velocity are related by the incompressible form of Bernoulli's equation

$$P_0 = P + (1/2) \rho V^2 \quad (1)$$

where P is the pressure, ρ is the density, and V is the velocity. The subscript "0" refers to total or stagnation conditions.

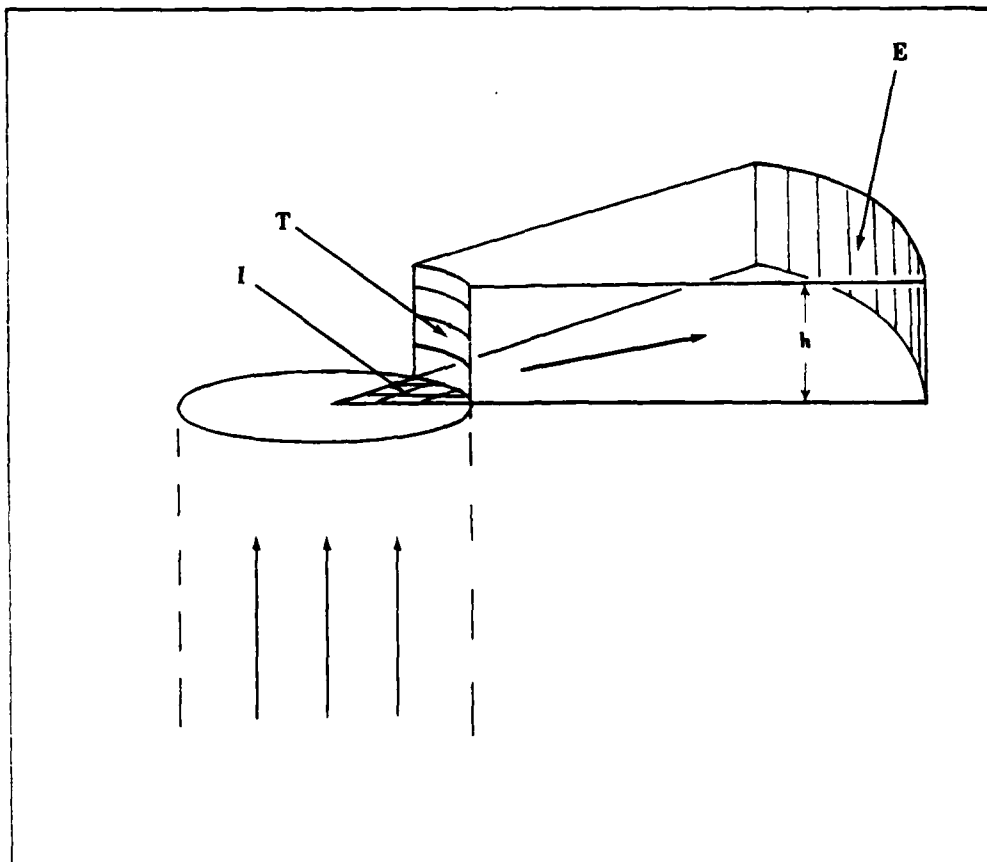


Figure 4. Sectional View of Flow Geometry

According to continuity, the mass flow rate

$$\dot{m} = \rho AV = \text{constant} \quad (2)$$

can be rearranged and differentiated to yield a relation for velocity and area in an incompressible, steady flow, so that

$$\frac{1}{V} \frac{dV}{dx} = - \frac{1}{A} \frac{dA}{dx} \quad (3)$$

This equation demonstrates that for subsonic, incompressible flow, an increase in the area of a given stream tube is accompanied with a decrease in the velocity of the fluid in the stream tube. Similarly, a decrease in area yields an increase in velocity. For the problem of the radial flow from the inlet annulus to the exit annulus, the area is increasing which indicates that the fluid velocity must decrease in the radial direction.

The radial decrease in velocity can also be identified with an increase in the static pressure. Referring back to Eq (1), a decrease in velocity for an incompressible fluid must be accompanied with an increase in static pressure for a fixed total pressure. Finally, for subsonic flow, the exit pressure must equal the ambient pressure at the exit, this being due to the ability of isentropic pressure signals to communicate upstream at the speed of sound. This communication is unavoidable because the flow is subsonic. The ambient pressure signal at the exit is able to

communicate upstream into the valve and modify the flow until the exit pressure exactly matches the pressure of the ambient environment.

The height of the valve plate above the base plate, h , is an interesting parameter of the valve problem. Because h is a factor in determining the area of the annular inlet collar (see Figure 4) it can dramatically alter the nature of the flow. If h is small, then the area of the inlet collar can be less than that of the inlet. This would effectively produce a channel area distribution which is similar to a convergent-divergent nozzle. A bit of reverse logic shows that indeed this is the only reasonable physical case to expect for a free-floating valve plate.

For a moment, let's assume that h is sufficiently large to insure that the inlet collar area (cf. Figure 4 and sectional area T) is greater than the area of the inlet. Also, assume that the flow is not allowed to separate. For flow to be in the desired direction, the inlet (reservoir) pressure must be greater than the ambient pressure, $P_{res} > P_a$. As the flow passes the inlet, the area increases and continues to increase to the exit. As shown before, this increase in the area of the flow channel is accompanied with a decrease in velocity and an increase in static pressure. This hypothetical case leads to the exit pressure being greater than the reservoir pressure or $P_e > P_{res} > P_a$. Recall however, that for a subsonic flow,

the exit pressure must equal the ambient pressure. Therefore, the exit pressure cannot be greater than that of the ambient pressure as described in this hypothetical case. This discrepancy shows that a large h is not compatible with a free floating valve plate. Since the flow will simply adjust until $P_e = P_a$, the proper sequence of pressures must be $P_{res} > P_e = P_a$. This sequence occurs when h is small enough to make the inlet collar area less than the inlet area; the inlet collar, in effect, throttles the flow in the valve.

The height of the valve plate is a function of the mass flow rate, as defined by continuity and the geometry of the inlet collar. The area of the collar is simply $A_c = 2\pi R_{inlet} h$. Combining this with Eq (2) completes a full specification of the incompressible problem.

This simplified incompressible look at the problem shows why the operator of the spool trick is unable to blow the paper off of the spool. The entire radial flow between the inlet collar and the exit collar is at a pressure below that of the ambient environment. The entire external side of the paper is acted upon by ambient pressure. This force imbalance is opposed by the force necessary to effect a momentum change in the flow to turn the corner at location T (see Figure 4) and possibly the weight of the paper. For geometries of the trick where the piece of paper is approximately the same size as the spool of thread, the

operator is physically unable to produce enough pressure to dislodge the paper. It will be shown that the flow enters the compressible regime and chokes at location T far before the force due to the momentum change can dislodge the paper.

Compressible Solution

Many of the basic features of the flow as identified in the incompressible discussion still hold. The concept of the area of the channel being similar to a convergent-divergent nozzle is valid, but the mathematical description in Eq (3) will require modification for compressible flow. With a proper pressure differential between the reservoir and the ambient environment, the flow may choke at the inlet collar and it is possible to have a supersonic section of the flow. A look at one-dimensional isentropic flow conditions shows why an increasing area accelerates the flow supersonically. The differential form of the continuity and momentum equations for one-dimensional flow is given by

$$VdV + \frac{dP}{\rho} = 0 \quad (4)$$

If we assume isentropic flow and incorporate the definition of the speed of sound, $(dP/ds)_s)^{0.5}$, and the continuity equation, Eq (4) may be manipulated (6:209-213) to yield

$$(M^2 - 1) \frac{1}{V} \frac{dV}{dx} = \frac{1}{A} \frac{dA}{dx} \quad (5)$$

Three cases must be considered.

For $M < 1$, dV/dx and dA/dx are opposite in sign. This is similar to Eq (3). Hence a subsonic flow decelerates in a diverging channel and accelerates in a converging channel.

For $M > 1$, dV/dx and dA/dx have the same sign. Hence a supersonic flow accelerates in an expanding channel and decelerates in a converging channel. Thus supersonic behavior in a channel is opposite to that of subsonic behavior.

For $M = 1$, the most appropriate consideration from physical grounds is that $dA/dx = 0$. We can conclude that the sonic condition can only occur at a constriction or throat.

Although, it may at first appear that the problem at hand is not suited to a one-dimensional analysis, the relative simplicity of the one-dimensional isentropic equations makes them attractive. Further, their use is compatible with a basic tenet of this work, to use techniques which are compatible with small computer systems. The reed-valve problem presents a geometry to the flow which is comparable to a convergent-divergent nozzle. The one-dimensional isentropic relations are applicable to a wide variety of nozzle-type problems, with reasonable results, even when the one-dimensionality of the problem is questionable. This work will use these relations and the

normal shock relations for the analytical solution to the problem, and, as will be shown, this method yields reasonably good agreement with experiment.

Numerical Solution

A computer program was written to solve the reed-valve problem. The program, SOLVE, is listed in Appendix A. SOLVE was written in BASIC and uses the assumption that the flow is steady, one-dimensional, at a minimum piece-wise isentropic and has the possibility of imbedded shocks. The flow is assumed to be air and was treated as a perfect gas. The program was run on a Columbia Data Products personal computer (IBM compatible) which has 256K RAM. SOLVE produces a solution to the reed-valve problem in approximately 60 seconds.

The analytical solution includes a number of isentropic flow parameters (7; 8:47-75). In the following discussion the "o" subscript again will refer to total or stagnation conditions for the specific parameter. Equations for the parameters of interest have been reduced to forms which require input of the total condition of the parameter and the local Mach number. A function of the local Mach number is a common factor to many of these calculations and is given by

$$FNBOB(M) = [1 + (\gamma - 1)M^2 / 2] \quad (6)$$

This function of Mach number was then used to determine the following properties:

Pressure was obtained by

$$P = \frac{P_0}{\left[\text{FNBOB}(M) \right]^{\gamma/(\gamma-1)}} \quad (7)$$

Density was found by applying

$$\rho = \frac{\rho_0}{\left[\text{FNBOB}(M) \right]^{1/(\gamma-1)}} \quad (8)$$

The local temperature was found using

$$T = \frac{T_0}{\text{FNBOB}(M)} \quad (9)$$

Also, using the total temperature, it was convenient to define a total sonic velocity

$$c_0 = (\gamma R T_0)^{1/2} \quad (10)$$

So that the local sonic velocity could be found using

$$c = \frac{c_0}{\left[\text{FNBOB}(M) \right]^{1/2}} \quad (11)$$

The local velocity of the flow was now found by

$$V = cM \quad (12)$$

In order to find the Mach number at each location of interest two equations relating the Mach number to the pressures and Mach number to area ratios were required. First, for an isentropic flow, the Mach number at the exit could be found by knowing the pressure ratio between the total pressure and the exit pressure. The relation is

$$M_e = \left[\frac{2}{\gamma-1} \left[\left[P_o / P_e \right]^{[(\gamma-1)/\gamma]} - 1 \right] \right]^{1/2} \quad (13)$$

Once the exit Mach number was known, the Mach number at any other location could be determined from

$$M_i = \left[\frac{R_e M_e}{R_i} \right] \left[\frac{FNBOB(M_e)}{FNBOB(M_i)} \right]^{(1/2)-[\gamma/(\gamma-1)]} \quad (14)$$

It is important to note that while the radius ratio is used in the preceeding equation; the usual ratio is that of the area ratios. For the circular reed-valve model, the radii ratio is identically the area ratio from the inlet collar to the exit collar. Recall that the area of the inlet collar is $A_c = 2\pi R_{inlet} h$ and the area of the exit collar is $A_e = 2\pi R_e h$. The common factor of $2\pi h$ cancels from the ratio of the two areas. It is emphasized here that this problem is, therefore, fully specified from this theoretical point of view without the variable h entering the problem.

If a shock occurs in the flow, several parameters undergo a change which was modeled by a jump discontinuity. The circular geometry of the reed valve model and the radial nature of the flow through the valve suggest that any shock in the flow will be normal to the flow. Although the shock will be circular when viewed from above, the flow sees a simple normal shock, thus the normal shock relations are appropriate for this case.

The subscripts "i" and "v" denote the upstream and downstream values, respectively, of a parameter across the shock. If the upstream Mach number is known, the downstream Mach number is given by

$$M_v = \left[\frac{2\gamma M_i^2 + 2}{2\gamma M_i^2 - (\gamma - 1)} \right]^{1/2} \quad (15)$$

The total pressure decreases across the normal shock. Total pressure is the parameter which is used in SOLVE to track the changes in the other parameters after the shock. Static pressure in particular is of interest because the flow after the normal shock will be subsonic and therefore the static pressure at the exit must match the ambient pressure. This was the parameter to be matched when determining the location of the shock. The total pressure on the downstream side of the shock is given by

$$P_{v0} = \left[\frac{(\gamma+1)M_x^2/2}{FNBOB(M_x)} \right]^{\gamma/(\gamma-1)} \left[\frac{\gamma+1}{2M_x^2 - (\gamma-1)} \right]^{1/(\gamma-1)} \quad (16)$$

With the background of the specific equations in place, a discussion of the logic of SOLVE follows. An overview of the entire program is given, followed by additional overviews of specifics of the subsonic and the supersonic solution techniques.

Figure 5 is a flow chart of SOLVE. Unless otherwise specified the program defaults to standard day conditions for temperature and pressure. The inlet radius for the valve is also set to default to the value of the actual reed-valve model tested. An alternate input section is interactively available to the user to allow specific inputs to match a specific problem. The default option is useful for a general understanding of a preliminary problem; however, it is important to use the alternate input section if one wishes to compare theoretical values with experimental data. Next, following the input section, SOLVE sets the definitions of various parameters, discretizes the radial domain of the flow field, and determines the nature of the problem.

Depending on the ratio of reservoir pressure to the exit (ambient) pressure the nature of the problem can be subsonic, supersonic with imbedded shocks, or fully

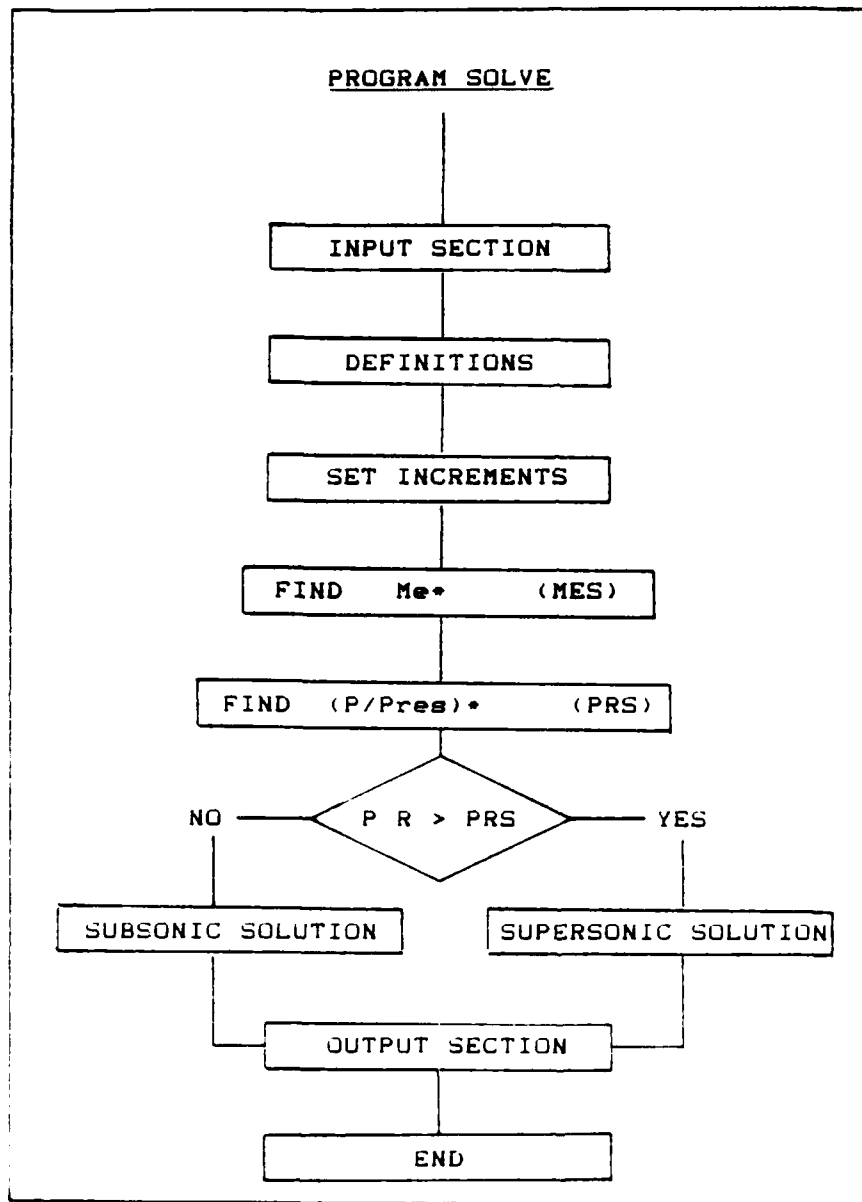


Figure 5. Flow Chart of Program SOLVE

supersonic. The main distinction which SOLVE is concerned with is whether the problem will require a subsonic or a supersonic solution technique. The program uses Eq (14) and a fixed point iteration scheme (9:88-95) to find the Mach number at the exit for the case where the flow is exactly sonic at the throat (inlet collar) but subsonic elsewhere. This condition will be referred to as the star condition for the problem. The flow is isentropic throughout the field for this case. Knowing the exit Mach number for the star condition the pressure ratio for the star condition can be found using Eq (7). By comparing the pressure ratio of the problem with the star condition pressure ratio, the nature of the problem is established. Following the appropriate solution technique, SOLVE outputs the data to the screen for viewing and will save pressure or pressure ratio data to a disk file. The files are formatted for easy use with graphics software.

If the specified pressure ratio is less than the pressure ratio for the star condition, the problem will be entirely subsonic. A flow chart of the subsonic solution is presented in Figure 6. Here the exit Mach number is found using Eq (13). The Mach numbers at the incremental locations are then found using Eq (14) and fixed point iteration. Finally, the remainder of the properties at the incremental locations are found using Eqs (7-12). The

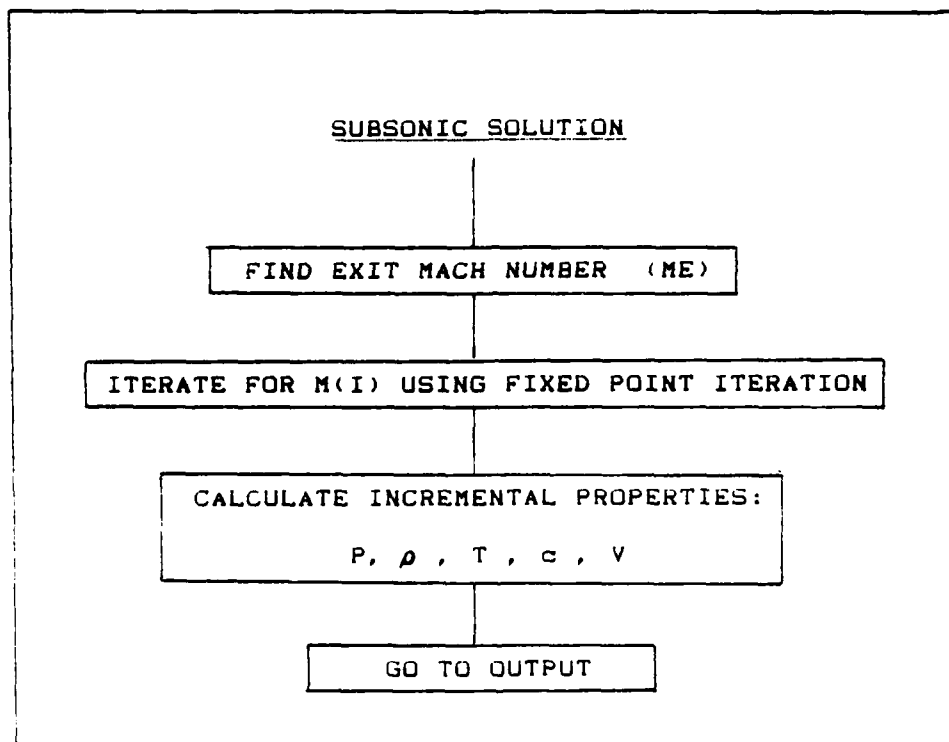


Figure 6. Flow Chart of Subsonic Solution

program branches to the output section with the subsonic description of the flow.

If the flow is supersonic in nature, the program assumes that the flow also has an imbedded normal shock. Schreier (8:75) gives a trial-and-error method for solving this problem. Some of his procedure has been modified to make it more applicable to a computer program and the reed-valve problem. A flow chart of the supersonic solution is shown in Figure 7. The steps used in SOLVE are:

1. Postulate an upstream Mach number for fixed shock.
2. Calculate the radius ratio using Eq (14).
3. Find the downstream Mach number using Eq (15).
4. Find the downstream total pressure using Eq (16).
5. Find the exit Mach number using Eq (13).
6. Find the exit pressure using Eq (7).
7. Compare this pressure with the ambient or back pressure. If they are equal to within a prescribed tolerance the shock is in the desired location. Otherwise, the process is repeated by changing the position of the shock. This is done by postulating a new upstream Mach number.

A marching technique is used to place the shock in the proper location. After the initial location is evaluated, the program takes a step increase or decrease in the upstream Mach number and re-evaluates the problem. This is repeated, stepping in the same direction, until it has

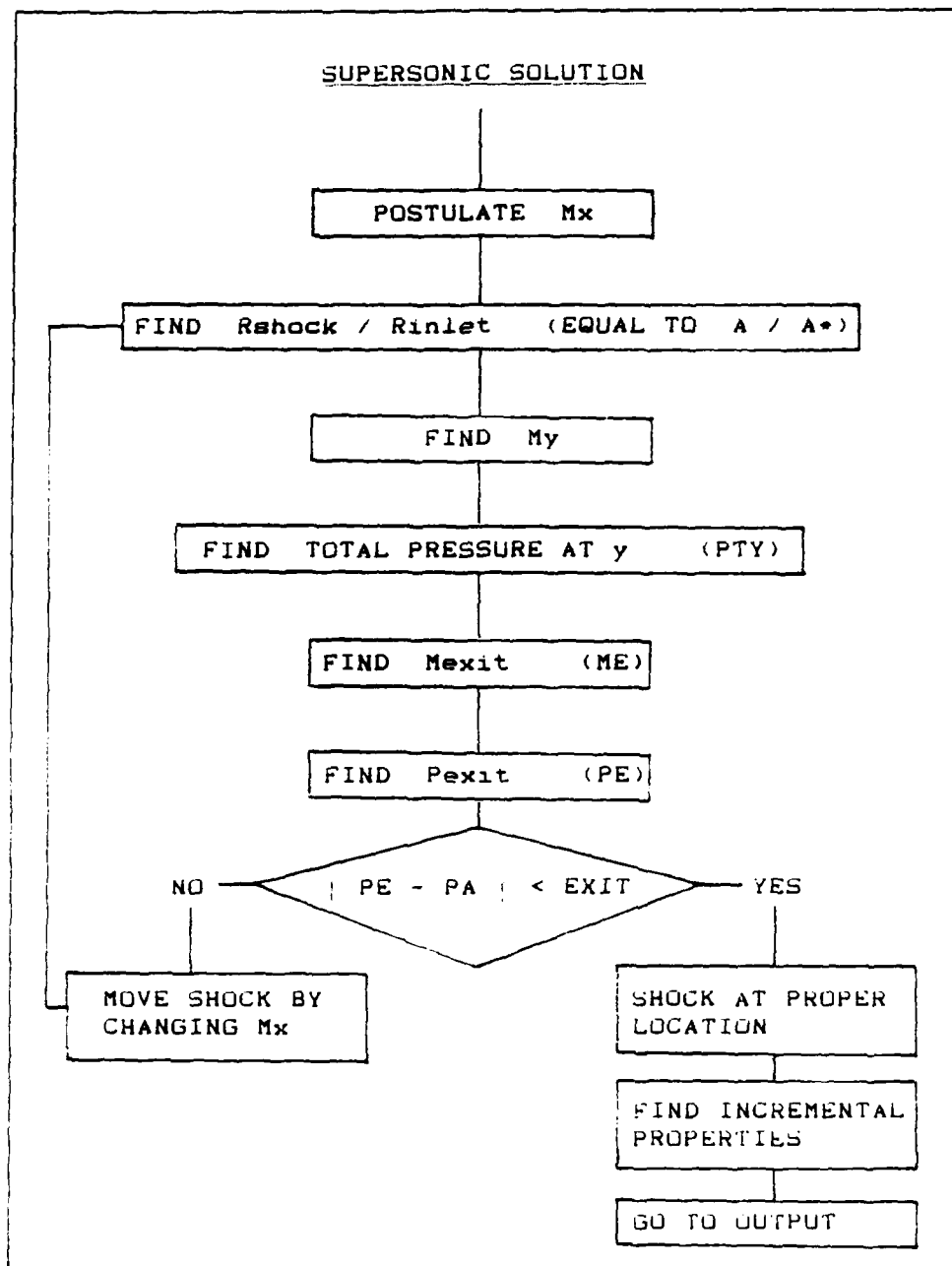


Figure 7. Flow Chart of Supersonic Solution

overstepped the solution. At that time the march changes direction and cuts the size of the step in half. The march continues in the new direction until the solution is again overstepped. This whole process continues until the exit pressure matches the prescribed back pressure to within a specified tolerance. This marching technique is also used to determine the Mach number at specified area ratios for the supersonic portion of the flow field because the fixed point iteration scheme does not converge to the supersonic value of Mach number. Once the shock has been determined to be in the proper location, the program delivers the incremental properties to the output section.

A collection of theoretical pressure ratio versus the radial location data from SOLVE is plotted in Figure 8. Figure 8 includes a subsonic curve, a nearly star condition curve, and several supersonic curves with imbedded shocks. One feature to keep in mind about Figure 8 is that the isentropic preshock portions of the supersonic curves lay on top of each other up to the point where they shock. This will be a pattern to be looking for when viewing the experimental data. The theoretical curves presented here are similar to those in texts describing the flow in a Laval nozzle (6:211-213, 242; 10:127-130) because the geometry of the flow in the reed valve is similar to a convergent-

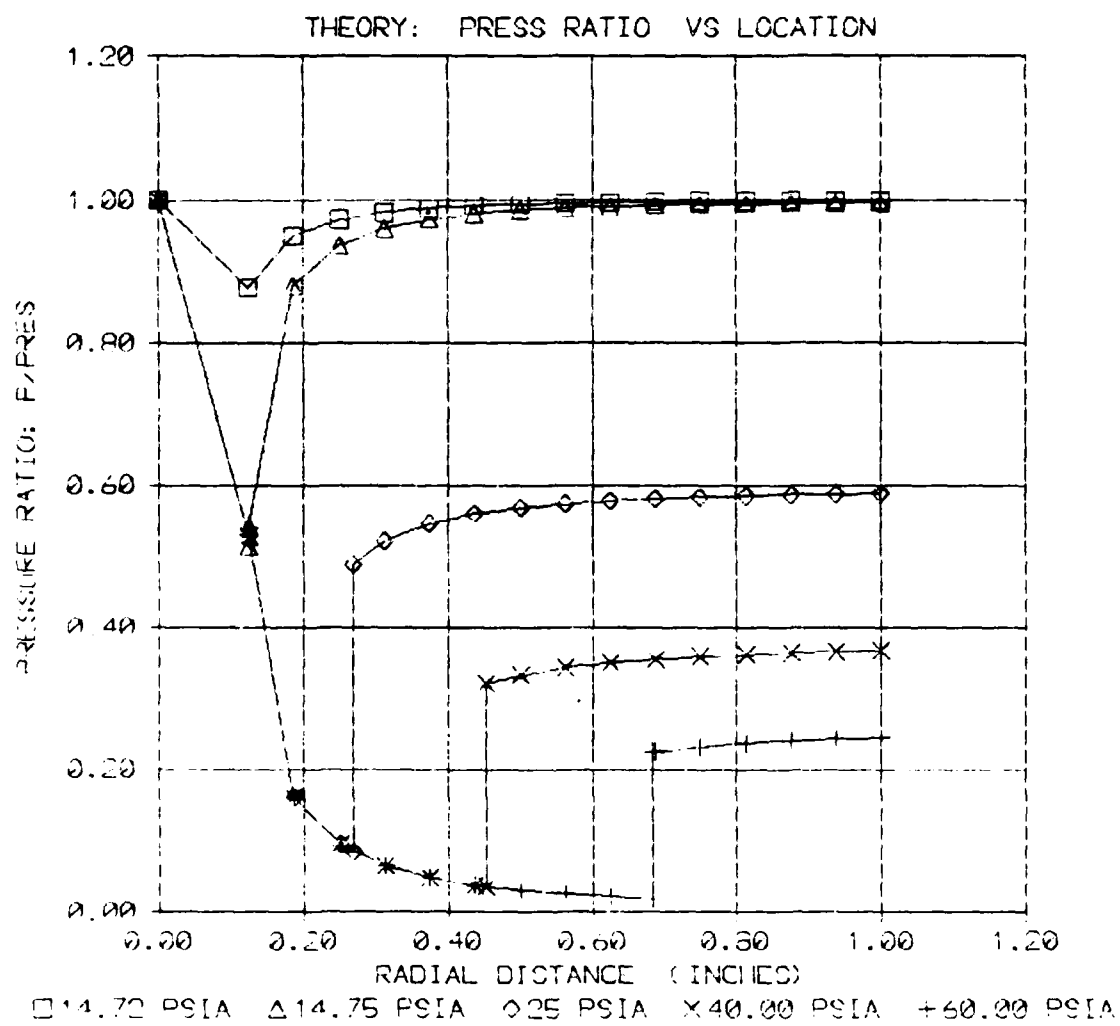


Figure B. Pressure Ratio vs. Location From Analytical Solution

divergent nozzle. It should be noted, however, that the convergence in the reed-valve problem is a very sharp decrease, basically a step, and the divergent section has a rapidly increasing area. An equivalent two-dimensional nozzle would have a divergence half angle, δ , of approximately 72.3 degrees ($\tan \delta = \pi$). For a circular duct nozzle, the applicable divergence half angle relationship is $\tan \delta = (2h/R_1)^{0.5}$. It is emphasized here that the reed-valve geometry does not match either the two-dimensional or three-dimensional equivalent nozzle, but a comparison with these "standard" nozzles is interesting.

Other Theoretical Considerations

It is interesting to look at what range of pressure ratios that cause the reed-valve or the spool problem to change from a subsonic nature to a supersonic problem. Assume an inlet, circular in cross section, with a radius of 1/8-inch and a reed-valve plate (or piece of paper) with a radius of 1-inch (representative of the spool trick). By using SOLVE, it can be seen that the problem changes character at a pressure approximately 0.055 psi above ambient (standard day assumed). This seems incredibly low and means that for inlet pressures greater than this, the flow will have a supersonic section with an imbedded shock. When performing the spool trick, an average adult can maintain a pressure on the order of 1 to 2 psi. Obviously,

even the spool trick must be treated as a compressible supersonic problem.

A more formal presentation of what pressure ratios are required to theoretically produce a supersonic problem is given in Figure 9. An example here is also instructive. For a radius ratio of 0.8 and the exit pressure at ambient, the valve would have sonic flow at the throat for a gauge pressure of approximately 3.6-psig. This example corresponds to a valve plate with a radius of 0.344-inches for an inlet of radius of 0.281-inches. The overlapping lip of the valve plate over the inlet hole then is 0.063-inches. This amount of overlapping for a valve lip, about 1/16 inch, is representative of the order of the measurements for an actual reed-valve configuration (see Figure 1).

Although the theoretical treatment of the reed-valve problem is inviscid, boundary layers should be expected to be present in the valve. When the air initially impinges on the valve plate a stagnation or Hiemenz flow (11:95-99) is likely. Further into the channel boundary layer growth for a divergent channel could be expected (11:106,223). The boundary layer will have a displacement thickness which should have an effect on the experimental results. The height of the valve plate above the base plate, if constant, is not a required parameter in the theoretical solution of the reed-valve problem; however, boundary-layer growth could

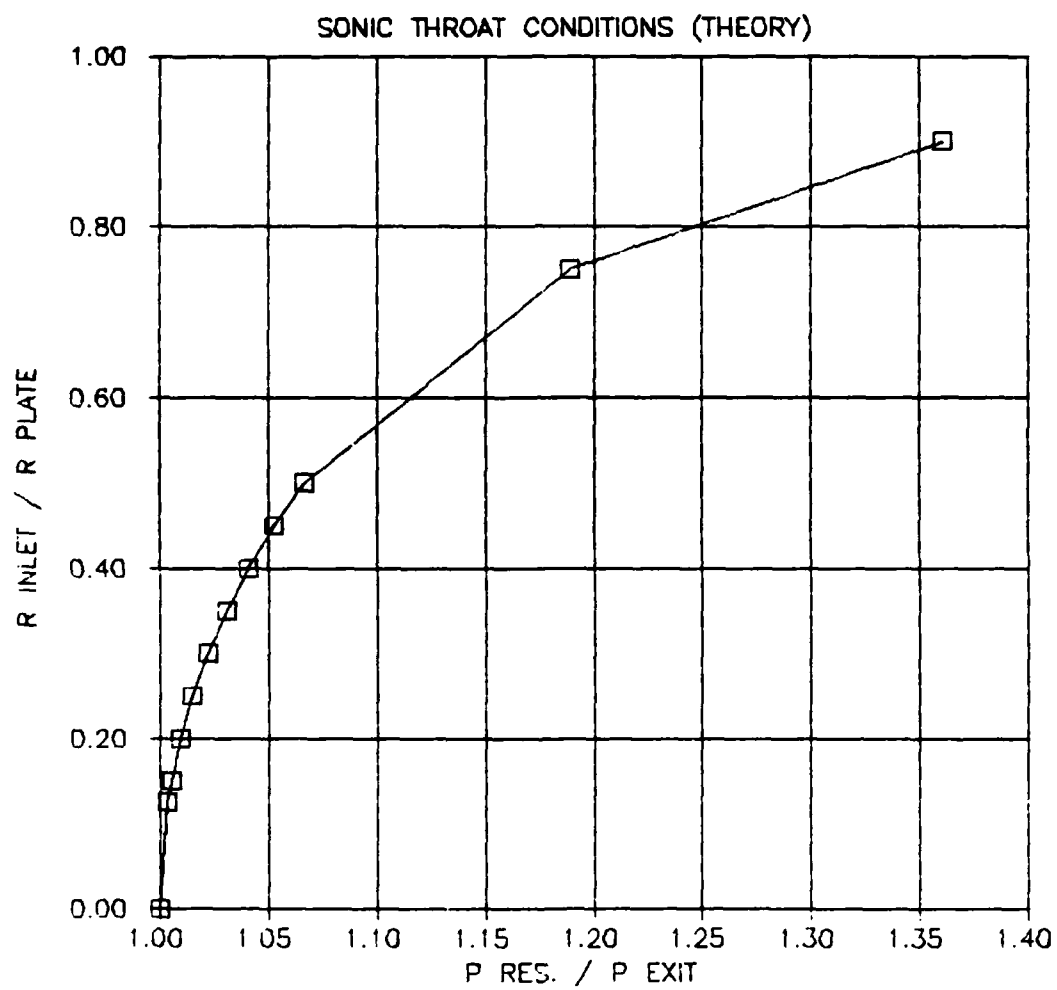


Figure 9. Radius Ratio vs. Pressure Ratio From Analytical Solution

change the effective channel height from a constant to a variable. For an increasing displacement thickness, the area of the channel would not grow as rapidly in the viscous case as in the theoretical case. One might assume, then, that the pressure ratios at a specific location would have a value corresponding to a smaller area ratio. One would also expect other considerations, such as separation of the flow, to effect the solution.

III. Apparatus and Instrumentation

General

Room 141, building 640 was the site of the experimental thesis work. The room has the necessary air supply and electrical power required for the work.

Figures 10A and 10B show the layout of the experimental work area. The majority of the test equipment fit neatly on a single table. A schematic depiction of the test set-up is given in Figure 11.

The heart of the experimental data gathering was a pressure transducer which is manufactured by Scanivalve Corporation of San Diego, CA. The transducer and the special sampler in which it is housed will be referred to simply as the scanivalve for this report. The scanivalve allowed rapid measurement of data from multiple pressure taps while using a single transducer.

The operation of the scanivalve was controlled by a computer. The computer commanded the scanivalve through a solenoid controller and scanivalve position was monitored by an odd-even decoder. The solenoid controller and the odd-even decoder are also products of Scanivalve Corporation. Power for the pressure transducer was provided by a separate power supply. The power supply output was monitored by a multimeter.

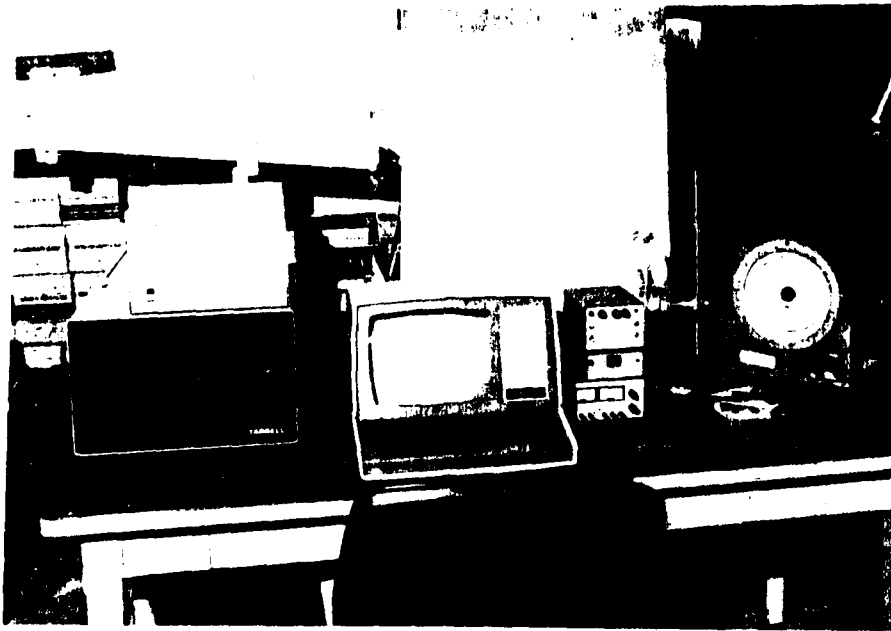


Figure 10A. Experimental Work Area, Front View

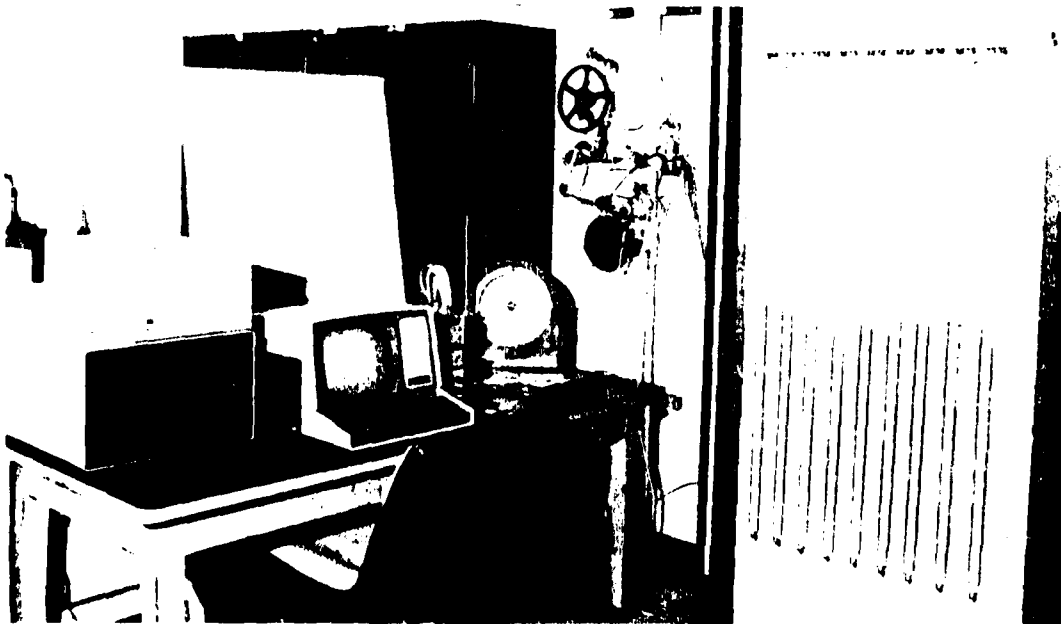


Figure 10B. Experimental Work Area, Oblique View

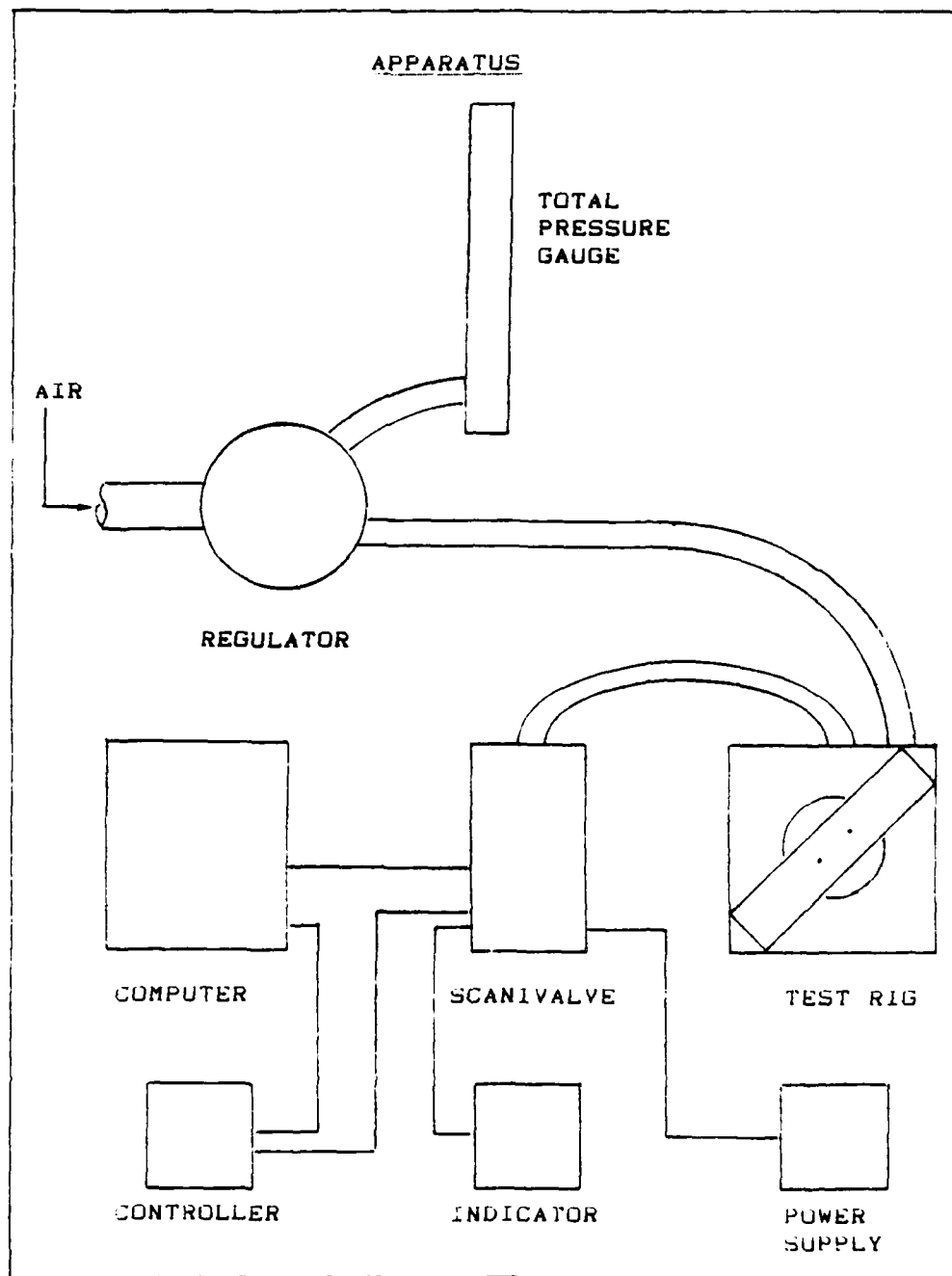


Figure 11. Schematic of Work Apparatus

The air which flowed to the test rig was metered through a regulator. Two air sources were available for the testing. The first was the building air supply and the second was bottled air. The building air was used for data runs up to about 80 psig, bottled air was used for higher pressures. The total pressure of the reservoir which supplied the air was measured on either a 100-inch mercury manometer or a 200-inch bourdon-type pressure gauge. A complete listing of the equipment used in the experimentation is presented in Appendix B.

Test Rig

The test rig used for the experimental investigation is shown in Figure 12A and 12B. As stated earlier, the design of the test rig followed from considering the reed valve (Figure 1) and the spool trick (Figure 2). The similarity of the spool trick and the test rig is again easily seen. Each provide a channel for the flow which expands radially outward. The channel is constrained by a floating valve plate above and the fixed base plate below. Due to the test rig being more adaptable to being connected to a high pressure reservoir, no formal measurements were taken using the spool of thread.

The test rig was fabricated by ARIT model shop personnel from aluminum stock. The 1/4-inch diameter inlet hole was centered in the base plate. Forty surface pressure

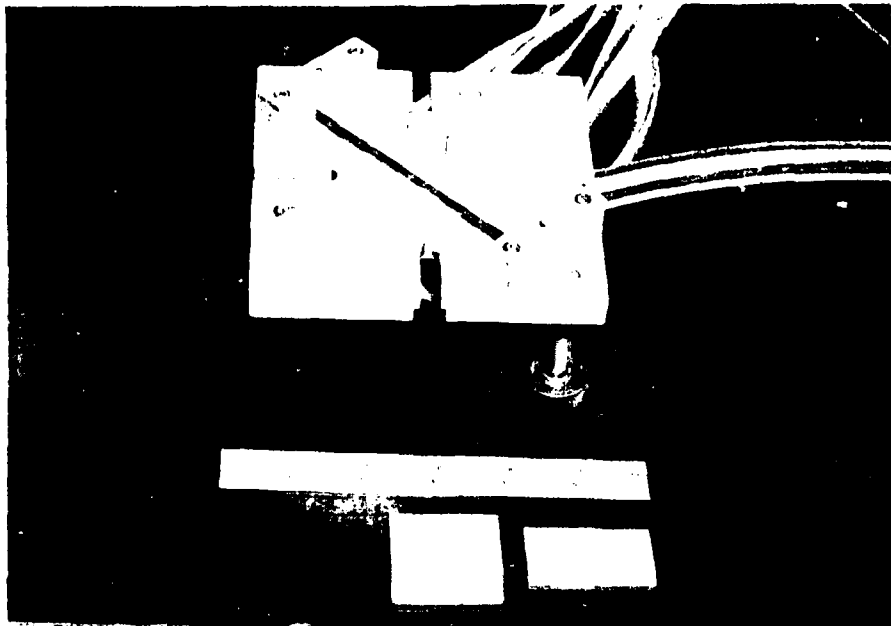


Figure 12A. Test Rig, Overhead View Showing Centering System, Pins, and Valve Plate

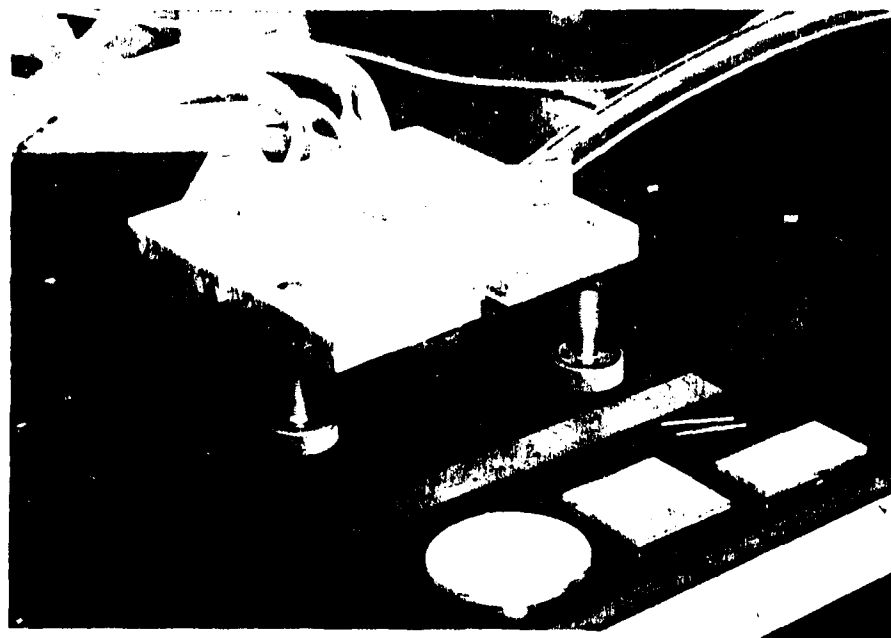


Figure 12B. Test Rig, Oblique View

taps were located in sets of five along eight radial arms. An overhead view of the inlet and the taps is shown in figure 13A. The surface pressure taps are 0.050-inch in diameter and located at 3/16-inch intervals from 3/16-inch to 15/16-inch radially from the center of the inlet. The bottom of the test rig is shown in Figure 13B.

Several disks were fabricated to serve as valve plates. Data were evaluated for three of the plates. The first plate was circular with a diameter of 2-inches. The second plate was square with dimensions of 1.5-inches on a side. Finally, the third plate to be evaluated was a 1-inch by 1.75-inch rectangle. The valve plates are also shown in Figure 13A.

Although the height of the valve plate above the base plate was self adjusting, the system need not be self centering. To keep the plate centered over the inlet, a technique using centering pins was developed. The pins set in recessed holes in the valve plates. The pins did not perforate the valve plates. The pins were free to rise up and down through holes in a cover plate which was rigidly fixed above the free floating valve plate. These components of the test rig can be seen in Figure 12A.

Scanivalve Operation

A 48-port Model 3 Scanivalve with a PCB-130-10P10 Scanivalve Corporation pressure transducer (figure 14) was

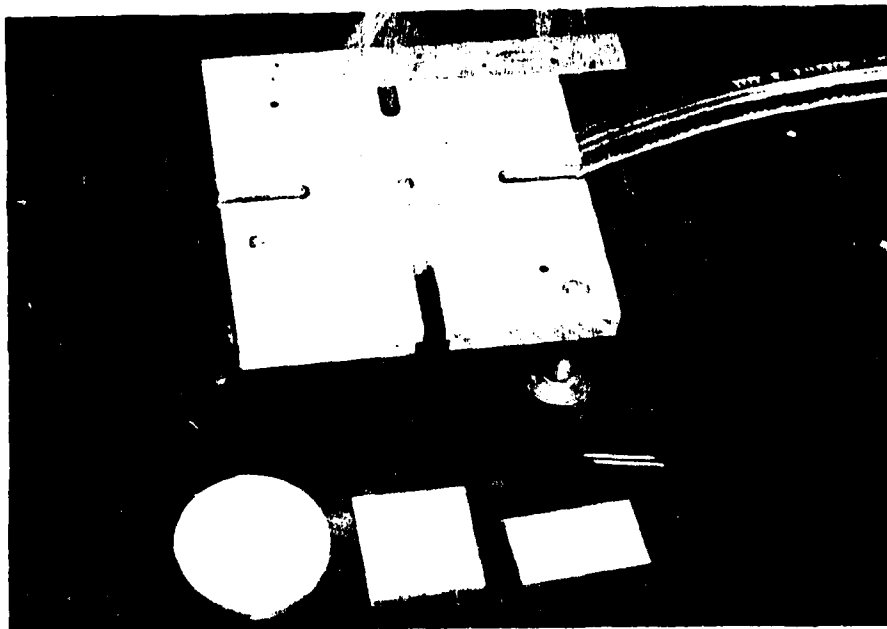


Figure 13A. Test Rig With Out Cover Plate, Showing Radial Arm Pattern of Pressure Taps

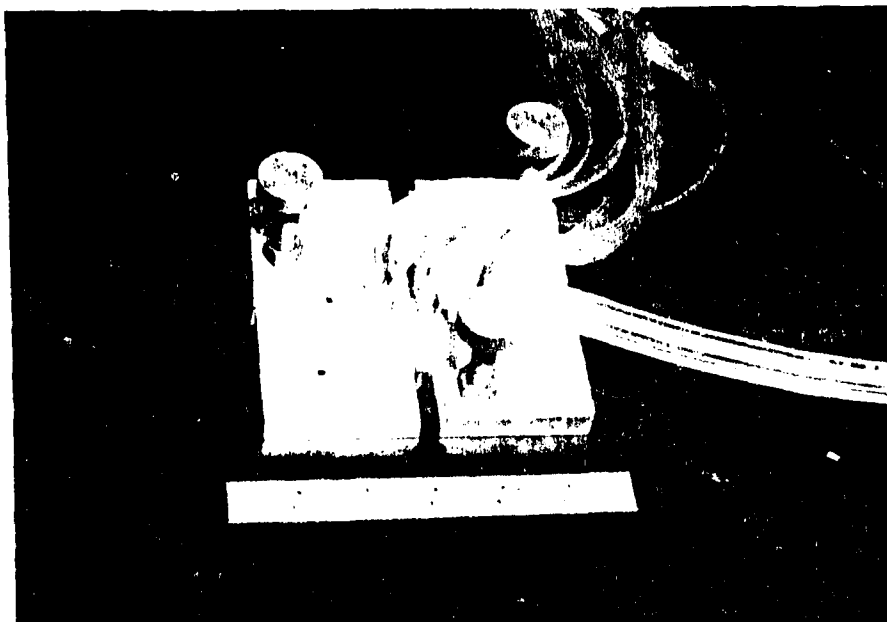


Figure 13B. Test Rig, Bottom View

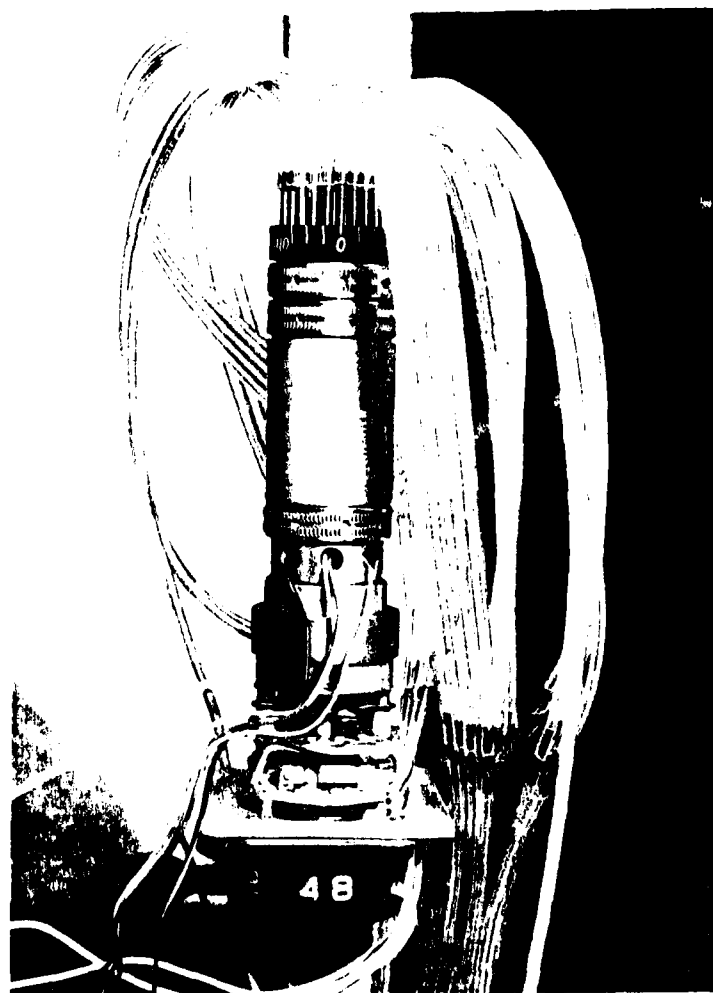


Figure 14. Scanivalve

used to gather the pressure data from the needle-valve model. The transducer had an operating pressure range of 25-psi and was configured to work by referencing differential pressure measurements. The transducer was a piezoresistive type employing an internal, four arm Wheatstone bridge. The bridge excitation voltage for the transducer was 10.00 volts.

Output from the transducer was directed to an Electronic Control Technology, Inc. (ECT) 8-bit-based computer. This input to the computer was digitized through a Dual Systems Control model AIM12 analog-to-digital card in the computer. An offset option on the card was set to midscale and the amplification was set so that signals from ± 20.0 -millivolts to ± 20.0 -millivolts could be read to one part in 4096. This provided a resolution of 0.0147 millivolts. Shielded cables were used to reduce the introduction of noise to the system. Also, the scanivalve sampled at a rate that allowed multiple samplings of the same port to get an average pressure reading. This averaging nearly eliminated any noticeable noise. A single port was usually sampled 20 times for the averaging. This technique worked well, and required less than one second per pressure tap. The 25-psi transducer was chosen in order to match the specific range of pressures which were encountered in the flow in the valve. Total pressure readings for several of the test conditions were too high for the

transducer. Total pressure readings were therefore made using other pressure gauges.

Once a pressure had been sampled, the scanivalve needed to be stepped. An electric stepper motor was attached directly to the scanivalve. This motor was directed by a solenoid controller. The controller issued the step command when it recieved a 5-volt signal from the computer. The 5-volt signal was produced with a Dual Systems Control model ADM-12 digital-to-analog card in the computer by using software commands.

The computer allowed the whole data gathering operation to be controlled through interactive software commands. The BASIC program for the operation of the data collection was named TEST, and is listed in Appendix C. TEST gives the operator the option to save the data to a disk file. The disk drives used with the computer were two Carbell 8-inch single-sided single-density disk drives.

In order to make the data accessible to programs operating on the author's personal computer, it was necessary to transfer files from the 8-inch disks, which were in DSK format, to 5 1/4-inch double-sided double-density format disks. This was made possible by the disk transfer system which is located in room 212, Bldg. 640.

IV. Calibration and Test Procedure

Calibration

One advantage to using the scanivalve for testing was that only one transducer was used for collecting the pressure data. Therefore, the calibration procedure was to compare the transducer signal against known pressures. From this comparison, a calibration curve (a plot of voltage versus pressure) was produced. The pressures for the calibration were measured with a 100-inch mercury manometer. This was the same manometer which was used to measure the total pressure of the reservoir. A pressure tap ran from this total pressure line to the scanivalve. This tap was used exclusively for calibration and was normally disconnected or closed during data runs to insure that the transducer was not inadvertently overpressurized. The computer and entire test station were in a ready-for-testing configuration during the calibration. The calibration curve for the scanivalve transducer is shown in Figure 15.

Once calibrated, it was a straight-forward procedure to measure a voltage corresponding to an unknown pressure. The unknown pressure was then found by computing the pressure which matched with the measured voltage. The calibration curve of the scanivalve transducer exhibited linearity to within 0.42 percent of full scale over the range of pressures of interest.

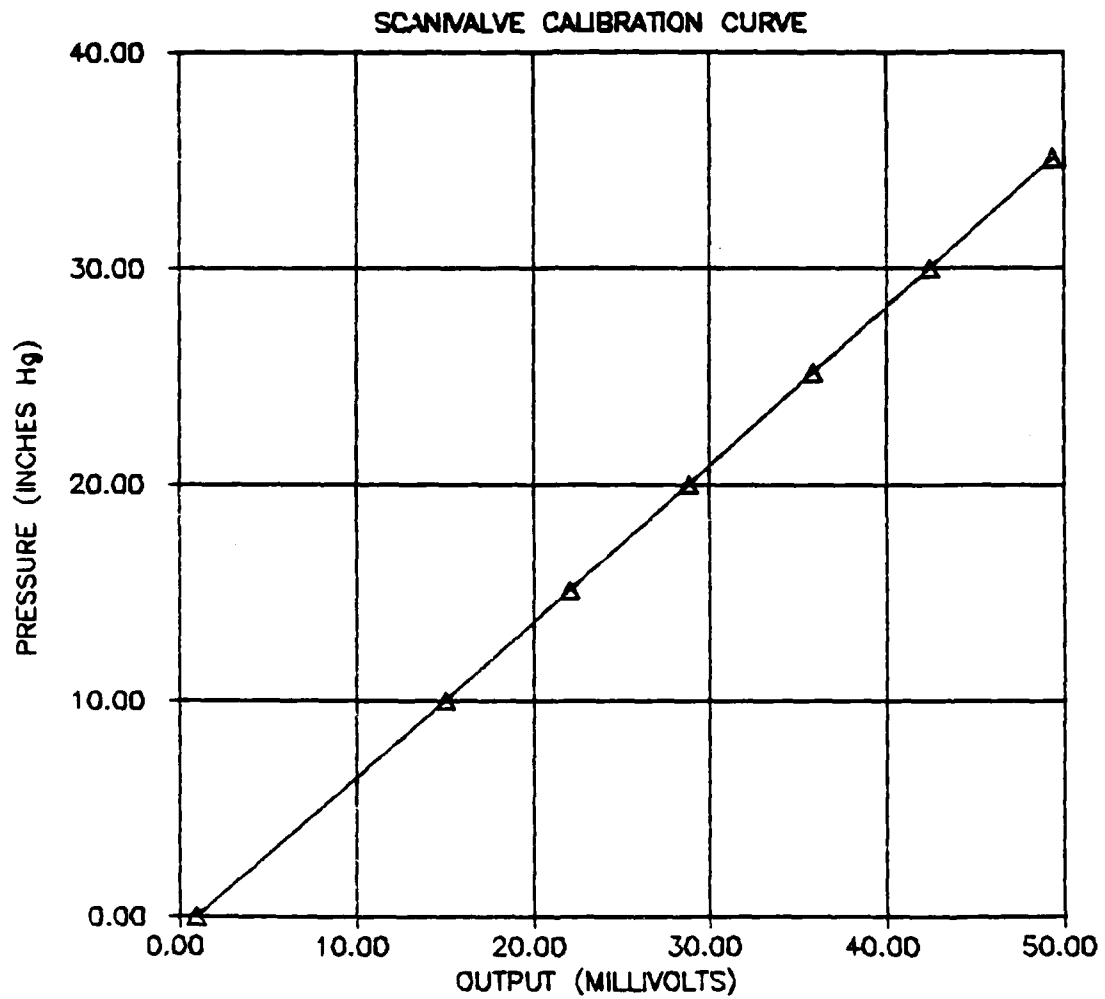


Figure 15. Pressure Transducer Calibration Curve

Test Procedure

A computer program, TEST, was written to direct the acquisition of the pressure measurements in the reed-valve model. The actual test procedure was straight forward. The equipment was turned on and allowed to warm up and stabilized for approximately 15 minutes. During the warm-up period barometric pressure and ambient temperature readings were made. After warming up, the bridge excitation voltage, which was sent from the power supply to the scanivalve, was checked and adjusted as necessary. A calibration run for the transducer was accomplished next. This calibration was done for each set of tests, but it is noted here that there was no measurable difference in the calibration curve over the entire duration of the testing. Once the calibration was checked, the testing was ready to procede.

The configuration to be tested was selected and set up on the test rig. The inlet pressure was set by adjusting the regulator on the inlet line. The system was again allowed to stabilize. While stabilizing, the program TEST was started with a run command. TEST interactively requested the test condition and then awaited a command to commence gathering data. When the system had stabilized the operator input a line feed (return) command and TEST directed the gathering of the data. The data runs lasted approximately 30 seconds. During the data run, all 40 surface pressure ports were sampled. Each port was

individually sampled 20 times before the scanivalve was stepped to the next port. The value of the reading for each port measurement was the average of the multiple sampling. Upon completion of the data run, TEST could be made to save the data to a disk file.

This procedure of testing continued until the operator was finished with the desired runs for the day. Finally, the barometric pressure and temperature were again measured.

Flow Visualization

In order to obtain a more specific idea of the shock location and shape, a flow visualization technique was devised. Wind tunnel flow visualization oil was used. Due to the oil mixture containing white pigment, the test rig was painted black to insure better contrast for photography. The oil was dotted on the base plate of the test rig as shown in Figure 16A. In order to keep the oil undisturbed (except by the flow) the tests were run with the rig up-side down as shown in Figure 16B. This required a slightly different configuration for the test rig. The legs were reversed in their holes and knife edge supports replaced the centering pins (cf. Figures 12 and 16C). After the oil was in place the rig was inverted and the air was turned on at a moderate rate. The valve plate was then raised slowly toward the inlet. Recall, that the problem is self adjusting for the height of the valve plate, so once the plate is close, the physics of the problem takes over and

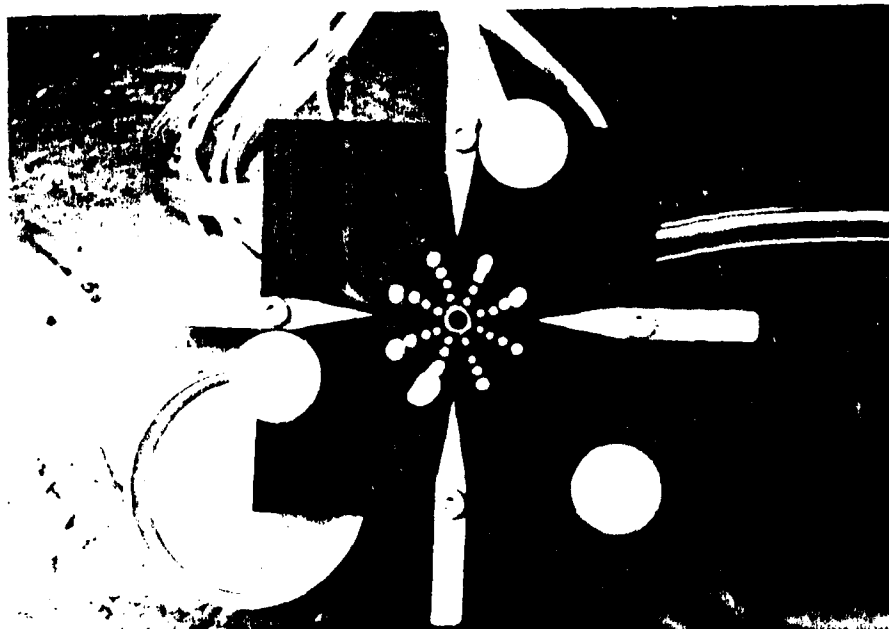


Figure 16A. Test Rig Showing Oil Drops for Flow Visualization

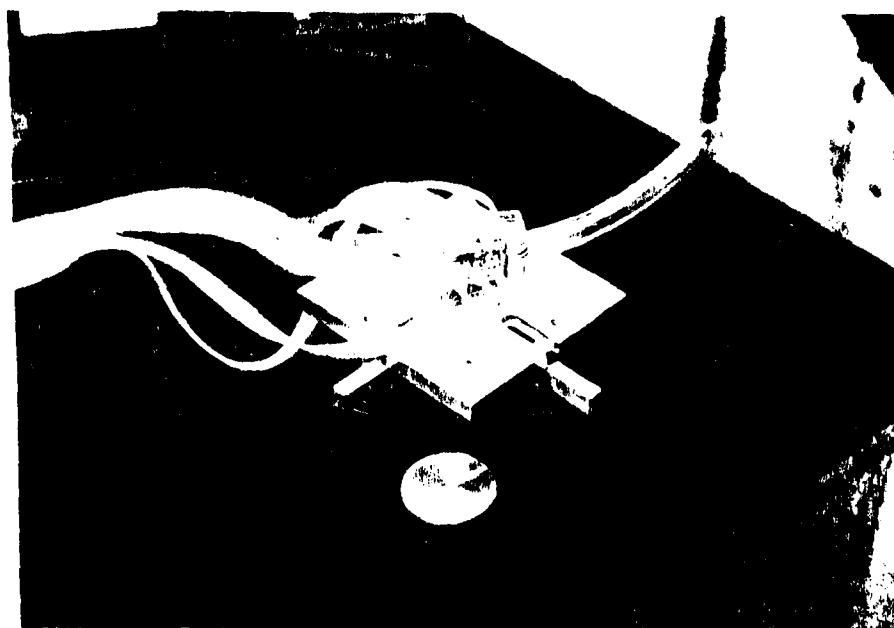


Figure 16B. Test Rig in Inverted Configuration. Note the Reversed Legs

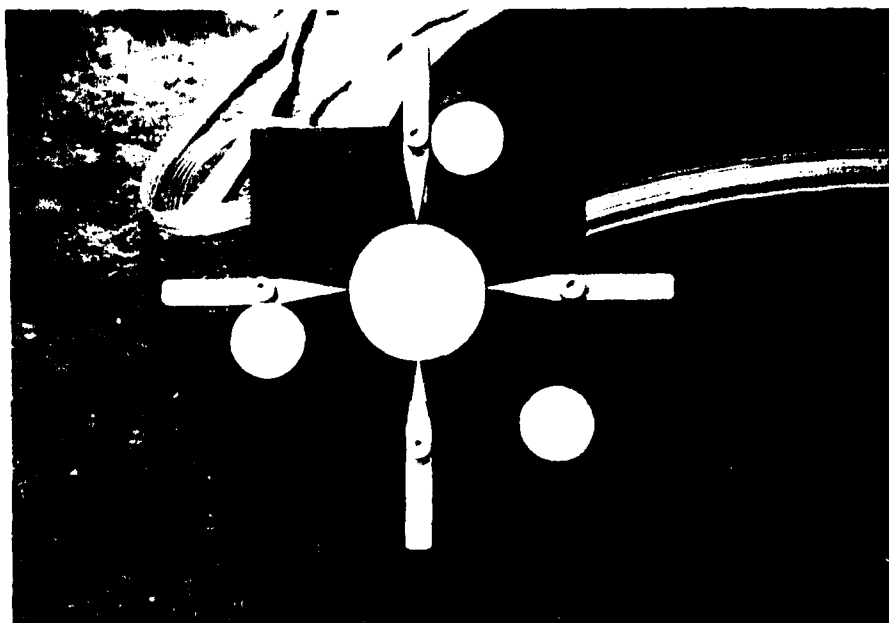


Figure 16C. Test Rig Showing Knife Edge Technique for Centering the Valve Plate

snatches the plate. After the valve plate is captured by the test rig, the reservoir pressure was adjusted to the test condition. The test pressure was maintained for approximately 20-seconds. The air supply was then cut off and the valve plate fell to the table, leaving the oil flow undisturbed. The rig was then turned back over for photographs of the flow pattern.

V. Data Reduction

The data were saved to a disk file during the test runs. These data files were accessed by a data reduction program, REDDATA. REDDATA was written in BASIC and is listed in Appendix D. The program took the raw data which was collected by TEST, applied the appropriate corrections to the data, converted the pressure readings to absolute pressure readings in psi, and then saved the reduced data to files for plotting.

The data which was collected by TEST was presented in millivolts. REDDATA took the millivolt readings and used the calibration curve to convert the millivolt readings to the equivalent manometer reading in inches of mercury. The readings required correction at this point. The equivalent manometer reading was corrected for temperature and gravity. The temperature correction accounted for thermal expansion. The gravity correction accounted for the elevation and latitude of the test site. Tables for the corrections are available in several experimental guides or meteorological texts (13; 14:13,138-202).

The pressure readings to this point were in inches of mercury. To get an absolute pressure, the ambient pressure had to be added to the data. The ambient barometric reading was taken at test time using a Fortin-type barometer. This reading was also in inches of mercury and had to be corrected. Once corrected, the pressure readings could be

added and converted to psi readings. Similarly, the total (reservoir) pressure reading was corrected and converted.

REDDATA took the absolute pressure readings and presented the data in a format similar to that which SOLVE used for the theoretical values. REDDATA used the symmetry of the problem to give an overall view of the flow field properties in the reed-valve test rig. For the circular valve plate the flow field along each radial arm was equivalent. REDDATA averaged the eight radial profiles to get the average description of the radial flow-field pressure under the valve plate. The reduced data was then saved to a disk file for plotting. REDDATA could save the data in a pressure ratio format or in an absolute pressure format.

Variations of REDDATA were used to reduce the data for the square and rectangular valve plates. The square plate had two sets of symmetric profiles. The radial arms which were parallel to the 0 and 90-degree axes of the square were symmetric and could be averaged. The +45 and -45-degree diagonals were also symmetric. For the rectangle, 3 sets of symmetric profiles are used. Figure 17 identifies the radial arms which display symmetry for the various plates. The variations to the REDDATA program required to present the data for the square and rectangular disks are straight forward and not presented.

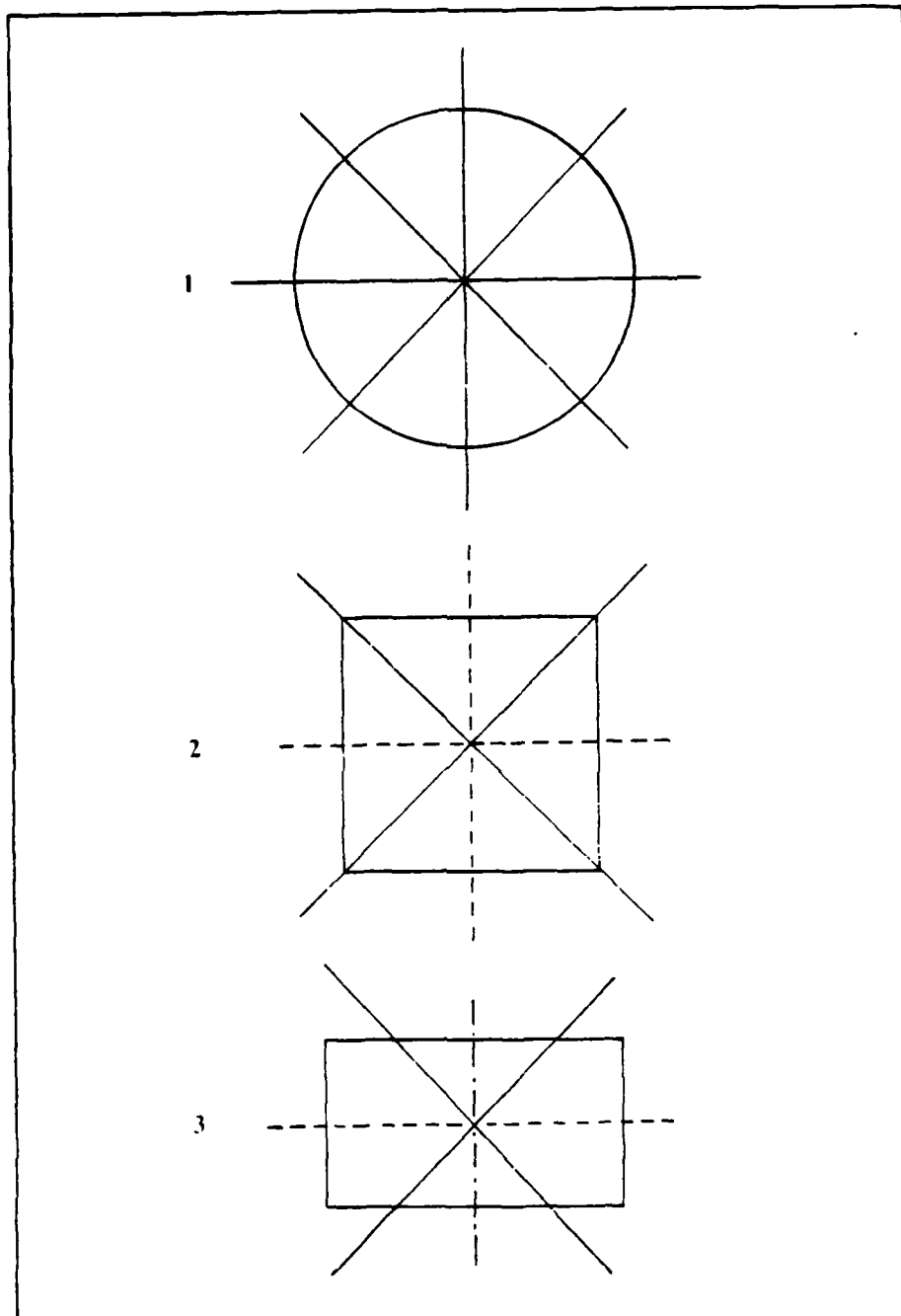


Figure 17. Radial Arm Symmetry for Various Valve Plates

A final program was written to compare the area presented by the reed-valve test rig with the equivalent or effective area of an ideal nozzle. This program, EFFAREA, is a modification of SOLVE. The purpose of writing EFFAREA was to look at various area ratio profiles in order to find a best-fit match of the data. The modifications to SOLVE consisted of replacing all references to radii ratios with area ratios and by specifying specific area ratios at all incremental locations. Two methods were used to define the effective area ratios.

The first profile, derived by method 1, was formed by fairing in the curve for the data which was analogous to the supersonic portion of the theoretical curve. Using the faired curve, pressures ratios could be projected back to the theoretical curve and effective area ratios could be determined.

The second profile, using method 2, was basically similar to the profile used in SOLVE. However, the area of the throat was varied while leaving the other incremental areas unchanged. This scheme may be similar to a profile which was due to a blockage at or near the corner which defined the throat. The location of the shock was used as the comparison criterion to determine what factor should multiply the throat area. After comparing several pressure profiles, the factor which multiplied the throat area was determined to be 0.64.

Due to the similarity of EFFAREA and SOLVE, the program is not presented. The area profiles for the two methods are presented in Appendix E.

VI. Results and Discussion

General

Data from 70 test runs were saved to disk files for reduction. Tests on three configurations were accomplished. In this section the configurations will be referred to as configuration 1, 2, and 3. The first configuration was the circular plate, the second was the square plate, and the third was the rectangular plate. Configuration 1 was tested in 33 runs; configuration 2, 31 runs; and configuration 3, 6 runs. Testing was accomplished on 5 separate days. Duplicate conditions were tested on different days to check the repeatability of the test data. The repeatability for all checks was excellent. The pressure ratio data points for similar runs from different days were basically coincident.

Configuration 1

Test runs for the circular, 2-inch diameter valve plate were performed for gauge pressures from 1.2-inches of mercury to 210-inches of mercury. Figure 18 shows a representative sampling of 5 data runs. A point to note from the figure is that portions of these curves closely overlay one another. This is very representative of the isentropic subsonic to supersonic branch of the one-dimensional theoretical analysis (cf. Figure 8). The exact locations of the normal shocks in these flows are unknown.

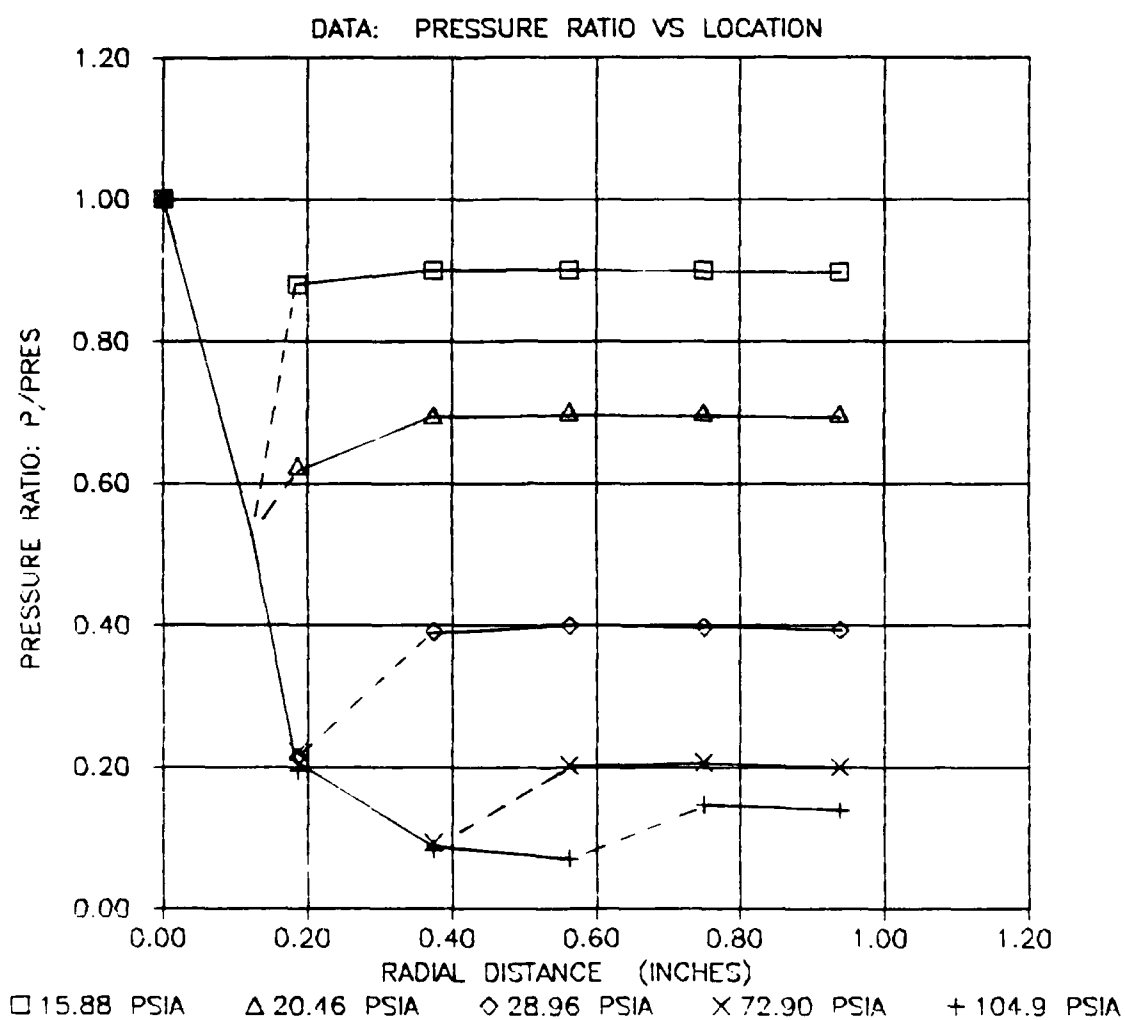


Figure 18. Representative Data; Pressure Ratio vs.
Radial Location; Five Runs

It is, however, fairly clear from the jump in the pressure ratio, that a shock must lay between certain data points. Data points on opposite sides of the shock are connected by a dotted line. Keep in mind that the shock caused a steeper jump in pressure ratio than this dotted line represents.

Figures 19-28 are direct comparisons of analytical and experimental data. Figure 29 is a compilation of several pressure ratio plots. The theoretical curve for a specific reservoir to exit pressure ratio is plotted as a solid line. The experimental data are represented by the individual points. These graphs provide a sequential look at what happens to the flow as the reservoir pressure is increased. The data indicate that the shock in the reed valve occurs at a smaller radial distance than the theory predicts. The data along the supersonic portions of the curve also match with smaller area ratios. This appears to be consistent with the idea of a blockage effect in the flow similar to a displacement thickness of a boundary layer (cf. Chapter 11). It should be noted that the flow in the supersonic section of the valve is influenced by an extreme pressure gradient. After the shock, the pressure gradient is adverse due to the subsonic nature of the problem and the geometry in this region. Also of interest is that the flow in the subsonic section of the test rig actually rose above ambient pressure. The theory shows that the pressure ratio should

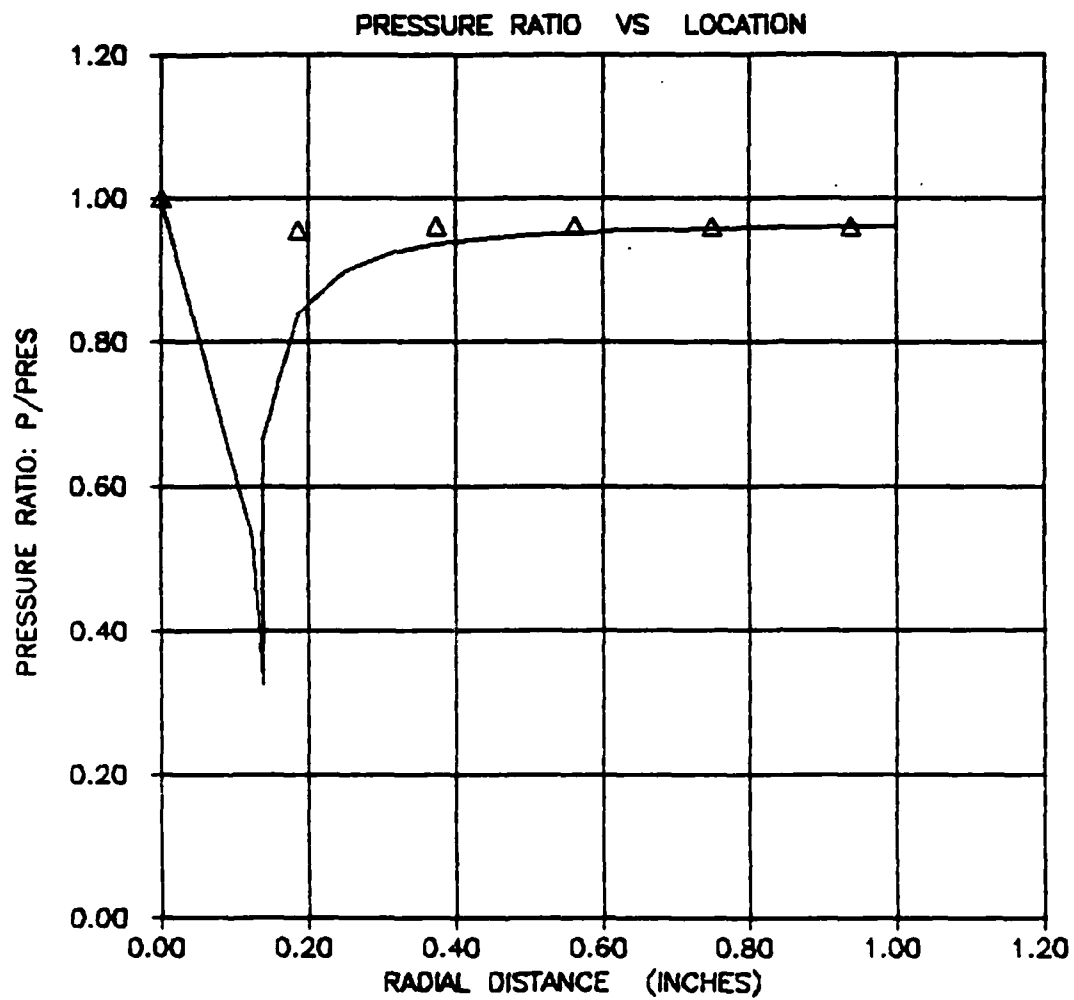


Figure 19. Pressure Ratio vs. Location Plots, Theory and Data, for Reservoir Pressure of 14.85 psia

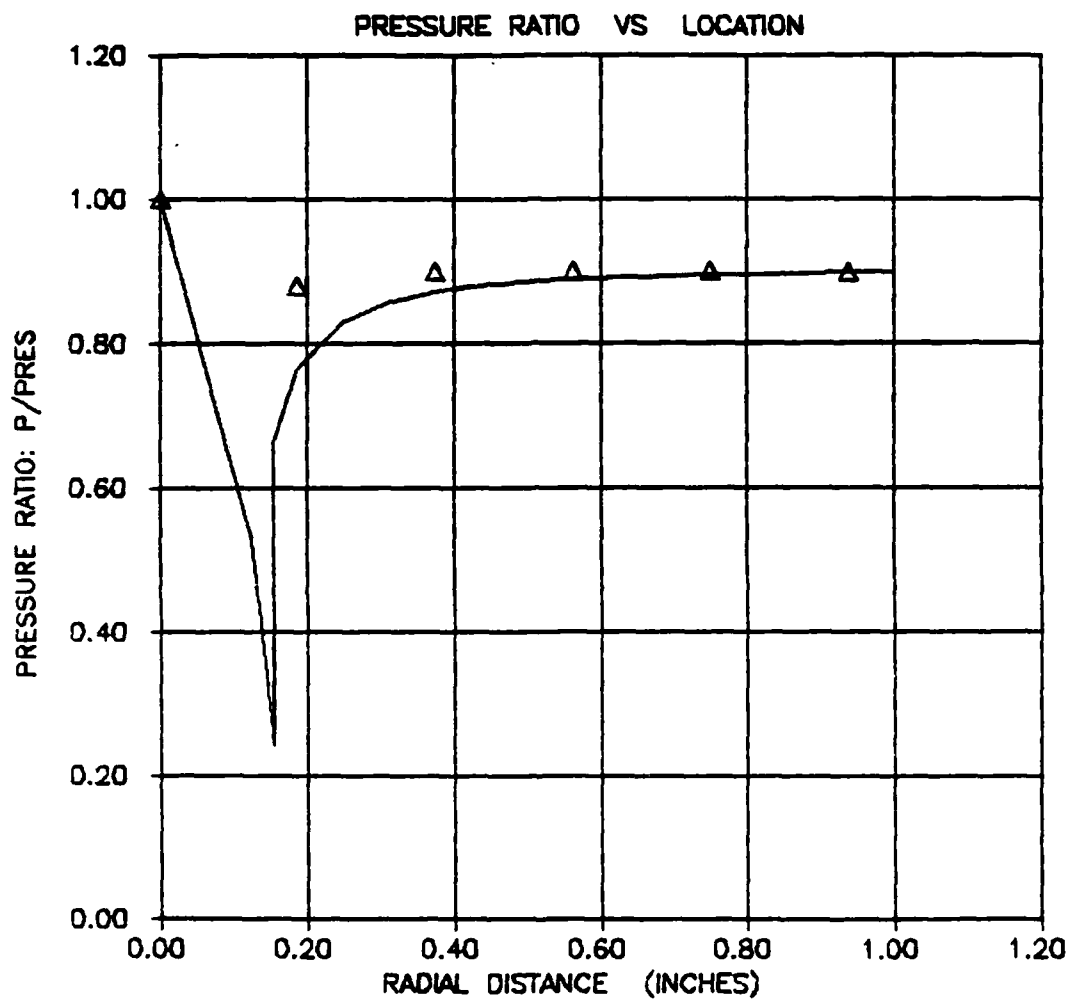


Figure 20. Pressure Ratio vs. Location Plots, Theory and Data, for Reservoir Pressure of 15.88 psia

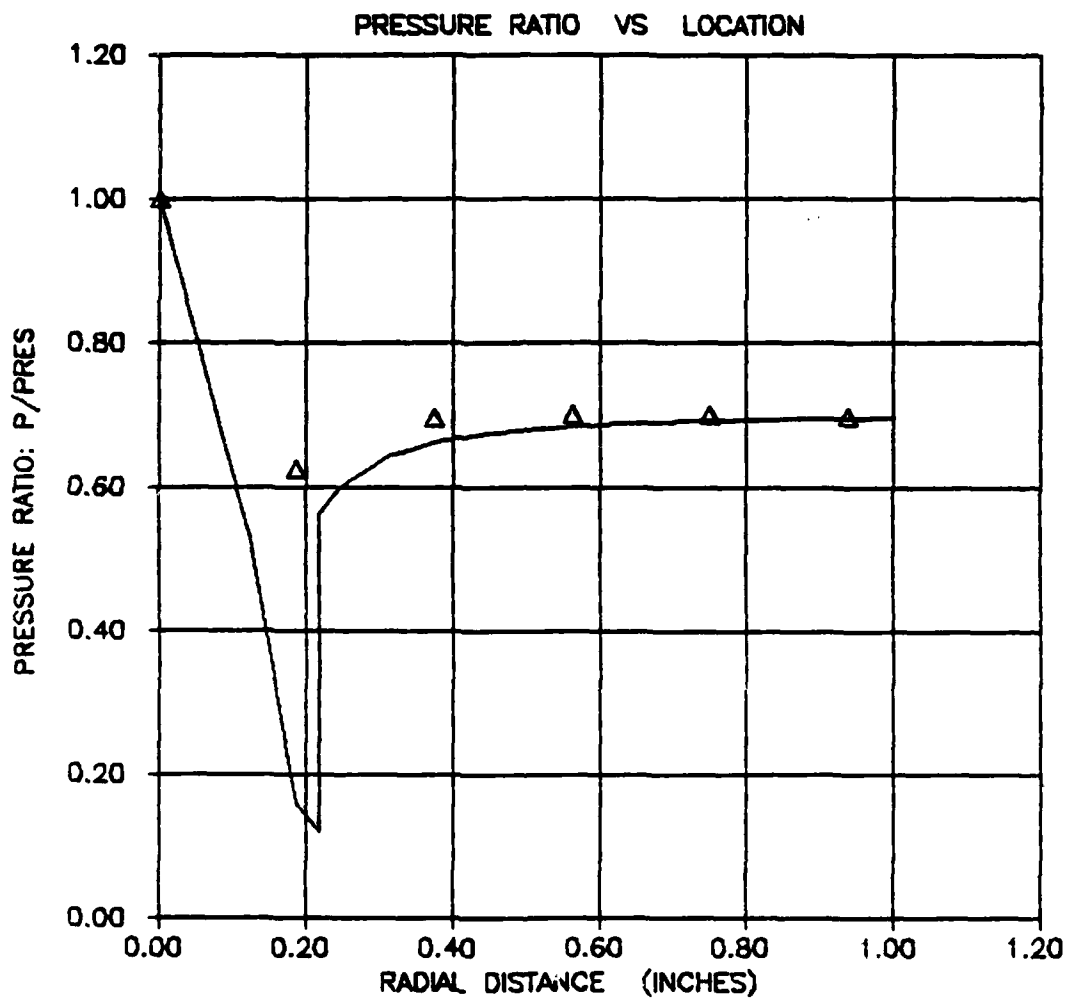


Figure 21. Pressure Ratio vs. Location Plots, Theory and Data, for Reservoir Pressure of 20.46 psia

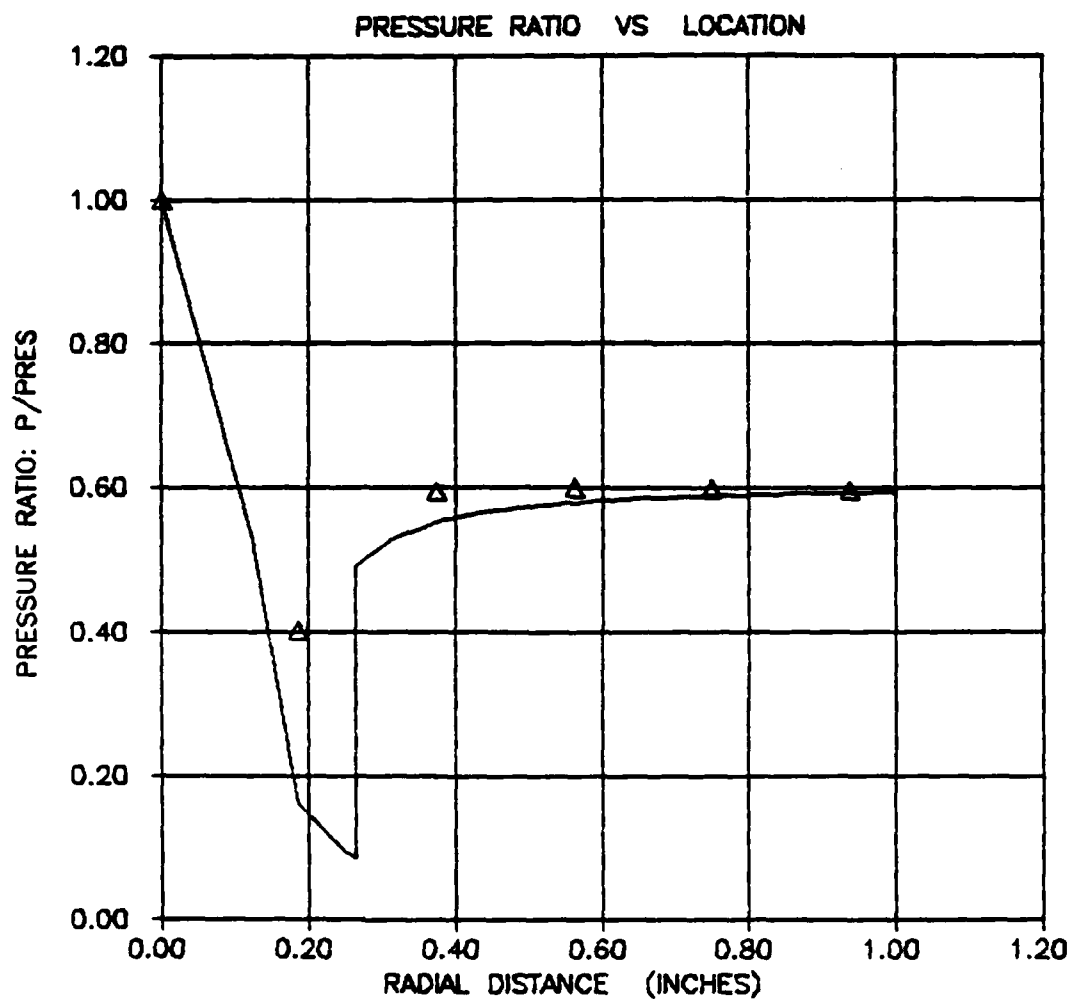


Figure 22. Pressure Ratio vs. Location Plots, Theory and Data, for Reservoir Pressure of 24.04 psia

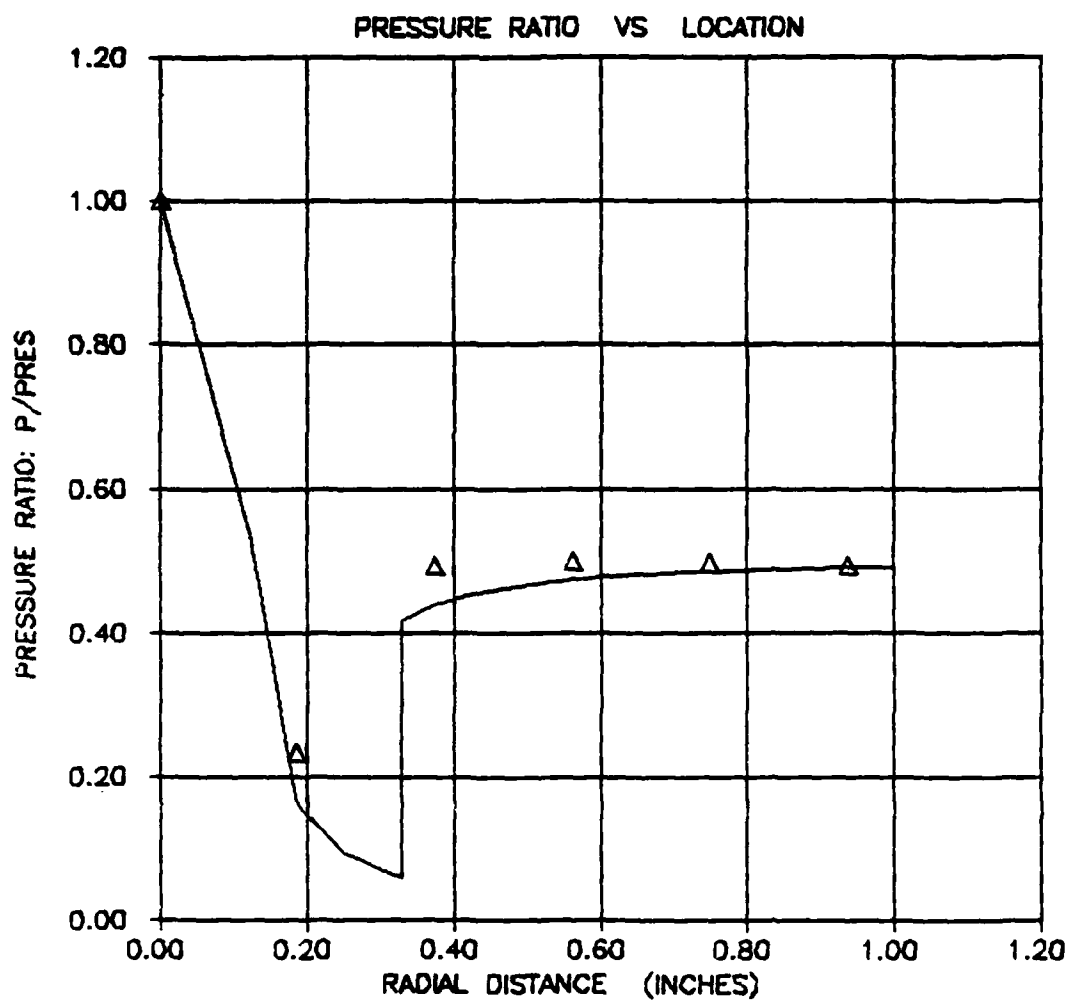


Figure 23. Pressure Ratio vs. Location Plots, Theory and Data, for Reservoir Pressure of 28.96 psia

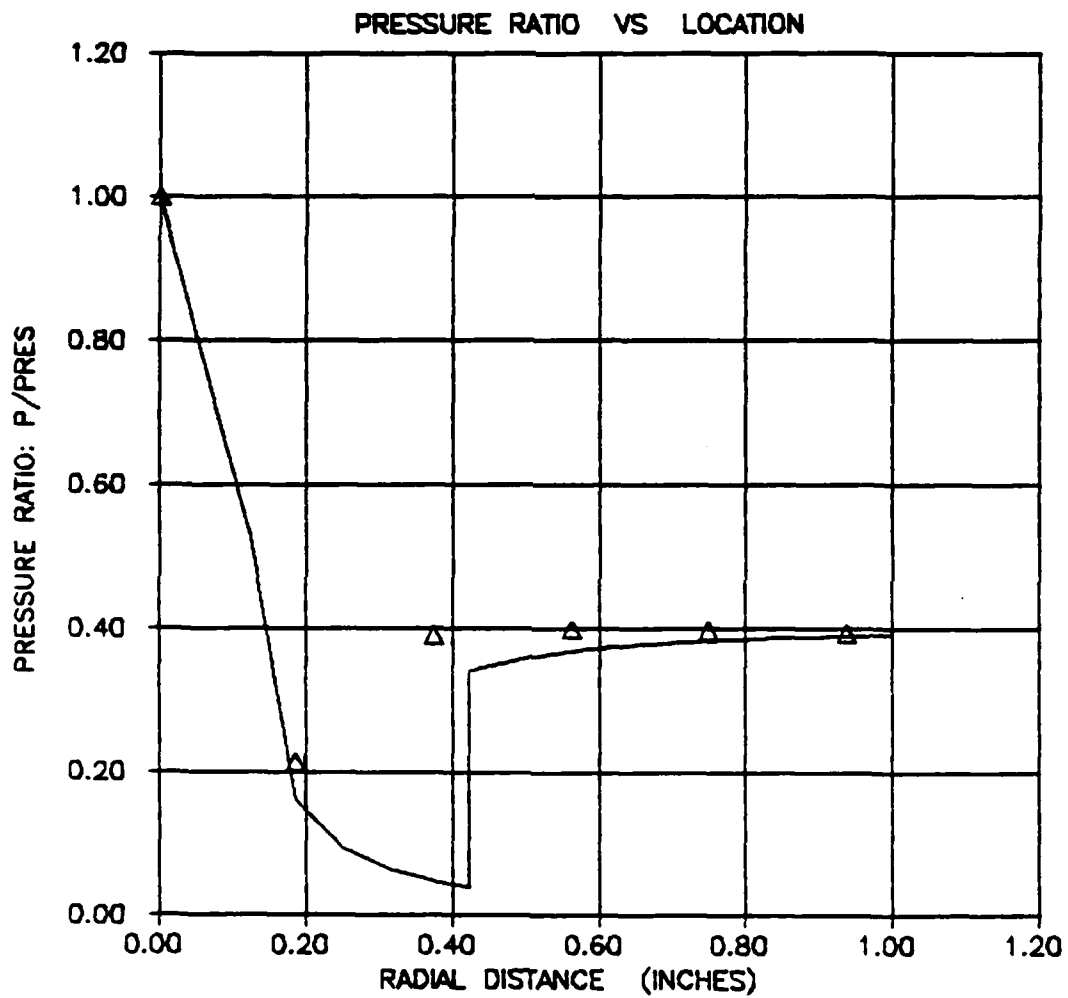


Figure 24. Pressure Ratio vs. Location Plots, Theory and Data, for Reservoir Pressure of 36.39 psia

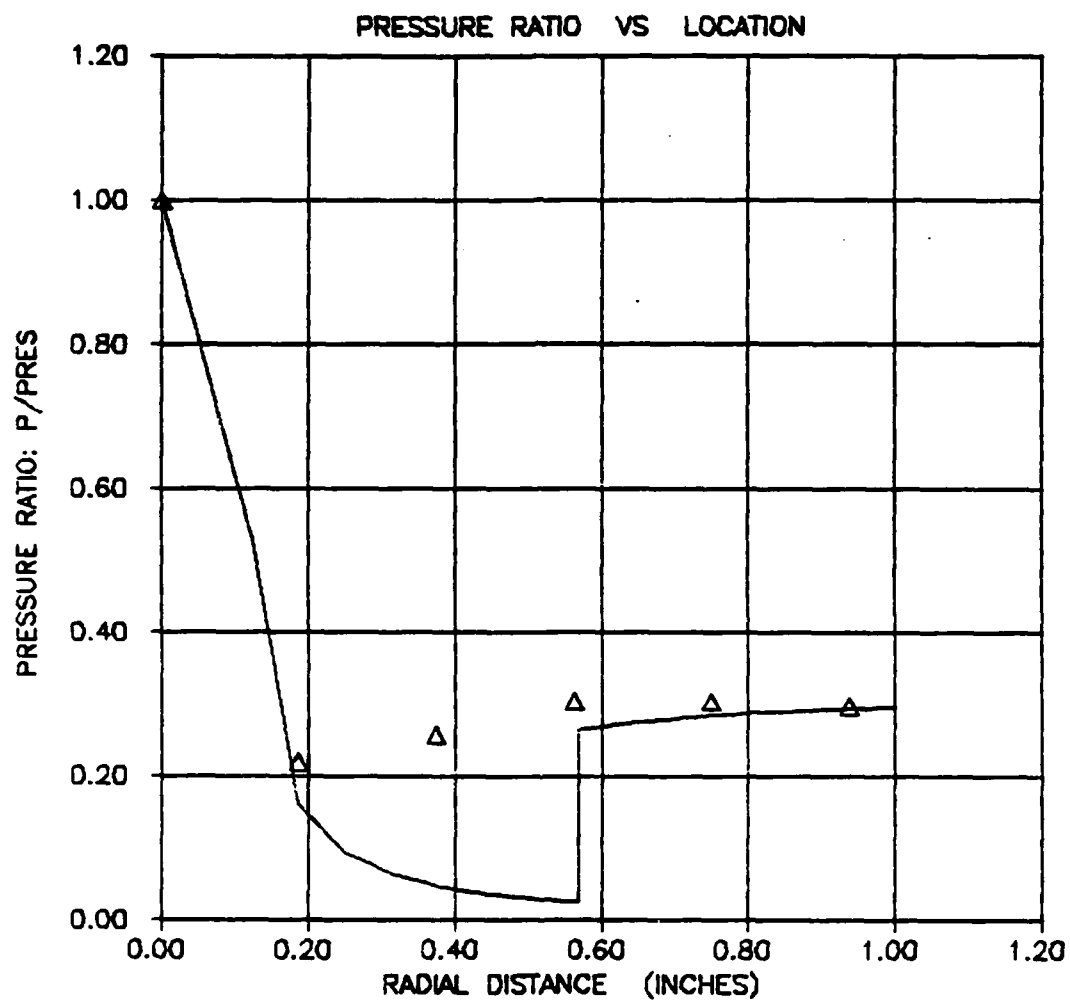


Figure 25. Pressure Ratio vs. Location Plots, Theory and Data, for Reservoir Pressure of 48.36 psia

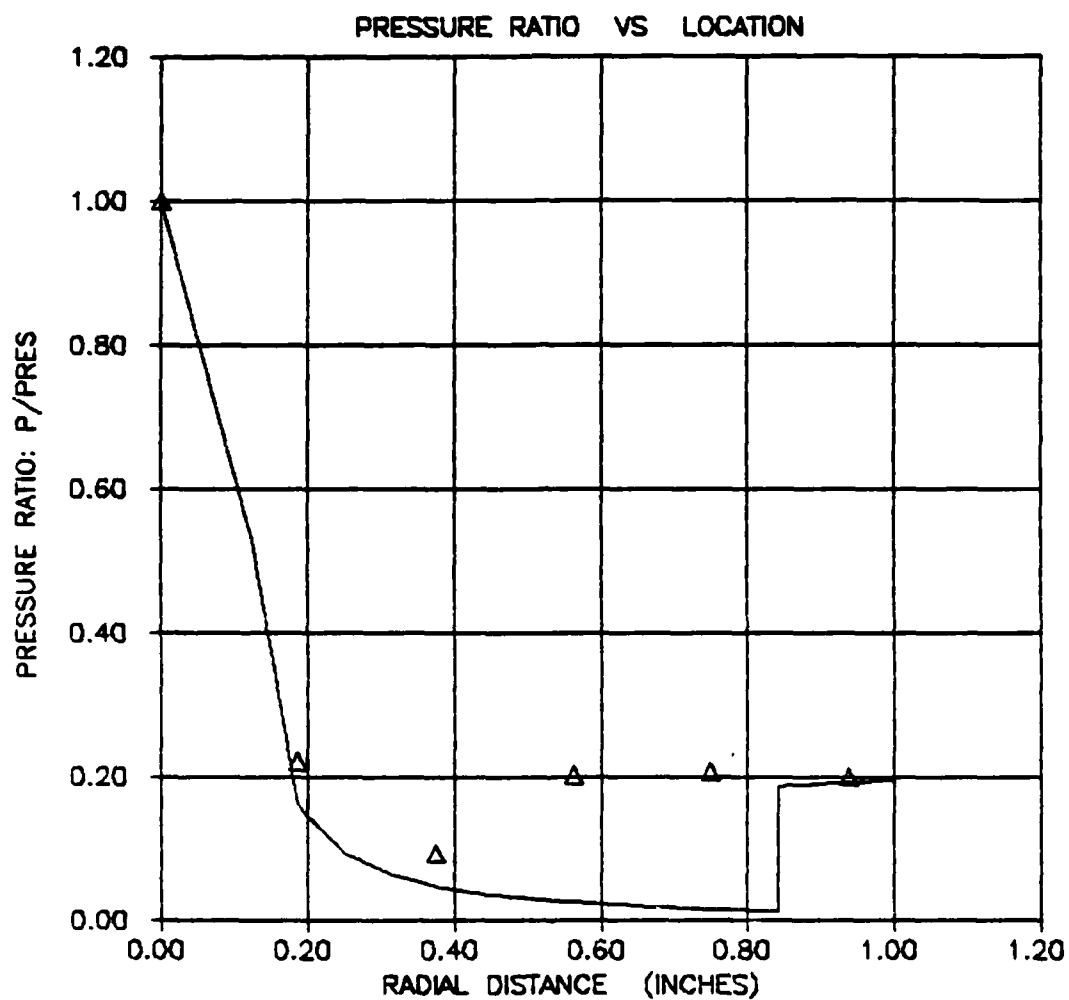


Figure 26. Pressure Ratio vs. Location Plots, Theory and Data, for Reservoir Pressure of 72.90 psia

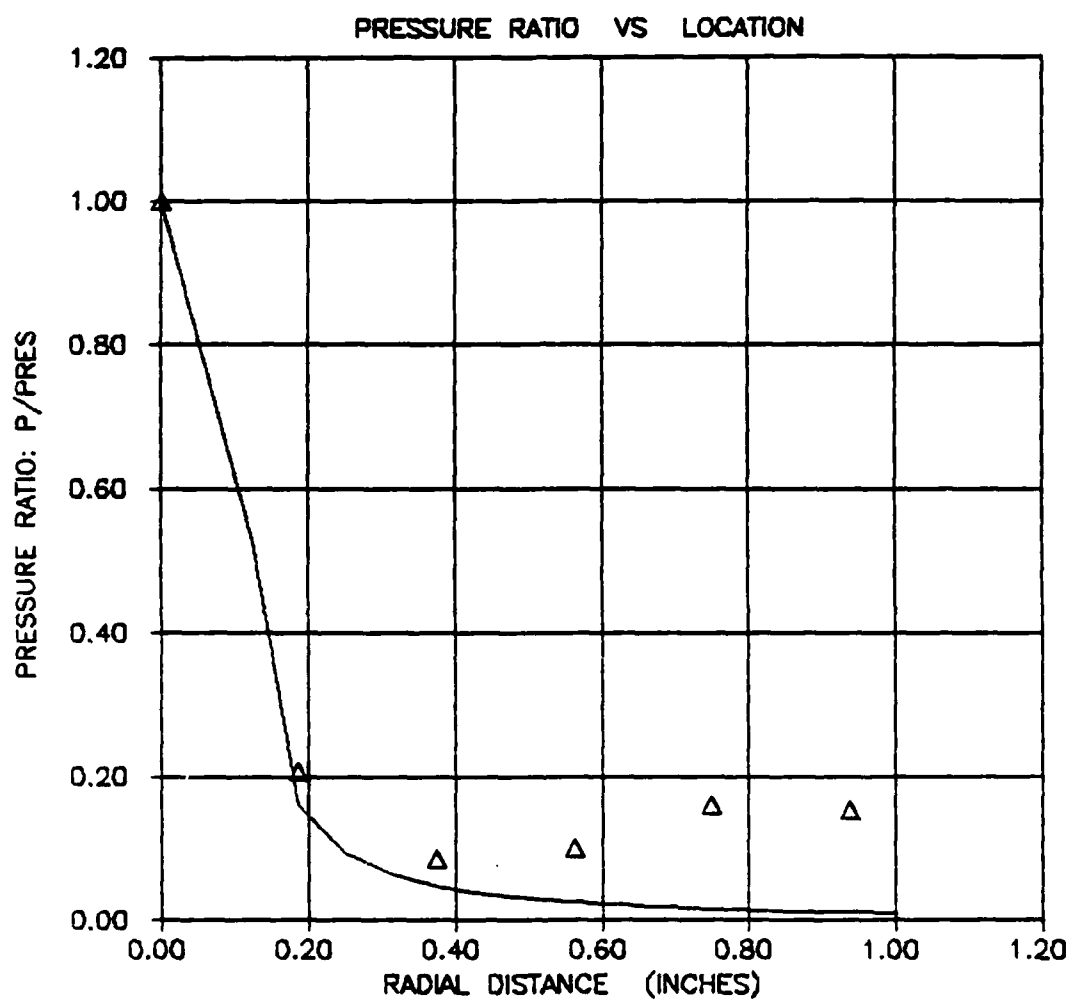


Figure 27. Pressure Ratio vs. Location Plots, Theory and Data, for Reservoir Pressure of 96.03 psia

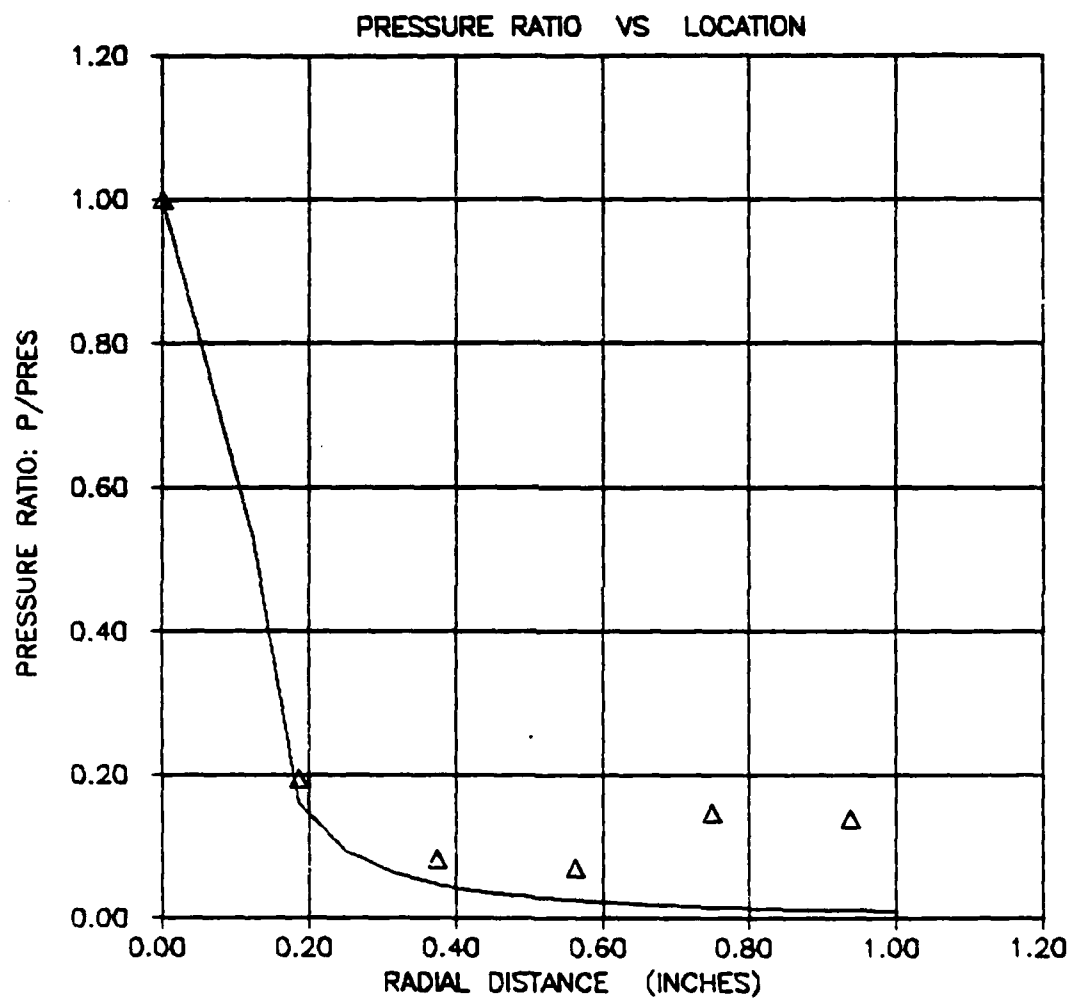


Figure 28. Pressure Ratio vs. Location Plots, Theory and Data, for Reservoir Pressure of 104.96 psia

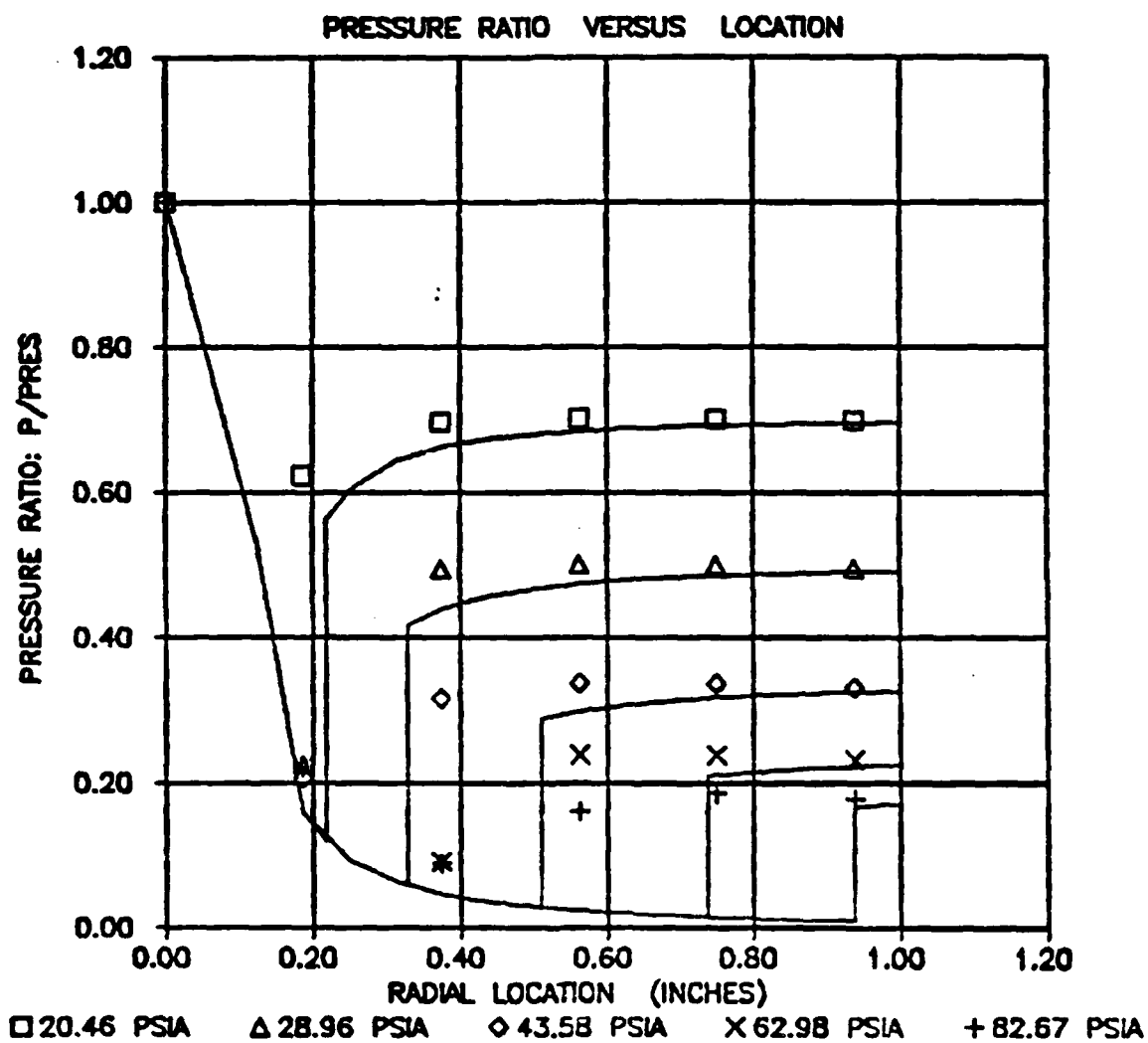


Figure 29. Overlay of Five Theoretical and Five Data Plots of Pressure Ratio vs. Location

approach the pressure ratio at the exit from below, with no overshoot. The data appears nearly flat, but close inspection reveals that the measured pressure ratio approaches the exit pressure ratio from above.

At reservoir pressures above 170-inches of mercury (pressure ratio of approximately 0.15) the valve plate began vibrating and the centering pins had to be held in place. At gauge pressures above 190-inches of mercury, the rig emitted a howling noise as the vibrations increased. Pressures above 210-inches of mercury were not attempted due to the intense noise and instability.

Figures 30A and 30B are included for a comparison of the data collected with the reed-valve model to data collected in a Laval nozzle (10:129). A striking similarity is apparent. The area ratio attained by the reed valve is much greater, but the jump in pressure due to a shock and the overshoot and return to ambient pressure near the exit are displayed in both. Further, it should be noted that Figure 30B is given as an example of how well the one-dimensional theory holds true in experiment (10:129).

The height of the valve plate was measured over a large range of pressures. The height was measured with an automotive feeler gauge and found to be constant to within the tolerance of this measurement technique. The height was found to be approximately 0.010-inches for the range of the test runs. The bourdon pressure gauge was hooked to the

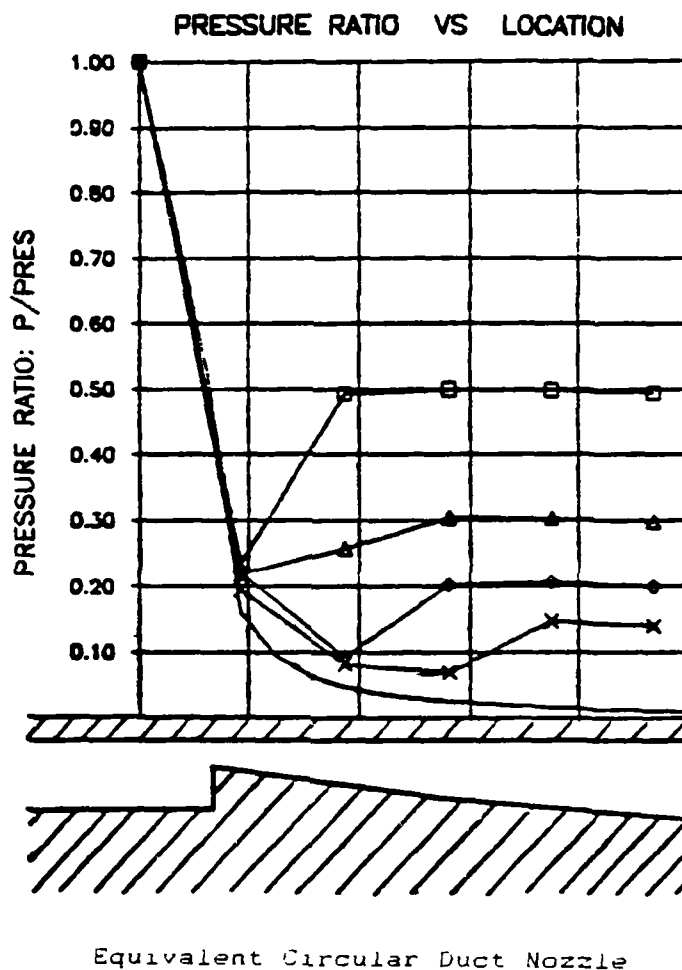


Figure 30A. Pressure Ratio vs. Location Data and Equivalent Nozzle Including Theoretical Supersonic Branch

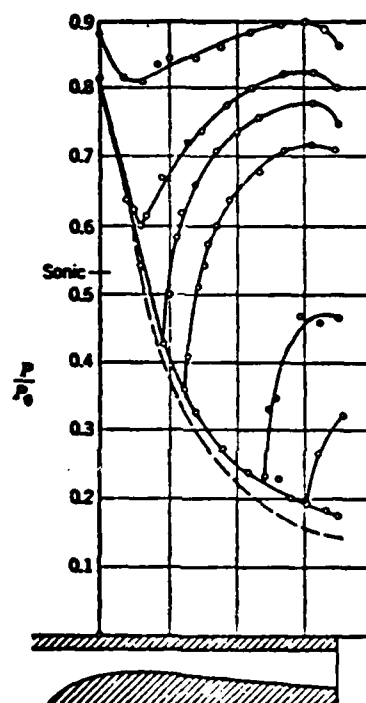


Figure 30B. Similar Plot for Laval Nozzle, Taken From
Liepmann and Roshko (10:129)

inlet line of the flow in order to make a static pressure reading. By forming the ratio of static inlet pressure to total pressure, the Mach number of the flow in the inlet was found to be approximately 0.205. Although it is most likely that the flow in the inlet is turbulent, a quick look at the problem assuming a laminar Hagen-Poiseuille profile (11:12) is a good order of magnitude check. The volumetric flow is given by

$$Q = (\pi/2) R_{\text{INLET}}^4 u_m \quad (17)$$

Where u_m is the maximum velocity of the flow. Recalling, that continuity may be written as

$$\dot{m} = \rho Q = \rho A V \quad (18)$$

The throat area may be chosen as the second location to do the comparison where $A = 2\pi R_{\text{INLET}} h$. Eq (18) is then solved for the height h .

$$h = (\rho_1 u_1 R_{\text{INLET}}) / (4 \rho_2 u_2) \quad (19)$$

For the Mach number of the inlet, the calculated height is $h = 0.0106$ -inches.

Configuration 2

The 1.5-inch by 1.5-inch square plate was tested for gauge pressures ranging from 8.2-inches of mercury to 140-inches of mercury. The plate became unstable at the upper

pressure. The plate was centered above the inlet at various orientations. This was made possible by drilling additional alignment holes in the overhead plate through which the centering pins could be inserted (See Figure 12). Pressure measurements were taken with the square aligned with the axes of the radial surface ports and at -15-degrees and at +30-degrees. The pressure profiles were expected to be different for different radial directions beneath the non-circular plates due to the variations in the lengths of the radial rays from inlet to the plate edge.

It came as a bit of a surprise that the data appeared to show little variation with respect to radial direction. The measurements taken with the plate turned either -15-degrees or +30-degrees also showed little variation. The data has the same appearance as the data gathered for the circular disk. REDDATA was put to use to determine if indeed there were variations in the data. Figure 31 contains three pressure profiles. The first is obtained by averaging data from the 0-degree and 90-degree radials. The second profile is pressure ratio data from the four 45-degree radials. The final curve is plotted as if the data were from a circular disk; all eight radial profiles are averaged to give this final curve. The three curves are nearly identical. Obviously, the distance travelled in the channel for this configuration did not effect the behavior of the flow. If one postulates that there is a significant

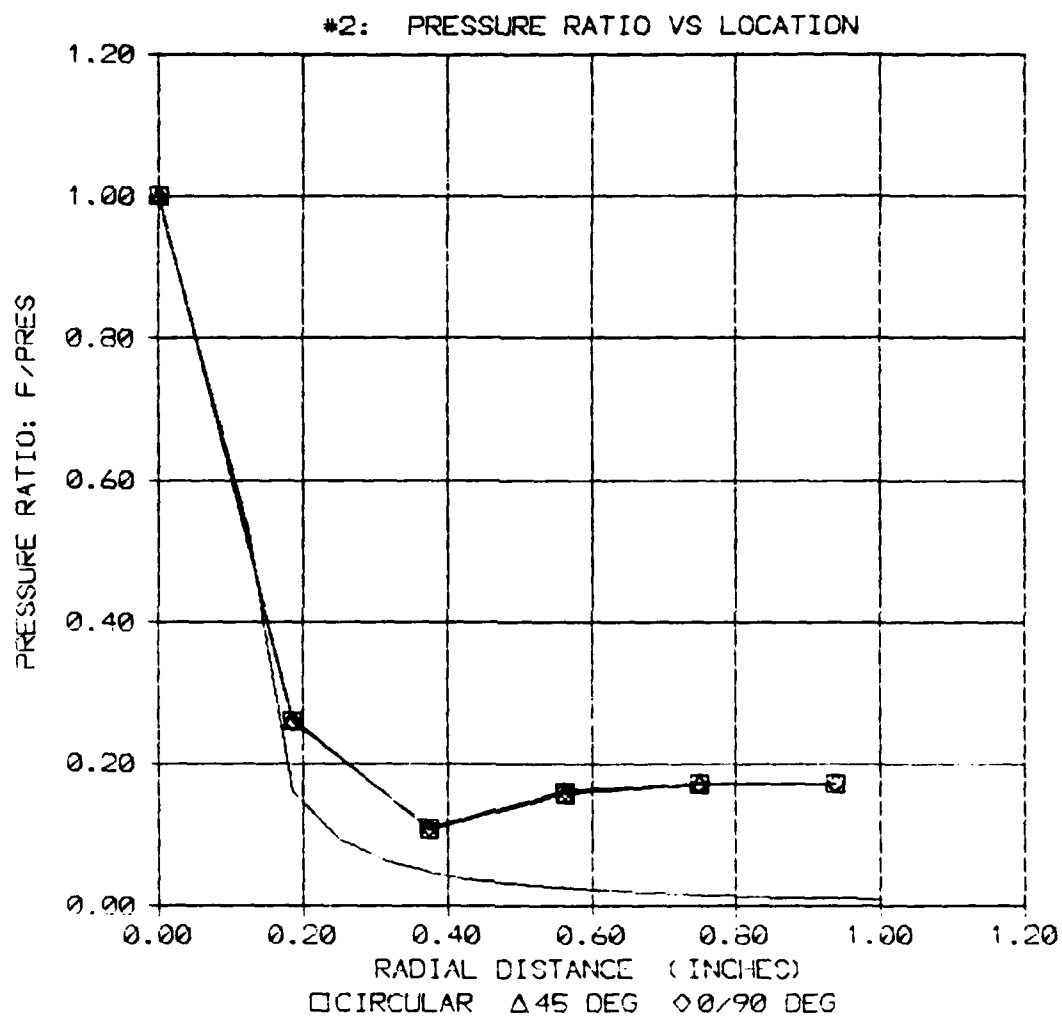


Figure 31.

Pressure Ratio vs. Location Data for Configuration 2: Three Data Plots; Two for Symmetric Arms, One for Circular Evaluation. Theoretical Plot for Circular Plate Included for Comparison

separation in the flow downstream of the shock, then the pressure in the region from the shock to the exit could be close to ambient along all ray directions. The pressure ratio curves are quite flat in this region so this seems like a reasonable possibility of what is happening. If this is the case, then a longer or shorter channel in this portion of the flow will probably have little effect on the overall characteristic of the flow in general. The geometry of the inlet is circular, the supersonic flow issues radially outward until it passes through what appears to be a circular jump discontinuity. It seems likely that the geometry of the inlet rather than the geometry of the valve plate disk is the determining factor of the flow.

It should be noted that the data on the supersonic portion of the curve for the square plate do not fall on the same curve as the points for the circular plate. The effective length of the flow channel in each case is different. The points are close, but a distinct difference is evident. The theoretical-isentropic subsonic to supersonic portion for the one-inch diameter circular plate is included in Figure 31 for comparison only.

Configuration 3

This rectangular valve plate measured 1.75-inches by 1-inch. Test runs were performed for gauge pressures from 20.5-inches of mercury to 100-inches of mercury. The plate

became unstable at the upper pressure. Only one orientation was tested for this valve plate. The results are very similar to what was found for configuration 2. A plot of the pressure ratios for various symmetric flows at the same inlet pressure are shown in Figure 32. Four data plots are presented. The first was obtained by averaging the two radial readings parallel to the primary axis of the rectangle. The second was obtained by averaging the two perpendicular radials. The third was the average of the four diagonal radial profiles. Finally, the fourth plot is obtained by treating the data as circular and averaging all eight radial profiles. Again, the curves are basically the same. Also, as was apparent with configuration 2, the data points on the supersonic portion of the curve do not match with the analogous points for the circular disk. The theoretical curve for the circular disk is again presented for comparison only.

Effective Area

Figure 33 is a plot with four sets of data. The plot is for configuration 1 operated at a reservoir pressure of 56.37 psia. The experimental data are plotted as individual points. The three solid curves represent analytic solutions obtained from SOLVE, EFFAREA method 1, and EFFAREA method 2. Note again that the data indicate a shock is occurring at a smaller radial distance than predicted by SOLVE. For method 1 of EFFAREA, the theoretical shock occurs at an even

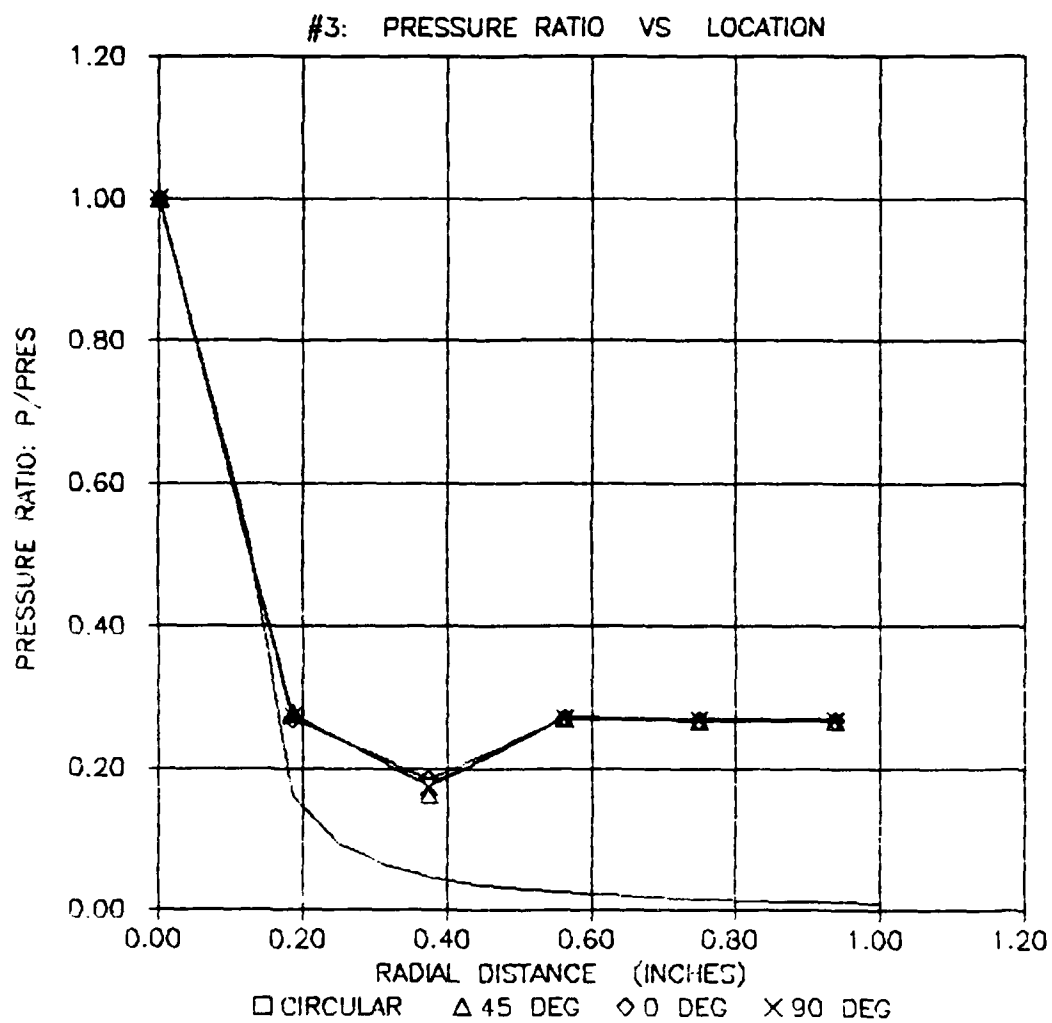


Figure 32.

Pressure Ratio vs. Location Data for Configuration 3: Four Data Plots; Three for Symmetric Arms, One for Circular Evaluation. Theoretical Plot for Circular Plate Included for Comparison

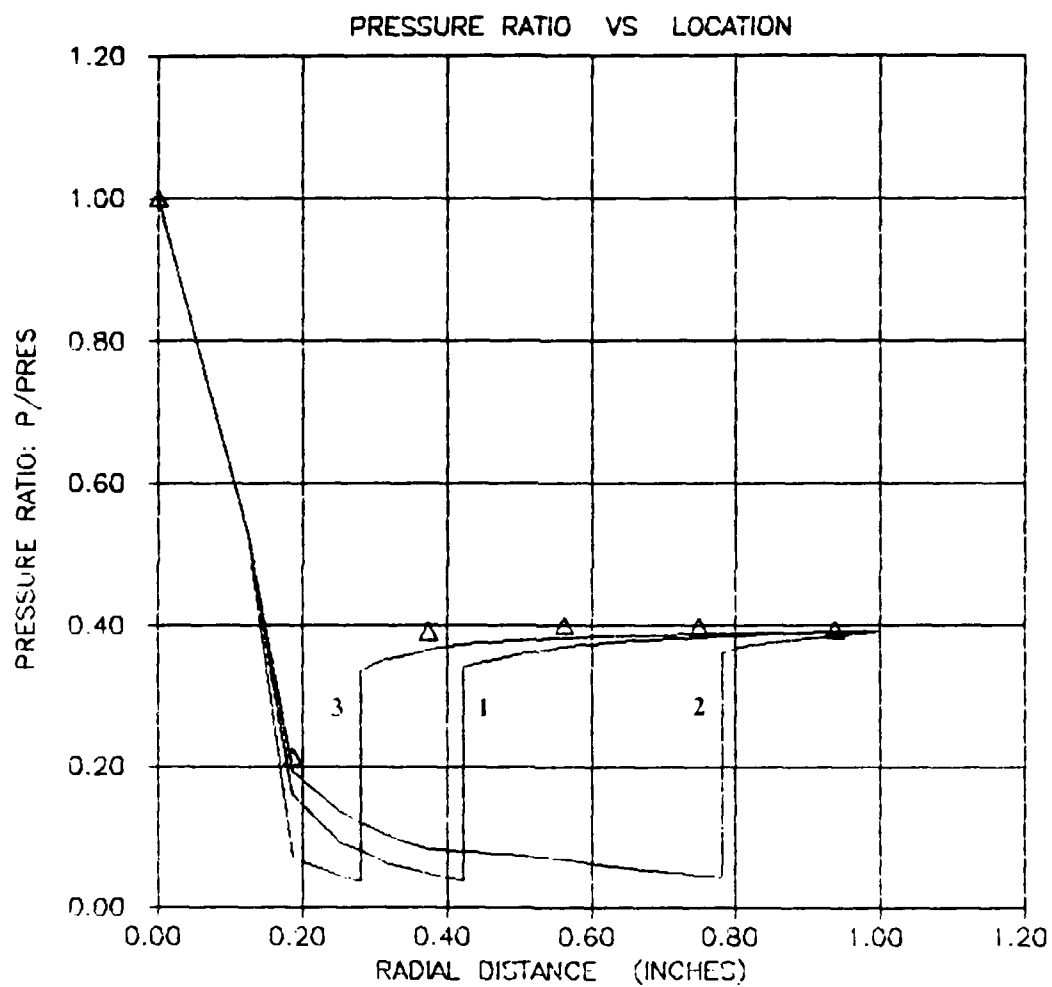


Figure 33.

Pressure Ratio vs. Location Plots of Data and
Three Analytic Techniques: (1) SOLVE,
(2) EFFAREA Method 1, (3) EFFAREA Method 2.
Reservoir Pressure is 36.39 psia

larger radial distance. Method 1 does match the data points on the supersonic curve fairly well. But, this should be no surprise, because the area ratios were derived from the supersonic portions of the data plots.

Method 2 predicts the shock location well using a value of 64.0 percent for the effective area of the throat. This value for the effective area matches the shock fairly well for the range of pressures tested. However, the values along the supersonic portion of the curve are incorrect. In fact, these values are worse than those predicted by SOLVE.

Neither method of EFFAREA is adequate to predict the flow. More work to attempt to match the data is probably in order, perhaps in a future study.

Flow Visualization

The oil flow-visualization procedure gave a distinct depiction of where the shock was located. A line was produced in the oil by the shock in most situations. Painting the base plate of the test rig black roughened the surface and slightly reduced the sharpness of the shock line.

For configuration 1, three test pressures were chosen. The test pressures were 44, 73, and 99 psia. These pressures were chosen from a study on the reduced pressure ratio data already gathered. The shock locations should be between ports 1 and 2, 2 and 3, and 3 and 4 respectively.

Figures 34A and 34B show the flow visualization for the first two runs. Each shock was well defined and at the expected location. The shock in each case was circular. Figure 35 shows the oil flow for the 99-psia run. This pressure corresponded to about 170-inches of mercury and, as reported earlier, the plate began vibrating. Close inspection of the oil flow does reveal that the shock was located at or just beyond port 3. However, the oil visualization is smeared as would be expected if the shock were oscillating.

One test run was performed with configuration 2. The oil flow is shown in Figure 36. The test pressure was 39-psia. Although the plate is square, the shock was circular. This supports the idea of separation discussed earlier (cf. Chapter VI Configuration 2).

Two test runs were performed with the rectangular plate (configuration 3). The first run was for a reservoir pressure of 39-psia and the flow visualization is presented in Figure 37A. Again, the shock was circular. The second run was performed to place the shock near the close edge of the plate. A pressure was chosen just below the threshold where the plate began to vibrate. The reservoir pressure was 34-psia. The shock was again circular as seen in Figure 37B.

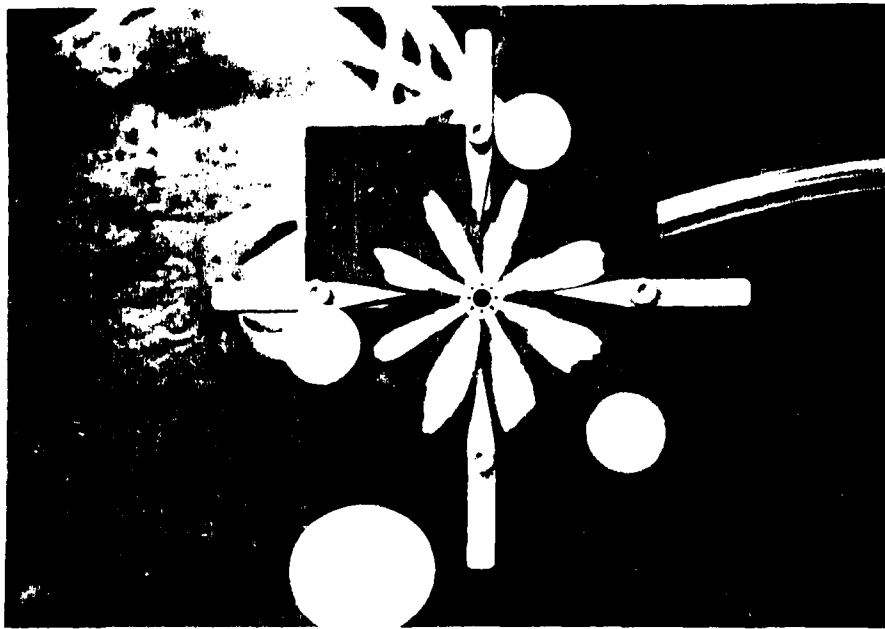


Figure 34A. Flow Visualization Configuration 1; Reservoir Pressure is 44 psia

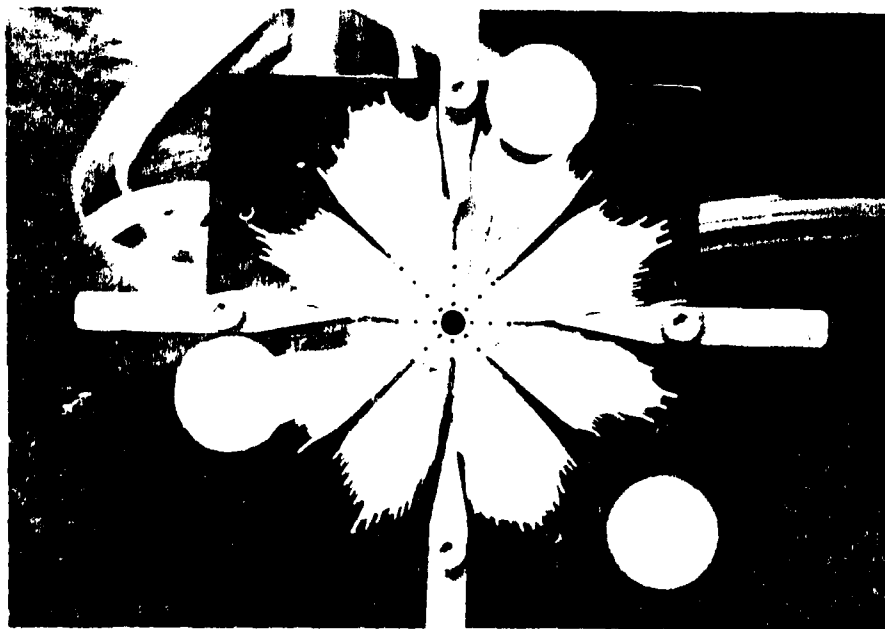


Figure 34B. Flow Visualization Configuration 1; Reservoir Pressure is 73 psia

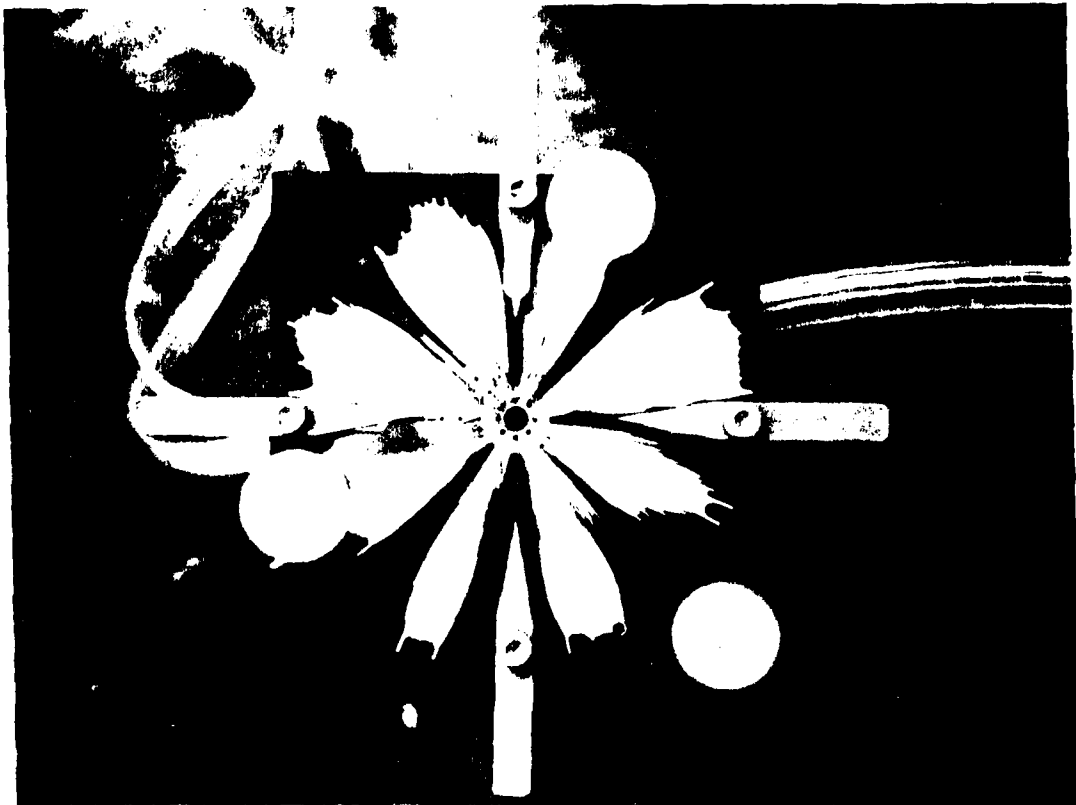


Figure 35. Flow Visualization Configuration 1; Reservoir Pressure is 99 psia. Note Smeared Shock

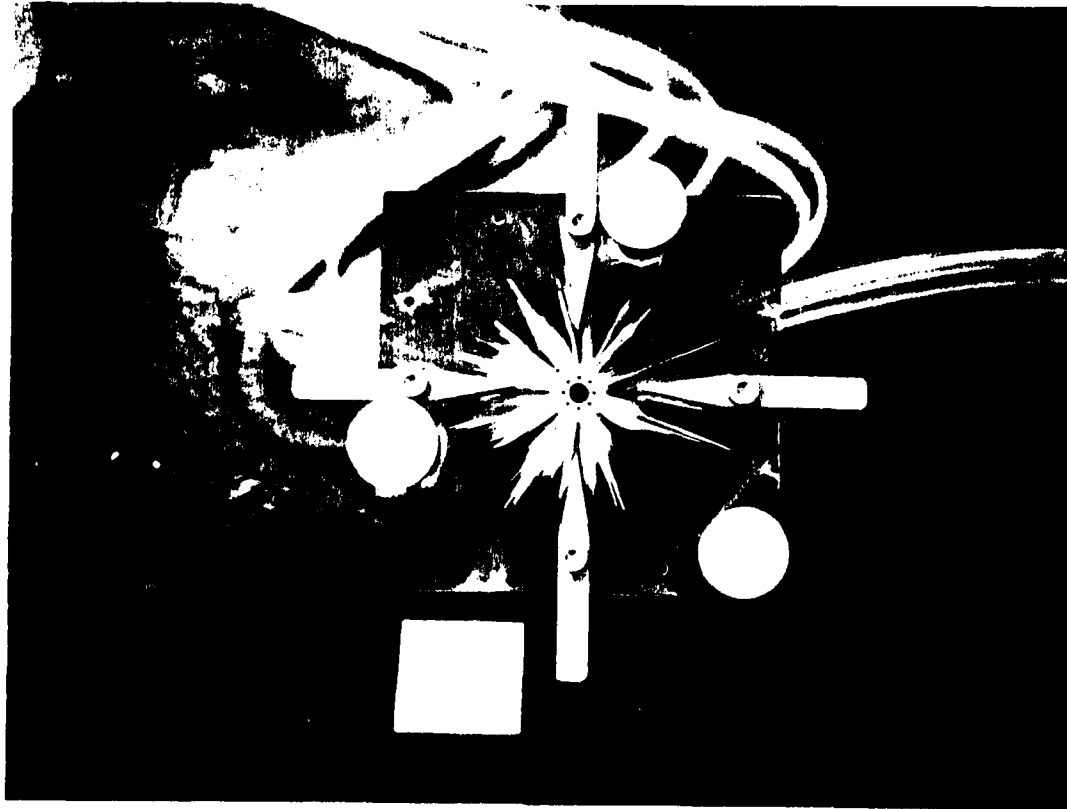


Figure 36. Flow Visualization Configuration 2; Reservoir Pressure is 39 psia

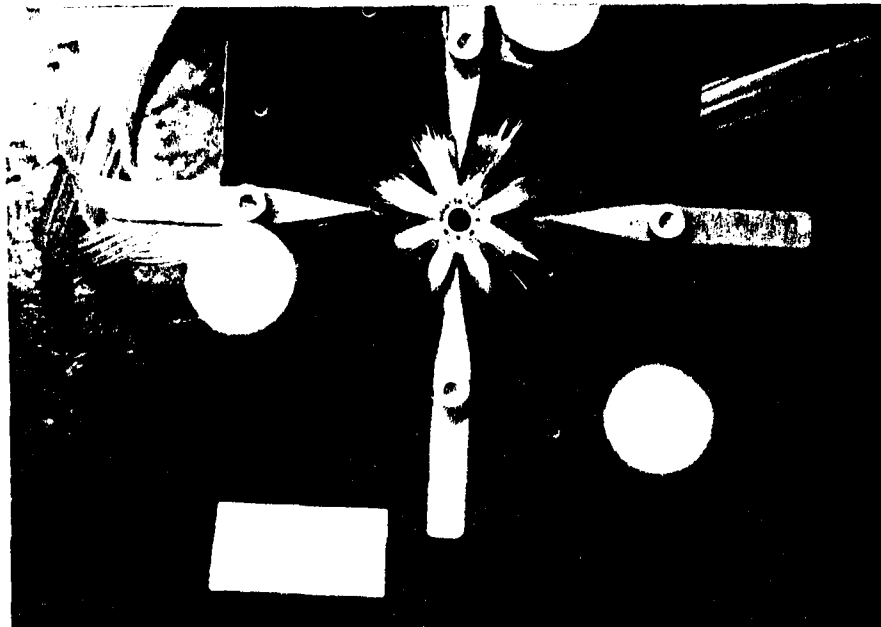


Figure 37A. Flow Visualization Configuration 3; Reservoir Pressure is 39 psia

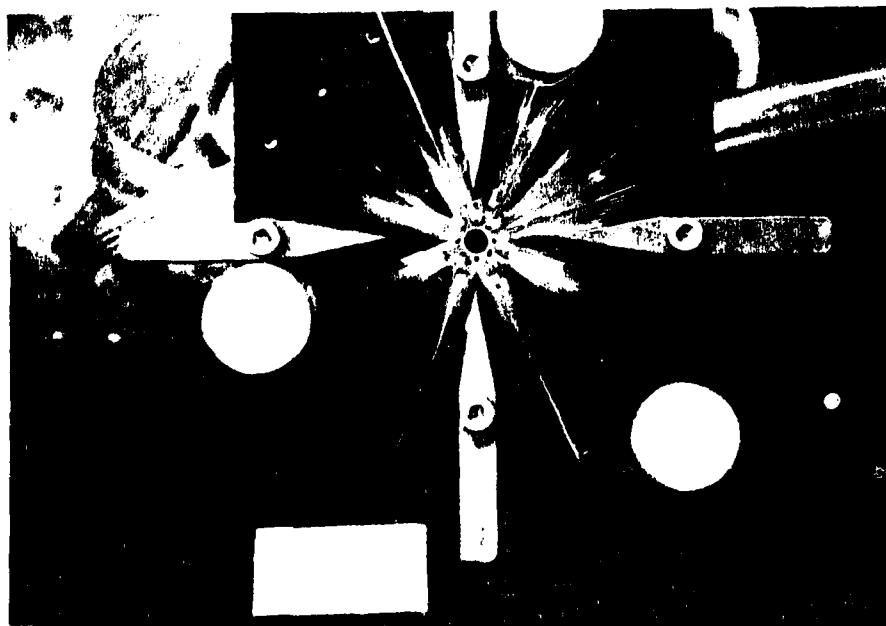


Figure 37B. Flow Visualization Configuration 3; Reservoir Pressure is 54 psia

AD-A164 102

A STUDY OF THE FLUID-DYNAMIC PRESSURE FIELDS ON
COMPRESSOR REED VALVES(U) AIR FORCE INST OF TECH
WRIGHT-PATTERSON AFB OH SCHOOL OF ENGINEERING R D HUNT
DEC 85 AFIT/GAE/AA/85D-09 F/G 28/4

2/2

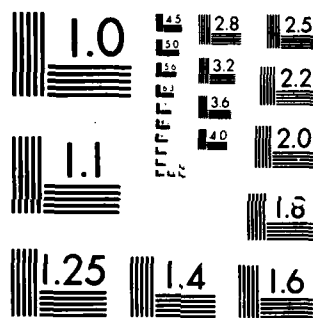
UNCLASSIFIED

F/G 20/4

NL

END

FILMED



MICROCOPY RESOLUTION TEST CHART
NATIONAL BUREAU OF STANDARDS-1963-A

The oil drop flow visualization worked well but was not suited for looking at the shock after the vibrations set in. Possibly a Schlieren technique with a plexiglass model would be a test bed to look at the higher pressure flows.

Discussion

The one-dimensional isentropic, inviscid model with normal shocks imbedded in the flow predicted the basic nature of the flow; in fact, as well as they predict for the Laval nozzle in Reference 10.

It is interesting that this reed-valve model so closely matched the performance of a Laval nozzle in the supersonic section, especially considering the equivalent divergence angle of the reed-valve model (cf. Chapter 11). Hill and Peterson (4:397-407) state that the best performance is obtained for conical nozzles with divergence half angles between 12 and 18-degrees. According to Reference 4, this preferred range of half angles is due to the stated "fact" that larger angles have the possibility of flow separation from the walls.

vii. Conclusions and Recommendations

Conclusions

The purpose of this project was to analytically predict and experimentally measure the flow-induced pressure field in a reed-valve arrangement. This pressure field was initially expected to be that for fully subsonic flow. The flow in both the reed-valve analytic model and experimental reed valve was supersonic in nature with imbedded shocks for all but the lowest total-pressure runs. Even the spool and paper trick can readily be made to have supersonic flow, a normal shock and finally a subsonic flow to the exit.

The one-dimensional isentropic-flow model with an imbedded normal shock is a good model for this flow. There is a definite phenomena in the flow channel which looks like a blockage due to the displacement thickness of a boundary layer, separation, or both. The phenomena did not yield to simple modeling techniques. The addition of a model to account for boundary layer growth might further enhance the model.

The effective area methods of analyzing the problem need more refinement. The task of closing the reed-valve problem to predict the valve height and the mass flow rate can be approached from simplified models to get a fair order of magnitude approximation.

The flow visualization technique worked well for getting a definite shock location and shape. From the

smearing of the shock line for test runs when the valve plate was vibrating, it seems that the vibration is due to an oscillation of the shock. A Schlieren technique may be effective for determining the shock characteristics for the high pressure flows.

The shocks were circular for all flow visualization runs for which an impression could be made. The circular shock beneath a non-circular valve plate suggests that the geometry of the inlet is a key factor in the shock shape and that there may be separation occurring in the subsonic section of the flow.

The analysis of the problem is certainly compatible with a small computer system when using the presented technique.

Recommendations

Based on the experiences and the results of this study the following recommendations are made:

1. Investigate methods to further analytically close the problem to determine the height of the valve plate above the base plate. A momentum approach is a likely candidate.
2. Investigate boundary-layer growth and the possibility of separation in the flow. Develop a model that predicts the effective area of the channel with these considerations in mind.

3. Predict mass-flow rates from the above extensions to the modelling. Verify the procedure by experimentally measuring the mass flow rate.

4. Investigate various inlet geometries to find the effect on the supersonic flow and the shape of the shock wave.

5. Use a Schlieren system in conjunction with a clear plexiglass reed-valve model to more precisely define the character of the shock at higher pressures.

Bibliography

1. Jumper, Eric J. Class lecture to AES.30, Chemical Rocket Propulsion and personal interview. School of Engineering, Air Force Institute of Technology (AU), Wright-Patterson AFB OH, October 1985.
2. Jumper, Eric J. Contract Report Prepared for Copland Corporation of Sidney, Ohio. Dayton OH, 1984.
3. Leone, S. Class material for AES.35, Low Speed Aerodynamics. School of Engineering, Air Force Institute of Technology (AU), Wright-Patterson AFB OH, 1984.
4. Hughes, W. F. and J. A. Brighton. Theory and Problems of Fluid Dynamics. New York: McGraw-Hill Book Company, 1967.
5. Hill, Philip G. and Carl A. Peterson. Mechanics and Thermodynamics of Propulsion. Reading MA: Addison-Wesley Publishing Company, 1970.
6. Kuethe, Arnold M. and Chuen-Yen Chow. Foundations of Aerodynamics: Bases of Aerodynamic Design. New York: John Wiley & Sons, 1976.
7. Staff, Ames Research. Equations, Tables, and Charts for Compressible Flow. Report 1135, NACA, 1953.
8. Schreier, Stefan. Compressible Flow. New York: John Wiley & Sons, 1982.
9. Conte, Samuel D. and Carl de Boor. Elementary Numerical Analysis an Algorithmic Approach. New York: McGraw-Hill Book Company, 1980.
10. Liepmann, Hans Wolfgang and Anatol Roshko. Elements of Gasdynamics. New York: John Wiley & Sons, 1962.
11. Schlichting, Hermann. Boundary-Layer Theory. New York: McGraw-Hill Book Company, 1979.
12. Keller, E. Evan. Mechanical Engineer. Personal interview. School of Engineering, Air Force Institute of Technology (AU), Wright-Patterson AFB OH, May 1985.

13. Cox, W. "Experiment 7, Pressure Measurement", Course Material for AE 6.50, Instrumentation. School of Engineering, Air Force Institute of Technology (AU), Wright-Patterson AFB OH, July 1985.

14. List, Robert J. Smithsonian Meteorological Tables. Washington D.C.: Smithsonian Institution Press, 1968.

Appendix A

SOLVE

A complete listing of the program SOLVE follows. SOLVE analytically solves the reed-valve problem for a circular valve plate and circular inlet. The assumptions which SOLVE uses are noted in Chapter II.

```

1000 '          PROGRAM - SOLVE
1010 '
1020 'THIS PROGRAM ANALYTICALLY SOLVES THE FLOW FIELD
1030 'UNDER A CIRCULAR DISK USING 1-D ISENTROPIC
1040 'AND NORMAL SHOCK FLOW RELATIONS.
1050 '
1060 DIM R(19),P(19),M(19),V(19),C(19),RHU(19),T(19),PR(19)
1070 '
1080 '    DEFINITIONS
1090 '
1100 GAMMA=1.4:'          RATIO OF SPECIFIC HEATS
1110 RG=1714.7:'         GAS CONST (FT^2/DEG RANKINE SEC^2)
1120 PA=14.6955:'        AMBIENT PRESSURE (PSI)
1130 TA=519:'            AMBIENT TEMP (RANKINE)
1140 TT=TA:'            TOTAL TEMPERATURE
1150 RI=.125:'           INLET RADIUS (INCHES)
1160 '
1170 '
1180 '    INPUT CONDITIONS
1190 '
1200 PRINT"DEFAULT OPTIONS ARE FOR A STD DAY
1210 INPUT"DO YOU WANT TO USE DEFAULT OPTIONS : ",Q19
1220 IF Q19="N" GOTO 1240
1230 IF Q19="n" GOTO 1240 ELSE GOTO 1270
1240 '
1250 GOSUB 1150:'          GO TO ALTERNATE INPUT SUBROUTINE
1260 '
1270 INPUT"INPUT THE RADIUS OF THE DISK (INCHES) : ",RE
1280 INPUT"INPUT THE INLET PRESSURE IN PSIA : ",PRES
1290 P=PRES
1300 '
1310 '    DEFINE FUNCTIONS
1320 DEF FNBU8(M)=(1+((GAMMA-1)/2)*M^2)
1330 '
1340 '    DEFINE EXPONENTS
1350 EX1=GAMMA/(GAMMA-1)
1360 EX2=1/(GAMMA-1)
1370 EX3=.5-(GAMMA/(GAMMA-1))

```

```

1380 EX4=(GAMMA-1)/GAMMA
1390 '
1400 '   DEFINE TOTAL PARAMETERS
1410 CT=(GAMMA*RG*TT)^.5:'   SONIC VEL FOR TOTAL COND.
1420 RHOT=PT/(RG*TT):'   TOTAL DENSITY
1430 '
1440 '   INCREMENTAL LOCATIONS FOR CALCULATIONS
1450 R=((RE-RI)*16)+1
1460 INCR=1/16:'   EVERY 1/16 INCH
1470 FOR I=1 TO R
1480 R(I)=RI+(I-1)*INCR
1490 NEXT I
1500 '
1510 '   DETERMINE PT/PE FOR SONIC THROAT
1520 '
1530 '   FIND MES - MACH @ EXIT FOR STAR COND
1540 MES=.1:'   JUST A FIRST HACK TO START ITERATING
1550 MES1=(RI/RE)*(FNBOB(MES)/FNBOB(1))^(EX3)
1560 IF ABS(MES-MES1)<.000001 THEN GOTO 1590
1570 MES=MES1
1580 GOTO 1550
1590 MES=MES1
1600 '   NOW USE MES TO FIND PT/PE FOR STAR COND
1610 '   CALL IT PRS -- FOR PRESSURE RATIO STAR
1620 PRS=(FNBOB(MES))^EX1
1630 '
1640 '   COMPARE PRESSURE RATIO, PR, WITH PRS
1650 PR=PI/PA:'   PR IS PRESSURE RATIO
1660 IF PR > PRS THEN GOTO 1680 ELSE GOTO 1720
1670 '
1680 GOSUB 2230:'   GOTO THE SUPERSONIC SUBROUTINE
1690 GOTO 3630:'   GOTO THE OUTPUT SECTION
1700 '
1710 '
1720 '   SUBSONIC SOLUTION
1730 PRINT
1740 PRINT"THIS IS A SUBSONIC PROBLEM"
1750 PRINT
1760 '
1770 ME=.12/(GAMMA-1)*((PR^EX4)-1)^.5:'   SCHREIER 149
1780 '
1790 '   WITH ME IN HAND FIND M(I) AT ALL RADIAL LOCATIONS
1800 FOR I=1 TO R
1810 GOSUB 1910
1820 NEXT I
1830 '
1840 '   WITH M(I)'S GET ALL OTHER PROPERTIES
1850 FOR I=1 TO R
1860 GOSUB 2020
1870 NEXT I
1880 GOTO 3630:'   GOTO THE OUTPUT SECTION
1890 '

```

```

1900 '
1910 '      SUBROUTINE -- INCREMENTAL MACH NUMBER
1920 '      INPUT -- EXIT MACH NUMBER
1930 MI=.5: 'ANOTHER HACK TO START THE ITERATION
1940 MI1=(RE*ME/R(1))*(FNBOB(ME)/FNBOB(MI))^EX3
1950 IF ABS(MI-MI1)<.000001 THEN GOTO 1980
1960 MI=MI1
1970 GOTO 1940
1980 M(1)=MI1
1990 RETURN
2000 '
2010 '
2020 '      SUBROUTINE -- INCREMENTAL PROPERTIES
2030 '      INPUT -- MACH NUMBER @ 1
2040 BOB=FNBOB(M(1))
2050 P(1)=PT/(BOB^EX1): '      PRESSURE (PSIA)
2060 PR(1)=P(1)/PRES: '      PRESSURE RATIO
2070 RHU(1)=RHUT/(BOB^EX2): '      DENSITY (SLOBS/CUBIC FOOT)
2080 RHO(1)=RHU(1)*1000: '      RHO(1)*E-03
2090 T(1)=TT/BOB: '      TEMP (DEGREES RANKINE)
2100 C(1)=CT/(BOB^.5): '      SONIC VELOCITY (FT/SEC)
2110 V(1)=M(1)*C(1): '      FLUID VELOCITY (FT/SEC)
2120 RETURN
2130 '
2140 '
2150 '      SUBROUTINE -- ALTERNATE INPUT
2160 INPUT"INPUT GAMMA : " , GAMMA
2170 INPUT"INPUT THE TOTAL TEMP IN DEGREES R : " , TT
2180 INPUT"INPUT THE EXIT PRESSURE IN PSIA : " , PA
2190 INPUT"INPUT THE RADIUS OF THE INLET (INCHES) : " , RI
2200 RETURN
2210 '
2220 '
2230 '      SUBROUTINE -- SUPERSONIC SOLUTION
2240 PRINT
2250 PRINT"      THIS IS A SUPERSONIC PROBLEM"
2260 PRINT
2270 SUPERS="YES"
2280 DIR=1: '      INITIAL MARCH DIRECTION = IN
2290 PACE=.5: '      SIZE OF MARCH STEP
2300 PRIN:"MARCH THE SHOCK IN/OUT UNTIL PE = PA":PRINT
2310 EXIT=.0001: '      PRESSURE DIFFERENTIAL @ EXIT
2320 MAX=1: '      INITIAL GUESS @ MAX MACH
2330 XY=(RI/MX)*((GAMMA+1)/2)/FNBOB(MX))^EX3
2340 MY=((GAMMA-1)*MX^2+2)/((2-GAMMA*MX^2)-(GAMMA-1)))^0.5
2350 GLOB1=((GAMMA+1)/2)*MX^2/FNBOB(MX))^EX1
2360 GLOB2=(GAMMA+1)/((2-GAMMA*MX^2)-(GAMMA-1))^EX2
2370 PLY=PI*GLOB1*GLOB2
2380 '
2390 '      ITERATE TO GET MACH AT THE EXIT -- ME
2400 '
2410 ME=.1: '      INITIAL GUESS @ ME

```

```

2420 ME1=(MY*RY/RE)*(FNBOB(ME)/FNBOB(MY))^(1-EX3)
2430 IF ABS(ME1-ME)<.0000001 THEN GOTO 2460
2440 ME=ME1
2450 GOTO 2420
2460 ME=ME1
2470 '
2480 PE=PTY/(FNBOB(ME))^EX1
2490 '
2500 '           COMPARE EXIT PRESSURE WITH AMBIENT
2510 '           MOVE SHOCK UNTIL THEY MATCH
2520 IF ABS(PE-PA)<EXIT THEN GOTO 2750
2530 IF PE<PA THEN GOTO 2650
2540 '
2550 '           MARCH OUT WITH THE SHOCK
2560 MARCH=0:PRINT"MARCHING OUT -- PE/PA = ",PE/PA
2570 IF MARCH-DIR=0 THEN 2580 ELSE 2600
2580 MX=MX+PACE
2590 GOTO 2330: '           UPDATED MX - RECALCULATE
2600 PACE=PACE*(.5)
2610 DIR=0
2620 MX=MX+PACE
2630 GOTO 2330
2640 '
2650 '           MARCH IN WITH THE SHOCK
2660 MARCH=1:PRINT"MARCHING IN --- PE/PA = ",PE/PA
2670 IF MARCH-DIR=0 THEN 2680 ELSE 2700
2680 MX=MX-PAVE
2690 GOTO 2330
2700 PACE=PACE*(.5)
2710 DIR=1
2720 MX=MX-PAVE
2730 GOTO 2330: '           UPDATED MX - RECALCULATE
2740 '
2750 ' THE SHOCK IS NOW AT THE RIGHT LOCATION
2760 PRINT:
2770 PRINT"THE SHOCK IS AT THE RIGHT LOCATION"
2780 PRINT"SHOCK LOCATED AT R = ",RY
2790 PRINT"AREA RATIO - ASHOCK/A* = ",RY/RI
2800 PRINT"EXIT PRESSURE = ",PE
2810 PRINT"AMBIENT PRESSURE = ",PA
2820 PRINT:PRINT:PRINT
2830 PX=PI/(FNBOB(MX))^EX1
2840 PRX=PX/PRES
2850 PY=PI/(FNBOB(MY))^EX1
2860 PRY=PY/PRES
2870 '
2880 '
2890 ' FIND BREAK POINT FOR SHOCK -- SUPER TO SUB -- ISH
2900 ISH=INT((RY-RI)/INCR)+1
2910 '
2920 ' FIND MACH NUMBERS @ I LOCATIONS
2930

```

```

2930 ' SUPERSONIC -- PRESHOCK SECTION
2940 ' COMPARE AREA RATIOS THEN ADJUST MACH
2950 ' NUMBER UNTIL THEY MATCH -- MARCH WITH
2960 ' MACH NUMBER
2970 '
2980 PRINT "MARCH UP/DOWN WITH MACH TO MATCH AREA RATIOS
2990 '
3000 FOR L=1 TO 3000:NEXT L: ' DELAY TO READ SCREEN
3010 '
3020 FOR I=1 TO ISH
3030 MIG=1: ' MACH @ 1 -- GUESS
3040 DIR=0
3050 PACE=.5
3060 EXIT=.001
3070 IF RI=RI1 THEN 3080 ELSE 3090
3080 MIG=1:GOTO 3090
3090 ARA=FR(1)/RI
3100 ARA1CALC=((FNBOB(1)/FNBOB(MIG))^(EX2))/MIG
3110 IF ABS(ARA1-ARA1CALC)<EXIT THEN 3160
3120 IF ARA1<ARA1CALC THEN 3250
3130 '
3140 ' MARCH UP WITH MACH TO MATCH A/A*
3150 PRINT "MARCHING UP
3160 MARCH=0
3170 IF (MARCH-DIR)=0 THEN 3180 ELSE 3200
3180 MIG=MIG+PACE
3190 GOTO 3100
3200 PACE=PACE*(.5)
3210 DIR=0
3220 MIG=MIG+PACE
3230 GOTO 3100
3240 '
3250 ' MARCH DOWN WITH MACH TO MATCH A/A*
3260 PRINT "MARCHING DOWN
3270 MARCH=1
3280 IF (MARCH-DIR)=0 THEN 3290 ELSE 3310
3290 MIG=MIG-PACE
3300 GOTO 3100
3310 PACE=PACE*(.5)
3320 DIR=1
3330 MIG=MIG-PACE
3340 GOTO 3100
3350 '
3360 ' AREA RATIO MATCH -- MIG = MACH AT A/A*
3370 A1=MIG
3380 PRINT "AT LOCATION ",I," THE MACH NUMBER IS: ",MIG
3390 NEXT I
3400 '
3410 ' SUBSONIC -- POSTSHOCK SECTION
3420 FOR I=ISH+1 TO R
3430 ' SUBSUB 1310
3440 NEXT I

```

```

3430      OK, I'VE FOUND M(1)'S
3460 '
3470 '   TAKE THE M(1)'S AND GO GET THE OTHER PROPERTIES
3480 '
3490 '           SUPERSONIC (PRESHOCK)
3500 FOR I=1 TO ISH
3510     GOSUB 2020
3520 NEXT I
3530 '
3540 '           SUBSONIC (POSTSHOCK)
3550 PT=PTY
3560 FOR I=ISH+1 TO R
3570     GOSUB 2020
3580 NEXT I
3590 PRINT:PRINT
3600 RETURN
3610 '
3620 '
3630 '   ----- OUTPUT SECTION
3640 '
3650 '   WITH ALL PROPERTIES CALCULATED - PRINT THEM OUT
3660 PRINT"FLOW PROPERTIES AT INCREMENTAL LOCATIONS
3670 PRINT
3680 PRINT"  I  DISTANCE  PRESSURE  PRES RAT  ";
3690 PRINT"MACH  VELOCITY  SONIC V    TEMP
3700 PRINT"      (INCHES)   (PSI)      ";
3710 PRINT"      (FT/SEC)   (FT/SEC)   (DEG R)
3720 PRINT
3730 FOR I=1 TO R
3740 PRINT USING" ##      #.###      ###.###      " ; I, R(I), P(I);
3750 PRINT USING"#.###      #.###      ###.###" ; PR(I), M(I), V(I);
3760 PRINT USING"      ###.##      ###.##" ; C(I), T(I)
3770 NEXT I
3780 PRINT
3790 INPUT"WALL 1 SAVE THE PRESSURE RATIO DATA ? ", Q19
3800 IF Q19="Y" THEN 3830 ELSE 3810
3810 IF Q19="Y" THEN 3830 ELSE 4110
3820
3830      OPEN DATA FILE FOR P/R PRES VS R DATA
3840 '
3850 INPUT"INPUT THE NAME OF THE DATA FILE : ", Q19
3860 PRINT
3870 OPEN "1", #1, Q19
3880 '   WRITE:  R(I), PR
3890 WRITE #1, 0, 1
3900 PRINT
3910 PRINT"           PRESSURE RATIO DATA
3920 PRINT
3930 PRINT"      R(I)           PR(I)
3940 PRINT 0, 1
3950 FOR I=1 TO ISH
3960 PRINT R(I), PR(I)

```



```

3970 WRITE #1,R(I),PR(I)
3980 NEXT I
3990 '
4000 IF SUPERS="YES" THEN 4010 ELSE 4060
4010 PRINT RY,PRX
4020 PRINT RY,PRY
4030 WRITE #1,RY,PRX
4040 WRITE #1,RY,PRY
4050 '
4060 FOR I=ISH+1 TO R
4070 PRINT R(I),PR(I)
4080 WRITE #1,R(I),PR(I)
4090 NEXT I
4100 CLOSE
4110 PRINT
4120 INPUT "SHALL I SAVE THE PRESSURE DATA : ",G3$
4130 IF G3$="Y" THEN 4160 ELSE 4140
4140 IF G3$="Y" THEN 4160 ELSE 5000
4150 '
4160 ' OPEN DATA FILE FOR PRESSURE VS R DATA
4170 '
4180 INPUT "INPUT THE NAME OF THE DATA FILE : ",G2$
4190 PRINT
4200 OPEN "O",#1,G2$
4210 ' WRITE: R(I),P(I)
4220 WRITE #1,0,PRES
4230 PRINT
4240 PRINT " PRESSURE DATA
4250 PRINT
4260 PRINT " R(I) P(I)
4270 PRINT 0,PRES
4280 FOR I=1 TO ISH
4290 PRINT R(I),P(I)
4300 WRITE #1,R(I),P(I)
4310 NEXT I
4320 '
4330 IF SUPERS="YES" THEN 4340 ELSE 4390
4340 PRINT RY,PX
4350 PRINT RY,PY
4360 WRITE #1,RX,PX
4370 WRITE #1,RX,PY
4380 '
4390 FOR I=ISH+1 TO R
4400 PRINT R(I),P(I)
4410 WRITE #1,R(I),P(I)
4420 NEXT I
5000 CLOSE
5010 END

```

Appendix B

Instrumentation List

Item	Serial Number
Electronic Control Technology S-100 Computer	---
Analog-to-Digital Card, Dual Systems Control Model AIM12 REV D	25315
Digital-to-Analog Card, Dual Systems Control Model AUM-12	1038
Disk Drive Assembly, Farbell	2267-0482
Terminal, Heathkit Model H-19	17-43722
Scanivalve, SCANCO Model 48S9 3012	003
Transducer, SCANCO Model PDCR23D-25PSID . . .	---
Dual DC Power Supply, Hewlett Packard 6205B .	1140A09045
Solenoid Controller, SCANCO CTRL2/S2-S6 . . .	1482
Odd-Even Decoder, SCANCO OED2	743600
100-inch Hg Manometer, King Engineering . . .	0257
100-inch Hg Equivalent Bourdon-type Pressure Gauge, Wallace and Tiernan	FA 145-NN10008
Digital Multimeter, Hewlett Packard Model 3438A	1717A-07469

Appendix C

TEST

A complete listing of program TEST follows. This program was used for data acquisition. A description of the application of TEST is given in Chapter IV.

```

100 '          PROGRAM -- TEST
110 '
120 '  THIS PROGRAM GATHERS DATA USING A SCANIVALVE.
130 '  IT STEPS THE VALVE THROUGH 40 PORTS AND SAMPLES
132 '  EACH PORT "K" TIMES.  THE AVERAGE OF THE "K"
140 '  SAMPLINGS IS PRINTED FOR EACH PORT.
150 '
160 '  BEFORE RUNNING THIS PROGRAM FOR DATA.  CHECK
162 '  THE POWER SUPPLY OUTPUT AND THE CORRESPONDING
170 '  OFFSET ( 10V AND ~.0009 ).
180 '
190 K=20: '          # OF SAMPLES TO BE AVERAGED
200 INPUT"INPUT CONFIGURATION # : ",CONFIG
210 INPUT"INPUT RESERVOIR PRESSURE : ",P0
220 P0=P0-.1
230 PRINT
240 PRINT
250 PRINT"CONFIGURATION",CONFIG,"RES PRESS =",P0,"in Hg"
260 PRINT
270 PRINT"          PORTS 1 THROUGH 5
280 PRINT"          VOLTAGE IN MILLIVOLTS"
290 PRINT
300 FOR IRAD =1 TO 8
310 FOR IPORT =1 TO 5
320
330 OUT 177,127: '          VOLTAGE ON -- VALVE STEPS
340 OUT 176,127
350 L=5: '          DELAY FOR SWITCHING
360 FOR J1=1 TO L
370 NEXT J1
380 OUT 177,0: '          VOLTAGE OFF
390 OUT 176,0
400 FOR K1=1 TO K
410 NEXT K1
420 OFFSET=.0009
430 AADD=0
440 '
450 '
460 FOR I =1 TO K
470 CH1=0

```

```

480 OUT 140, CH1
490 OUT 141, 0
500 A=INP(142) + (INP(143) AND 15)*256
510 A=A-2048
520 A=(10/4096)*A/100
530 AADD=AADD+A
540 NEXT I
550 AAVE=AADD/K
560 AADJ(IRAD, IPORT)=(AAVE-OFFSET)*1000
570 NEXT IPORT
580 PRINT USING "###.###"      "; IRAD, AADJ(IRAD, 1);
582 PRINT USING "###.###"      "; AADJ(IRAD, 2), AADJ(IRAD, 3);
584 PRINT USING "###.###"      "; AADJ(IRAD, 4), AADJ(IRAD, 5)
590 NEXT IRAD
600 '
610 FOR I2=1 TO 8: '          STEP VALVE TO HOME
620 OUT 177, 127
630 OUT 176, 127
640 FOR J2=1 TO L
650 NEXT J2
660 OUT 177, 0
670 OUT 176, 0
680 FOR K2=1 TO L
690 NEXT K2
700 NEXT I2
710 '
720 '          SAVE DATA TO DATA FILE
730 PRINT
740 INPUT "DO YOU WANT TO SAVE THIS DATA ? ", Q$
750 IF Q$= "Y" GOTO 800
760 INPUT "HOW ABOUT ANOTHER RUN ? ", Q2$
770 IF Q2$= "Y" GOTO 100
780 PRINT "IT'S BEEN A PLEASURE DOING BUSINESS WITH YOU !"
790 GOTO 920
800 PRINT "INPUT FILE NAME:      B:RMMDB##.DAT
810 INPUT "FILE NAME:      ", F$
820 OPEN "O", #1, F$
830 WRITE# 1, CONFIG
840 WRITE# 1, P0
850 FOR JS=1 TO 8
860 FOR IS=1 TO 5
870 WRITE# 1, AADJ(JS, IS)
880 NEXT IS
890 NEXT JS
900 CLOSE #1
910 GOTO 750
920 END

```

Appendix D

REDDATA

A complete listing of program REDDATA follows. This program was used to reduce the data which were generated by program TEST. The details of the program are described in Chapter V.

```

1000 '          PROGRAM -- REDDATA
1010 PRINT
1020 PRINT"PROGRAM ACCESSES DATA FILES GENERATED BY TEST"
1030 PRINT"THE DATA ARE PRESENTED IN ABSOLUTE PRESSURES"
1040 '
1050 SLOPE = .7261:'SLOPE OF CAL CURVE (mv TO in. Hg)
1060 PRINT
1070 INPUT "ENTER .DAT FILE NAME : ",GS
1080 PRINT
1090 INPUT"ENTER AMBIENT PRESS (in. Hg) : ",PA
1100 '
1110 '  CORRECT PA FOR TEMP. AND GRAVITY
1120 '  CORRECTIONS BASED ON 80 DEG F @ 1000' AND 40 DEG N
1130 '  IF CONDITIONS ARE DIFFERENT FROM THIS RECALCULATE !!
1140 '  TEMP= -.015/28"  GRAV= -.12/28"
1150 CORR=(-.145)/28
1160 PA=PA+(PA*CORR)
1170 '
1180 PRINT
1190 PA1=PA/2.036:'          AMBIENT PRESS (PSIA)
1200 PRINT"CORRECTED AMBIENT PRESSURE IS :",PA1,"PSIA"
1210 OPEN "1",#1,BS
1220 INPUT #1,CONFID
1230 INPUT #1,P0
1240 '
1250 '  CORRECT P0 FOR TEMP. AND GRAVITY
1260 P0=P0+(P0*CORR)
1270 '
1280 P0A=P0+PA/2.036
1290 '
1300 FOR IRAD = 1 TO 8
1310 FOR IPORT = 1 TO 5
1320 INPUT #1, AADJ(IRAD,IPORT)
1330 '  CHANGE mv READING TO inches Hg
1340 AHG(IRAD,IPORT)=AADJ(IRAD,IPORT)*SLOPE
1350 '  CORRECT AHG FOR TEMP. AND GRAVITY
1360 AHG(IRAD,IPORT)=AHG(IRAD,IPORT)+(AHG(IRAD,IPORT)*CORR)
1370 '  CHANGE inches Hg TO PSIA

```

```

1380 APSIA(IRAD, IPORT)=(ARGC(IRAD, IPORT)+PA)/2.036
1390 NEXT IPORT
1400 NEXT IRAD
1410 FOR I=1 TO 5
1420 PADD=0
1430 FOR J=1 TO 8
1440 PADD=PADD+APSIA(J, I)
1450 NEXT J
1460 PAVG(I)=PADD/8
1470 PRAT(I)=PAVG(I)/P0A
1480 NEXT I
1490 '          PRINT DATA TO SCREEN
1500 PRINT
1510 PRINT
1520 PRINT"CONFIG", CONFIG, "RES PRESS =", P0A, "PSIA"
1530 PRINT
1540 PRINT"          PORTS 1 THROUGH 5
          PRESSURE (PSIA)"
1550 PRINT
1560 FOR IRAD = 1 TO 8
1580 PRINT USING "###.###"      "; IRAD, APSIA(IRAD, 1);
1590 PRINT USING "###.###"      "; APSIA(IRAD, 2), APSIA(IRAD, 3);
1600 PRINT USING "###.###"      "; APSIA(IRAD, 4), APSIA(IRAD, 5)
1610 NEXT IRAD
1620 PRINT:PRINT"AVERAGE PRESSURES":PRINT
1630 PRINT USING "###.###"      "; 0, PAVG(1), PAVG(2);
1640 PRINT USING "###.###"      "; PAVG(3), PAVG(4), PAVG(5)
1650 PRINT:PRINT"PRESSURE RATIOS":PRINT
1660 PRINT USING "###.###"      "; 0, PRAT(1), PRAT(2);
1670 PRINT USING "###.###"      "; PRAT(3), PRAT(4), PRAT(5)
1680 CLOSE 1
1690 PRINT
1700 R17=.1875
1710 R127=.1475
1720 R137=.0625
1730 R147=.75
1740 R157=.9375
1750 '
1760 INPUT"SHALL I SAVE THE PRESSURE RATIO DATA ? ", Q15
1770 IF Q15="Y" THEN 1800 ELSE 1780
1780 IF Q15="N" THEN 1800 ELSE 1900
1790 '
1800 ' OPEN DATA FILE FOR P/PRES VS R DATA
1810
1820 INPUT"INPUT THE NAME OF THE DATA FILE : ", Q16
1830 PRINT
1840 OPEN "Q", #1, Q16
1850 PRINT"PRESSURE RATIO DATA"
1860 PRINT
1870 WRITE #1, 0, 1
1880 PRINT 0, 1
1890 FOR I=1 TO 5

```

```

1900 WRITE #1,R(I),PRAT(I)
1910 PRINT R(I),PRAT(I)
1920 NEXT I
1930 CLOSE 1
1940 '
1950 INPUT"SHALL I SAVE THE PRESSURE DATA ? ",Q2$
1960 IF Q2$="Y" THEN 1990 ELSE 1970
1970 IF Q2$="Y" THEN 1990 ELSE 2140
1980 '
1990 ' OPEN DATA FILE FOR PRESS VS R DATA
2000 '
2010 INPUT"INPUT THE NAME OF THE DATA FILE : ",Q2$
2020 PRINT
2030 OPEN "O",#1,Q2$
2040 PRINT"PRESSURE DATA
2050 PRINT
2060 WRITE #1,0,POA
2070 PRINT 0,POA
2080 FOR I=1 TO 5
2090 WRITE #1,R(I),PAVG(I)
2100 PRINT R(I),PAVG(I)
2110 NEXT I
2120 CLOSE 1
2130 '
2140 END

```

Appendix E

EFFAREA

The program EFFAREA solved the reed-valve problem by two analytic methods. Descriptions of the techniques are presented in Chapter VI. The major difference between EFFAREA and SOLVE is in the area distribution of the reed-valve flow channel. The area distributions are listed below for the applicable method. The line numbers correspond to the locations where they should be substituted into SOLVE. Other minor modifications are described in Chapter VI.

Method 1 area ratios:

```
1462 FOR I=1 TO R
1464 R(I)=R1+(I-1)*INCR
1466 NEXT I
1468 '
1470 A(1)=1
1472 A(2)=1.367
1474 A(3)=1.629
1476 A(4)=1.892
1478 A(5)=2.154
1480 A(6)=2.416
1482 A(7)=2.678
1484 A(8)=2.940
1486 A(9)=3.202
1488 A(10)=3.464
1490 A(11)=3.726
1492 A(12)=3.988
1494 A(13)=4.250
1496 A(14)=4.512
1498 A(15)=4.774
1500 '
1502 A(16)=5.036
1504 A(17)=5.298
1506 A(18)=5.560
1508 A(19)=5.822
1510 A(20)=6.084
1512 A(21)=6.346
1514 A(22)=6.608
1516 A(23)=6.870
1518 A(24)=7.132
1520 A(25)=7.394
1522 A(26)=7.656
1524 A(27)=7.918
1526 A(28)=8.180
1528 A(29)=8.442
1530 A(30)=8.704
1532 A(31)=8.966
1534 A(32)=9.228
1536 A(33)=9.490
1538 A(34)=9.752
1540 A(35)=10.014
1542 A(36)=10.276
1544 A(37)=10.538
1546 A(38)=10.800
1548 A(39)=11.062
1550 A(40)=11.324
1552 A(41)=11.586
1554 A(42)=11.848
1556 A(43)=12.110
1558 A(44)=12.372
1560 A(45)=12.634
1562 A(46)=12.896
1564 A(47)=13.158
1566 A(48)=13.420
1568 A(49)=13.682
1570 A(50)=13.944
1572 A(51)=14.206
1574 A(52)=14.468
1576 A(53)=14.730
1578 A(54)=14.992
1580 A(55)=15.254
1582 A(56)=15.516
1584 A(57)=15.778
1586 A(58)=16.040
1588 A(59)=16.302
1590 A(60)=16.564
1592 A(61)=16.826
1594 A(62)=17.088
1596 A(63)=17.350
1598 A(64)=17.612
1600 A(65)=17.874
1602 A(66)=18.136
1604 A(67)=18.398
1606 A(68)=18.660
1608 A(69)=18.922
1610 A(70)=19.184
1612 A(71)=19.446
1614 A(72)=19.708
1616 A(73)=19.970
1618 A(74)=20.232
1620 A(75)=20.494
1622 A(76)=20.756
1624 A(77)=21.018
1626 A(78)=21.280
1628 A(79)=21.542
1630 A(80)=21.804
1632 A(81)=22.066
1634 A(82)=22.328
1636 A(83)=22.590
1638 A(84)=22.852
1640 A(85)=23.114
1642 A(86)=23.376
1644 A(87)=23.638
1646 A(88)=23.900
1648 A(89)=24.162
1650 A(90)=24.424
1652 A(91)=24.686
1654 A(92)=24.948
1656 A(93)=25.210
1658 A(94)=25.472
1660 A(95)=25.734
1662 A(96)=26.000
1664 A(97)=26.260
1666 A(98)=26.520
1668 A(99)=26.780
1670 A(100)=27.040
1672 A(101)=27.300
1674 A(102)=27.560
1676 A(103)=27.820
1678 A(104)=28.080
1680 A(105)=28.340
1682 A(106)=28.600
1684 A(107)=28.860
1686 A(108)=29.120
1688 A(109)=29.380
1690 A(110)=29.640
1692 A(111)=29.900
1694 A(112)=30.160
1696 A(113)=30.420
1698 A(114)=30.680
1700 A(115)=30.940
1702 A(116)=31.200
1704 A(117)=31.460
1706 A(118)=31.720
1708 A(119)=31.980
1710 A(120)=32.240
1712 A(121)=32.500
1714 A(122)=32.760
1716 A(123)=33.020
1718 A(124)=33.280
1720 A(125)=33.540
1722 A(126)=33.800
1724 A(127)=34.060
1726 A(128)=34.320
1728 A(129)=34.580
1730 A(130)=34.840
1732 A(131)=35.100
1734 A(132)=35.360
1736 A(133)=35.620
1738 A(134)=35.880
1740 A(135)=36.140
1742 A(136)=36.400
1744 A(137)=36.660
1746 A(138)=36.920
1748 A(139)=37.180
1750 A(140)=37.440
1752 A(141)=37.700
1754 A(142)=37.960
1756 A(143)=38.220
1758 A(144)=38.480
1760 A(145)=38.740
1762 A(146)=39.000
1764 A(147)=39.260
1766 A(148)=39.520
1768 A(149)=39.780
1770 A(150)=40.040
1772 A(151)=40.300
1774 A(152)=40.560
1776 A(153)=40.820
1778 A(154)=41.080
1780 A(155)=41.340
1782 A(156)=41.600
1784 A(157)=41.860
1786 A(158)=42.120
1788 A(159)=42.380
1790 A(160)=42.640
1792 A(161)=42.900
1794 A(162)=43.160
1796 A(163)=43.420
1798 A(164)=43.680
1800 A(165)=43.940
1802 A(166)=44.200
1804 A(167)=44.460
1806 A(168)=44.720
1808 A(169)=44.980
1810 A(170)=45.240
1812 A(171)=45.500
1814 A(172)=45.760
1816 A(173)=46.020
1818 A(174)=46.280
1820 A(175)=46.540
1822 A(176)=46.800
1824 A(177)=47.060
1826 A(178)=47.320
1828 A(179)=47.580
1830 A(180)=47.840
1832 A(181)=48.100
1834 A(182)=48.360
1836 A(183)=48.620
1838 A(184)=48.880
1840 A(185)=49.140
1842 A(186)=49.400
1844 A(187)=49.660
1846 A(188)=49.920
1848 A(189)=50.180
1850 A(190)=50.440
1852 A(191)=50.700
1854 A(192)=50.960
1856 A(193)=51.220
1858 A(194)=51.480
1860 A(195)=51.740
1862 A(196)=52.000
1864 A(197)=52.260
1866 A(198)=52.520
1868 A(199)=52.780
1870 A(200)=53.040
1872 A(201)=53.300
1874 A(202)=53.560
1876 A(203)=53.820
1878 A(204)=54.080
1880 A(205)=54.340
1882 A(206)=54.600
1884 A(207)=54.860
1886 A(208)=55.120
1888 A(209)=55.380
1890 A(210)=55.640
1892 A(211)=55.900
1894 A(212)=56.160
1896 A(213)=56.420
1898 A(214)=56.680
1900 A(215)=56.940
1902 A(216)=57.200
1904 A(217)=57.460
1906 A(218)=57.720
1908 A(219)=57.980
1910 A(220)=58.240
1912 A(221)=58.500
1914 A(222)=58.760
1916 A(223)=59.020
1918 A(224)=59.280
1920 A(225)=59.540
1922 A(226)=59.800
1924 A(227)=60.060
1926 A(228)=60.320
1928 A(229)=60.580
1930 A(230)=60.840
1932 A(231)=61.100
1934 A(232)=61.360
1936 A(233)=61.620
1938 A(234)=61.880
1940 A(235)=62.140
1942 A(236)=62.400
1944 A(237)=62.660
1946 A(238)=62.920
1948 A(239)=63.180
1950 A(240)=63.440
1952 A(241)=63.700
1954 A(242)=63.960
1956 A(243)=64.220
1958 A(244)=64.480
1960 A(245)=64.740
1962 A(246)=65.000
1964 A(247)=65.260
1966 A(248)=65.520
1968 A(249)=65.780
1970 A(250)=66.040
1972 A(251)=66.300
1974 A(252)=66.560
1976 A(253)=66.820
1978 A(254)=67.080
1980 A(255)=67.340
1982 A(256)=67.600
1984 A(257)=67.860
1986 A(258)=68.120
1988 A(259)=68.380
1990 A(260)=68.640
1992 A(261)=68.900
1994 A(262)=69.160
1996 A(263)=69.420
1998 A(264)=69.680
2000 A(265)=69.940
2002 A(266)=70.200
2004 A(267)=70.460
2006 A(268)=70.720
2008 A(269)=70.980
2010 A(270)=71.240
2012 A(271)=71.500
2014 A(272)=71.760
2016 A(273)=72.020
2018 A(274)=72.280
2020 A(275)=72.540
2022 A(276)=72.800
2024 A(277)=73.060
2026 A(278)=73.320
2028 A(279)=73.580
2030 A(280)=73.840
2032 A(281)=74.100
2034 A(282)=74.360
2036 A(283)=74.620
2038 A(284)=74.880
2040 A(285)=75.140
2042 A(286)=75.400
2044 A(287)=75.660
2046 A(288)=75.920
2048 A(289)=76.180
2050 A(290)=76.440
2052 A(291)=76.700
2054 A(292)=76.960
2056 A(293)=77.220
2058 A(294)=77.480
2060 A(295)=77.740
2062 A(296)=78.000
2064 A(297)=78.260
2066 A(298)=78.520
2068 A(299)=78.780
2070 A(300)=79.040
2072 A(301)=79.300
2074 A(302)=79.560
2076 A(303)=79.820
2078 A(304)=80.080
2080 A(305)=80.340
2082 A(306)=80.600
2084 A(307)=80.860
2086 A(308)=81.120
2088 A(309)=81.380
2090 A(310)=81.640
2092 A(311)=81.900
2094 A(312)=82.160
2096 A(313)=82.420
2098 A(314)=82.680
2100 A(315)=82.940
2102 A(316)=83.200
2104 A(317)=83.460
2106 A(318)=83.720
2108 A(319)=83.980
2110 A(320)=84.240
2112 A(321)=84.500
2114 A(322)=84.760
2116 A(323)=85.020
2118 A(324)=85.280
2120 A(325)=85.540
2122 A(326)=85.800
2124 A(327)=86.060
2126 A(328)=86.320
2128 A(329)=86.580
2130 A(330)=86.840
2132 A(331)=87.100
2134 A(332)=87.360
2136 A(333)=87.620
2138 A(334)=87.880
2140 A(335)=88.140
2142 A(336)=88.400
2144 A(337)=88.660
2146 A(338)=88.920
2148 A(339)=89.180
2150 A(340)=89.440
2152 A(341)=89.700
2154 A(342)=89.960
2156 A(343)=90.220
2158 A(344)=90.480
2160 A(345)=90.740
2162 A(346)=91.000
2164 A(347)=91.260
2166 A(348)=91.520
2168 A(349)=91.780
2170 A(350)=92.040
2172 A(351)=92.300
2174 A(352)=92.560
2176 A(353)=92.820
2178 A(354)=93.080
2180 A(355)=93.340
2182 A(356)=93.600
2184 A(357)=93.860
2186 A(358)=94.120
2188 A(359)=94.380
2190 A(360)=94.640
2192 A(361)=94.900
2194 A(362)=95.160
2196 A(363)=95.420
2198 A(364)=95.680
2200 A(365)=95.940
2202 A(366)=96.200
2204 A(367)=96.460
2206 A(368)=96.720
2208 A(369)=96.980
2210 A(370)=97.240
2212 A(371)=97.500
2214 A(372)=97.760
2216 A(373)=98.020
2218 A(374)=98.280
2220 A(375)=98.540
2222 A(376)=98.800
2224 A(377)=99.060
2226 A(378)=99.320
2228 A(379)=99.580
2230 A(380)=99.840
2232 A(381)=100.100
2234 A(382)=100.360
2236 A(383)=100.620
2238 A(384)=100.880
2240 A(385)=101.140
2242 A(386)=101.400
2244 A(387)=101.660
2246 A(388)=101.920
2248 A(389)=102.180
2250 A(390)=102.440
2252 A(391)=102.700
2254 A(392)=102.960
2256 A(393)=103.220
2258 A(394)=103.480
2260 A(395)=103.740
2262 A(396)=104.000
2264 A(397)=104.260
2266 A(398)=104.520
2268 A(399)=104.780
2270 A(400)=105.040
2272 A(401)=105.300
2274 A(402)=105.560
2276 A(403)=105.820
2278 A(404)=106.080
2280 A(405)=106.340
2282 A(406)=106.600
2284 A(407)=106.860
2286 A(408)=107.120
2288 A(409)=107.380
2290 A(410)=107.640
2292 A(411)=107.900
2294 A(412)=108.160
2296 A(413)=108.420
2298 A(414)=108.680
2300 A(415)=108.940
2302 A(416)=109.200
2304 A(417)=109.460
2306 A(418)=109.720
2308 A(419)=110.000
2310 A(420)=110.260
2312 A(421)=110.520
2314 A(422)=110.780
2316 A(423)=111.040
2318 A(424)=111.300
2320 A(425)=111.560
2322 A(426)=111.820
2324 A(427)=112.080
2326 A(428)=112.340
2328 A(429)=112.600
2330 A(430)=112.860
2332 A(431)=113.120
2334 A(432)=113.380
2336 A(433)=113.640
2338 A(434)=113.900
2340 A(435)=114.160
2342 A(436)=114.420
2344 A(437)=114.680
2346 A(438)=114.940
2348 A(439)=115.200
2350 A(440)=115.460
2352 A(441)=115.720
2354 A(442)=115.980
2356 A(443)=116.240
2358 A(444)=116.500
2360 A(445)=116.760
2362 A(446)=117.020
2364 A(447)=117.280
2366 A(448)=117.540
2368 A(449)=117.800
2370 A(450)=118.060
2372 A(451)=118.320
2374 A(452)=118.580
2376 A(453)=118.840
2378 A(454)=119.100
2380 A(455)=119.360
2382 A(456)=119.620
2384 A(457)=119.880
2386 A(458)=120.140
2388 A(459)=120.400
2390 A(460)=120.660
2392 A(461)=120.920
2394 A(462)=121.180
2396 A(463)=121.440
2398 A(464)=121.700
2400 A(465)=121.960
2402 A(466)=122.220
2404 A(467)=122.480
2406 A(468)=122.740
2408 A(469)=123.000
2410 A(470)=123.260
2412 A(471)=123.520
2414 A(472)=123.780
2416 A(473)=124.040
2418 A(474)=124.300
2420 A(475)=124.560
2422 A(476)=124.820
2424 A(477)=125.080
2426 A(478)=125.340
2428 A(479)=125.600
2430 A(480)=125.860
2432 A(481)=126.120
2434 A(482)=126.380
2436 A(483)=126.640
2438 A(484)=126.900
2440 A(485)=127.160
2442 A(486)=127.420
2444 A(487)=127.680
2446 A(488)=127.940
2448 A(489)=128.200
2450 A(490)=128.460
2452 A(491)=128.720
2454 A(492)=128.980
2456 A(493)=129.240
2458 A(494)=129.500
2460 A(495)=129.760
2462 A(496)=130.020
2464 A(497)=130.280
2466 A(498)=130.540
2468 A(499)=130.800
2470 A(500)=131.060
2472 A(501)=131.320
2474 A(502)=131.580
2476 A(503)=131.840
2478 A(504)=132.100
2480 A(505)=132.360
2482 A(506)=132.620
2484 A(507)=132.880
2486 A(508)=133.140
2488 A(509)=133.400
2490 A(510)=133.660
2492 A(511)=133.920
2494 A(512)=134.180
2496 A(513)=134.440
2498 A(514)=134.700
2500 A(515)=134.960
2502 A(516)=135.220
2504 A(517)=135.480
2506 A(518)=135.740
2508 A(519)=136.000
2510 A(520)=136.260
2512 A(521)=136.520
2514 A(522)=136.780
2516 A(523)=137.040
2518 A(524)=137.300
2520 A(525)=137.560
2522 A(526)=137.820
2524 A(527)=138.080
2526 A(528)=138.340
2528 A(529)=138.600
2530 A(530)=138.860
2532 A(531)=139.120
2534 A(532)=139.380
2536 A(533)=139.640
2538 A(534)=139.900
2540 A(535)=140.160
2542 A(536)=140.420
2544 A(537)=140.680
2546 A(538)=140.940
2548 A(539)=141.200
2550 A(540)=141.460
2552 A(541)=141.720
2554 A(542)=141.980
2556 A(543)=142.240
2558 A(544)=142.500
2560 A(545)=142.760
2562 A(546)=143.020
2564 A(547)=143.280
2566 A(548)=143.540
2568 A(549)=143.800
2570 A(550)=144.060
2572 A(551)=144.320
2574 A(552)=144.580
2576 A(553)=144.840
2578 A(554)=145.100
2580 A(555)=145.360
2582 A(556)=145.620
2584 A(557)=145.880
2586 A(558)=146.140
2588 A(559)=146.400
2590 A(560)=146.660
2592 A(561)=146.920
2594 A(562)=147.180
2596 A(563)=147.440
2598 A(564)=147.700
2600 A(565)=147.960
2602 A(566)=148.220
2604 A(567)=148.480
2606 A(568)=148.740
2608 A(569)=149.000
2610 A(570)=149.260
2612 A(571)=149.520
2614 A(572)=149.780
2616 A(573)=150.040
2618 A(574)=150.300
2620 A(575)=150.560
2622 A(576)=150.820
2624 A(577)=151.080
2626 A(578)=151.340
2628 A(579)=151.600
2630 A(580)=151.860
2632 A(581)=152.120
2634 A(582)=152.380
2636 A(583)=152.640
2638 A(584)=152.900
2640 A(585)=153.160
2642 A(586)=153.420
2644 A(587)=153.680
2646 A(588)=153.940
2648 A(589)=154.200
2650 A(590)=154.460
2652 A(591)=154.720
2654 A(592)=154.980
2656 A(593)=155.240
2658 A(594)=155.500
2660 A(595)=155.760
2662 A(596)=156.020
2664 A(597)=156.280
2666 A(598)=156.540
2668 A(599)=156.800
2670 A(600)=157.060
2672 A(601)=157.320
2674 A(602)=157.580
2676 A(603)=157.840
2678 A(604)=158.100
2680 A(605)=158.360
2682 A(606)=158.620
2684 A(607)=158.880
2686 A(608)=159.140
2688 A(609)=159.400
2690 A(610)=159.660
2692 A(611)=159.920
2694 A(612)=160.180
2696 A(613)=160.440
2698 A(614)=160.700
2700 A(615)=160.960
2702 A(616)=161.220
2704 A(617)=161.480
2706 A(618)=161.740
2708 A(619)=162.000
2710 A(620)=162.260
2712 A(621)=162.520
2714 A(622)=162.780
2716 A(623)=163.040
2718 A(624)=163.300
2720 A(625)=163.560
2722 A(626)=163.820
2724 A(627)=164.080
2726 A(628)=164.340
2728 A(629)=164.600
2730 A(630)=164.860
2732 A(631)=165.120
2734 A(632)=165.380
2736 A(633)=165.640
2738 A(634)=165.900
2740 A(635)=166.160
2742 A(636)=166.420
2744 A(637)=166.680
2746 A(638)=166.940
2748 A(639)=167.200
2750 A(640)=167.460
2752 A(641)=167.720
2754 A(642)=167.980
2756 A(643)=168.240
2758 A(644)=168.500
2760 A(645)=168.760
2762 A(646)=169.020
2764 A(647)=169.280
2766 A(648)=169.540
2768 A(649)=169.800
2770 A(650)=170.060
2772 A(651)=170.320
2774 A(652)=170.580
2776 A(653)=170.840
2778 A(654)=171.100
2780 A(655)=171.360
2782 A(656)=171.620
2784 A(657)=171.880
2786 A(658)=172.140
2788 A(659)=172.400
2790 A(660)=172.660
2792 A(661)=172.920
2794 A(662)=173.180
2796 A(663)=173.440
2798 A(664)=173.700
2800 A(665)=173.960
2802 A(666)=174.220
2804 A(667)=174.480
2806 A(668)=174.740
2808 A(669)=175.000
2810 A(670)=175.260
2812 A(671)=175.520
2814 A(672)=175.780
2816 A(673)=176.040
2818 A(674)=176.300
2820 A(675)=176.560
2822 A(676)=176.820
2824 A(677)=177.080
2826 A(678)=177.340
2828 A(679)=177.600
2830 A(680)=177.860
2832 A(681)=178.120
2834 A(682)=178.380
2836 A(683)=178.640
2838 A(684)=178.900
2840 A(685)=179.160
2842 A(686)=179.420
2844 A(687)=179.680
2846 A(688)=179.940
2848 A(689)=180.200
2850 A(690)=180.460
2852 A(691)=180.720
2854 A(692)=180.980
2856 A(693)=181.240
2858 A(694)=181.500
2860 A(695)=181.760
2862 A(696)=182.020
2864 A(697)=182.280
2866 A(698)=182.540
2868 A(699)=182.800
2870 A(700)=183.0
```


Method - area ratios:

```
1461 FOR I=1 TO R
1464 R(I)=R1+(I-1)*INCR
1466 NEXT I
1468 '
1470 INPUT "INPUT A(1) = ";A(1)
1471 A1=A(1)
1472 A(2)=1.5
1473 A(3)=2.0
1474 A(4)=2.5
1475 A(5)=3.0
1476 A(6)=3.5
1477 A(7)=4.0
1478 A(8)=4.5
1479 A(9)=5.0
1480 A(10)=5.5
1481 A(11)=6.0
1482 A(12)=6.5
1483 A(13)=7.0
1484 A(14)=7.5
1485 A(15)=8.0
1486 AE=A(15)
1488 '
```

Vita

Captain Robert D. Hunt was born on 30 July 1955 in Shelby, Montana. He was raised in the Treasure State and graduated from high school in Helena in 1973. He attended Montana State University for four quarters before transferring to the University of Hawaii, where he recieved the degree of Bachelor of Science in Meteorology in December 1979. Bob was recruited into the USAF to attend AFIT in an undergraduate degree conversion program. He recieved his commission as a distinguished graduate of OTS and after the 18-month program at AFIT, recieved a Bachelor of Science degree in Aeronautical Engineering in 1982. He spent two years working in the 3246 Test Wing as a flight test engineer at Eglin AFB, FL. He became the lead test engineer on F-16 flutter, loads, and stability and control testing at the Armament Division. Captain Hunt re-entered the School of Engineering, Air Force Institute of Technology, in the Aeronautical Engineering Master of Science program, in May 1984.

Permanent Address: 3725 West 44th

Anchorage, Alaska 99517

AD-A164102

REPORT DOCUMENTATION PAGE

1a. REPORT SECURITY CLASSIFICATION UNCLASSIFIED			1b. RESTRICTIVE MARKINGS		
2a. SECURITY CLASSIFICATION AUTHORITY			3. DISTRIBUTION/AVAILABILITY OF REPORT		
2b. DECLASSIFICATION/DOWNGRADING SCHEDULE			Approved for public release; distribution unlimited		
4. PERFORMING ORGANIZATION REPORT NUMBER(S) AFIT/GAE/AA/85D-09			5. MONITORING ORGANIZATION REPORT NUMBER(S)		
6a. NAME OF PERFORMING ORGANIZATION School of Engineering		6b. OFFICE SYMBOL (If applicable) AFIT/ENY	7a. NAME OF MONITORING ORGANIZATION		
6c. ADDRESS (City, State and ZIP Code) Air Force Institute of Technology Wright-Patterson AFB, Ohio 45433			7b. ADDRESS (City, State and ZIP Code)		
8a. NAME OF FUNDING/SPONSORING ORGANIZATION		8b. OFFICE SYMBOL (If applicable)	9. PROCUREMENT INSTRUMENT IDENTIFICATION NUMBER		
8c. ADDRESS (City, State and ZIP Code)			10. SOURCE OF FUNDING NOS.		
			PROGRAM ELEMENT NO.	PROJECT NO.	TASK NO.
11. TITLE (Include Security Classification) See Box 19			WORK UNIT NO.		
12. PERSONAL AUTHOR(S) Robert D. Hunt, B.S., Capt, USAF					
13a. TYPE OF REPORT MS Thesis		13b. TIME COVERED FROM _____ TO _____		14. DATE OF REPORT (Yr., Mo., Day) 1985 December	
				15. PAGE COUNT 119	
16. SUPPLEMENTARY NOTATION					
17. COSATI CODES			18. SUBJECT TERMS (Continue on reverse if necessary and identify by block number)		
FIELD	GROUP	SUB. GR.	Compressor, Valves, Scanivalve, Radial Flow, Supersonic		
20	04				
13	07				
19. ABSTRACT (Continue on reverse if necessary and identify by block number)					
<p>Title: A STUDY OF THE FLUID-DYNAMIC FIELDS ON COMPRESSOR REED VALVES</p> <p>Thesis Chairman: Eric J. Jumper, Lt Col, USAF</p> <p style="text-align: right;">Approved for public release: LAW AFR 180-17 <i>Ly. Wolaver</i> 16 JAN 86 LYON E. WOLAVER Dean for Research and Professional Development Air Force Institute of Technology (AFIT) Wright-Patterson AFB OH 45433</p>					
20. DISTRIBUTION AVAILABILITY OF ABSTRACT UNCLASSIFIED/UNLIMITED <input checked="" type="checkbox"/> SAME AS RPT <input type="checkbox"/> DTIC USERS <input type="checkbox"/>			21. ABSTRACT SECURITY CLASSIFICATION UNCLASSIFIED		
22a. NAME OF RESPONSIBLE INDIVIDUAL Eric J. Jumper, Lt Col, USAF			22b. TELEPHONE NUMBER (Include Area Code) 513-255-3517		22c. OFFICE SYMBOL AFIT/ENY

UNCLASSIFIED

SECURITY CLASSIFICATION OF THIS PAGE

The flow-induced pressure field in a reed-valve arrangement was analytically predicted and experimentally measured for steady-state conditions. The flow was found to be supersonic in nature with an imbedded shock for all but the lowest pressure runs.

The analytic method used one-dimensional isentropic and normal shock relations. The technique provides a good "first-look" at the nature of the flow and is compatible for use on a small computer system.

The experimental data was obtained by using an idealized reed-valve model. The data acquisition system was computerized and used a scanivalve system to measure the pressure in the valve model. Circular, square, and rectangular valve plate geometries were investigated. The inlet was circular for all cases. Flow-visualization oil was also used in a qualitative approach to determine the location and shape of the shock in the flow. The pressure measurements and the flow visualization showed the shock to be circular for all geometries and pressures tested. At high total pressure runs the valve plate began vibrating and the shock location became smeared, suggesting the the shock was also oscillating.

UNCLASSIFIED

SECURITY CLASSIFICATION OF THIS PAGE

END

FILMED

3-86

DTIC